Cellulose Nanocrystals: Renewable Property Modifiers for Pressure Sensitive Adhesives

Zahra Dastjerdi

A thesis submitted in partial fulfilment of the requirements for the
Doctorate in Philosophy degree in Chemical Engineering

Department of Chemical and Biological Engineering
Faculty of Engineering
University of Ottawa

Statement of Contributions of Collaborators

I hereby declare that I am the sole author of this thesis. I performed all the *in situ* emulsion polymerization experiments, polymer nanocomposite characterization and pressure-sensitive adhesive (PSA) performance testing as well as the associated data analysis. PSA nanocomposite film surface tension measurements and CNC/latex particle size analysis were carried out by me in the Department of Chemical and Biological Engineering at the University of Ottawa.

The scientific guidance throughout the project and editorial comments of the written work were provided by my thesis supervisor Dr. Marc A. Dubé of the Department of Chemical and Biological Engineering at the University of Ottawa and Dr. Emily D. Cranston of the Department of Chemical Engineering at McMaster University.

Name: Zahra Dastjerdi

Date: September/2017

Abstract

Pressure sensitive adhesives (PSAs) are polymeric materials with versatile applications in industrial and consumer products such as protective films, product labels, masking tape, and sticky notes, to name a few applications. World demand for emulsion–based products is on the rise due to worldwide legislation on solvent emissions. In order to completely replace emulsion-based PSAs with their solvent-based counterpart, the property modification of emulsion-based PSAs is required. The use of nanomaterials to modify polymer properties is well established. The aim of this thesis was to use cellulose nanocrystals (CNCs) as property modifiers for emulsion-based PSAs.

CNCs are recognized as a highly efficient reinforcement nanofiller. Owing to their environmentally friendly characteristics, low density, high aspect ratio, non-toxicity, and abundant availability, the application of CNCs in composite materials is gaining increasing attention. In this thesis, the inclusion of CNCs in emulsion-based PSAs was carried out through *in situ* emulsion polymerization and blending technique. To the best of our knowledge, there is limited information about the synthesis of CNC/PSAs nanocomposites via *in situ* emulsion polymerization and the evaluation of their mechanical performance.

The addition of CNCs to the polymerization formulation caused latex instability due to the negatively charged surfaces of the CNCs. After numerous attempts to overcome the stability issues, a stable polymerization formulation and protocol were developed. CNC/PSAs were synthesized via *in situ* seeded-semi batch emulsion polymerization, which is a common commercial production pathway for PSAs. The mechanical performance of the resulting PSA nanocomposite films, namely, shear strength, tack, and peel strength, was evaluated at several CNC loadings. All three PSA adhesive properties were simultaneously enhanced with increasing

CNC loading. The inclusion of CNCs into the films increased their hydrophilicity. Consequently, the PSA films' improved wettability on a stainless steel substrate imparted greater tack and peel strength. The blending of the CNCs with a base latex also led to improved adhesive properties. However, the property modification through blending was not as effective as that for the CNC/PSA films synthesized via *in situ* emulsion polymerization. Thus, CNCs are safe nanomaterials that have been shown to provide remarkable property enhancement of emulsion-based PSA films at low loadings (1wt%).

Résumé

Les adhésifs sensibles à la pression (PSA) sont des matériaux polymériques avec des applications polyvalentes dans des produits industriels et de consommation tels que des films protecteurs, des étiquettes de produits, des rubans adhésifs et des notes collantes, pour nommer quelques applications. La demande de produits à base d'émulsion augmente en raison de la législation mondiale sur les émissions de solvants. Afin de remplacer complètement les PSA à base d'émulsion par leur contrepartie à base de solvant, la modification de la propriété des PSA à base d'émulsion est requise. L'utilisation de nanomatériaux pour modifier les propriétés des polymères est bien établie. L'objectif de cette thèse était d'utiliser des nanocristaux de cellulose (CNC) comme modificateurs de propriété pour les PSA à base d'émulsion. Les CNC sont reconnus comme un nanofiller de renforcement hautement efficace. En raison de leurs caractéristiques respectueuses de l'environnement, de leur faible densité, de leur haut rapport d'aspect, de leur non toxicité et de leur disponibilité abondante, l'application de CNC dans des matériaux composites prend de plus en plus d'attention. Dans cette thèse, l'inclusion de CNC dans des PSA à base d'émulsion a été effectuée par une polymérisation en émulsion in situ et une technique de mélange. À notre connaissance, il existe peu d'informations sur la synthèse des nanocomposites CNC / PSA par polymérisation en émulsion in situ et l'évaluation de leur performance mécanique.

L'addition de CNC à la formulation de polymérisation a provoqué une instabilité du latex due aux surfaces chargées négativement des CNC. Après de nombreuses tentatives pour surmonter les problèmes de stabilité, une formulation et un protocole de polymérisation stable ont été développés. Les CNC/PSA ont été synthétisés via une polymérisation en émulsion semi-discontinue semée in situ, qui est une voie de production commerciale commune. La performance

mécanique des films nanocomposites PSA résultants, à savoir la résistance au cisaillement, l'adhérence et la résistance au pelage, a été évaluée à plusieurs charges de CNC. Les trois propriétés adhésives des PSA ont été augmentées simultanément avec l'augmentation du chargement CNC. L'inclusion des CNC dans les films a augmenté leur hydrophilie. En conséquence, la mouillabilité améliorée des films PSA sur un substrat en acier inoxydable a permis une adhérence accrue et une résistance au pelage. Le mélange des CNC avec un latex de base a également conduit à des propriétés adhésives améliorées. Cependant, la modification de la propriété par mélange n'a pas été aussi efficace que pour les films CNC/PSA synthétisés par polymérisation en émulsion in situ. Ainsi, les CNC sont des nanomatériaux non-toxiques qui se sont révélés de fournir une amélioration remarquable des propriétés des films PSA à base d'émulsion à faible charge (1% en poids).

Acknowledgments

I would like to express my gratitude to those individuals who supported and assisted me during my PhD journey and make it pleasant and memorable chapter of my life.

First and foremost, I would like to thank my supervisor, Prof Marc. A. Dubé, for his insightful supervision, guidance, and constructive feedback throughout my PhD.

I would also like to thank Prof Emily. D. Cranston for her thoughtful comments and sound advice.

My special thanks go to technical support Louis Tremblay and Gérard Nina at Faculty of Chemical & Biological Engineering.

I extend my deepest appreciation to my family for their love, support, patience and encouragement.

Last but not least, I am indebted to my friends and fellows for their support and friendship during my study.

This thesis is dedicated to the memory of my mother who taught me the importance of curiosity and experimentation to knowledge and learning.

Nomenclature

G'= Storage modulus (Pa)

G''= Loss modulus (Pa)

G* = Composite modulus (Pa)

T = temperature (C)

T_g = Glass transition temperature (°C)

Greek Symbols

ρ = Density (g cm^{-3})

θ = Contact angle (^{o})

γ = Surface tension (N m^{-1})

μ = Dynamic viscosity (mPa.s)

List of Abbreviations

AMA = Allyl methacrylate

BA = Butyl acrylate

CAN = Ammonium cerium (IV) nitrate

CTA = Chain transfer agent

CTAB = cetrimonium bromide

CMC = Critical micelle nucleation

CNCs= Cellulose nanocrystals

DDI H_2O = Deionized distilled water

DLS = Dynamic light scattering

DMA = Dynamic mechanical analysis

DSC = Differential scanning calorimetry

HQ = Hydroquinone

KPS = Potassium persulfate

MMA = Methyl methacrylate

MPS = ϒ-methacryloxypropyl triethoxysilane

MWD = Molecular weight distribution

NDM = n-Dodecyl mercaptan

PDI = Polydispersity index

PVDF = Poly (vinylidene fluoride)

phm = parts per hundred parts of monomer

PSA = Pressure sensitive adhesive

PSD = Particle size distribution

PTFE = Polytetrafluoroethylene

SC = Solids content

SDS = Sodium dodecyl sulphate

TEM = Transmission electron microscopy

THF = Tetrahydrofuran

List of Molecular Formulae

Allyl methacrylate: $CH_2=C(CH_3)-COO-CH_2-CH=CH_2$

Ammonium cerium (IV) nitrate: $H_8N_8CeO_{18}$

Butyl acrylate: $CH_2=CH-COO-(CH_2)_3-CH_3$

Cellulose nano crystal: $(C_6H_{10}O_5)_n$

n-Dodecyl mercaptan: $CH_3-(CH_2)_{11}-SH$

Hydroquinone: $HO-(C_6H_4)-OH$

Methyl methacrylate: $CH_2=C(CH_3)-COO-CH_3$

Potassium persulfate: $K_2(SO_4)_2$

Sodium bicarbonate: $NaHCO_3$

Sodium dodecyl sulfate: $CH_3-(CH_2)_{11}-(SO_4)-Na$

Table of Contents

List of Figures

Chapter 1

Chapter 3

Chapter 4

Chapter 5

Chapter 6

Appendix

List of Tables

Chapter 3

Chapter 4

Chapter 5

Chapter 6

Appendix

Chapter 1:

Introduction

Pressure sensitive adhesives (PSAs) are polymeric materials which instantly adhere to a substrate with light finger pressure and leave no residue when removed [1,2]. PSAs are commonly employed in a variety of products such as tapes, note pads, labels, packaging, electronic parts and health care products, to name a few. PSA adhesive properties are highly dependent on their bulk properties (i.e., microstructural and viscoelastic properties) as well as their surface properties. Adhesive properties can be varied by the incorporation of different monomers, microstructural modifiers, and their synthetic process. PSA films are typically evaluated by tack, peel strength (adhesion) and shear strength (cohesion) measurements. PSAs must be able to wet the adherent surface to achieve close contact and must therefore be able to flow at their application temperature to achieve high adhesion energy. A PSA also must have sufficient cohesive (or internal) strength so that the adhesive itself is not responsible for failure of the adhesion process. Therefore, a careful balance between microstructural, viscoelastic and surface properties is required.

Adhesion and cohesion are molecular phenomena. All molecules adhere to one another with considerable force. When two solid bodies approach within a distance on the order of nanometers, they jump into contact as a result of molecular adhesion [3]. Cohesion is an attraction between similar or identical surfaces while adhesion is an attraction between dissimilar surfaces. The adhesion mechanism of PSAs can be explained by several adhesion theories including electrostatic theory, diffusion theory, mechanical theory, weak boundary layer theory, and the adsorption theory [4].

Electrostatic theory proposes that materials adhere to each other by forming a double layer of electrical charge at the interface [4]. The basis of this theory is that there is always an electrochemical potential difference across the interface between two materials in contact, e.g., adhesive and substrate. Free electronic or ionic charge carriers will tend to move across the contact

interface, and an electric double layer is established. This theory is effective to materials with substantially different electronegativities. Diffusion theory postulates that the molecules of the two parts of the specimen interdiffuse, so that the interface becomes diffuse and eventually disappears [4]. Therefore, the mutual solubility of polymers which facilitates the interdiffusion of polymer chains is regarded as an important feature of adhesion phenomena. Mechanical theory relies on the mechanical interlocking between liquid adhesives and the irregularities (peaks and valleys) of a substrate surface [4]. Sufficient adhesion strength is developed after adhesives are solidified. Weak boundary layer theory is a debonding theory which explains the locus of bond failure [4]. A weak boundary is a cohesively weak layer in the interfacial region of an adhesive joint, which may cause the joint itself to be weak, i.e., to fail at a low stress or with low fracture energy. Adsorption theory is the most accepted theory in adhesion science [4]. It proposes that materials with an intimate contact adhere to one another through molecular interactions such as van der Waals bonds, hydrogen bonds, acid-basic interactions, and covalent bonds. These forces are generally considered sufficient to give a high bond strength as long as the extent of wetting is good.

PSAs are mainly composed of monomers yielding low glass transition temperature (T_g) polymers (ranging from -60 to -20^{o}C,) which provide tack and flexibility and monomers giving high T_g polymers (ranging from 105 to 125^{o}C) which offer shear strength [1,2]. The copolymerization of "low T_g" monomers with "high T_g" monomers is required to obtain a T_g (-20 to 50^{o}C) which results in a balanced combination of tack, peel strength, and shear strength appropriate to a particular application (e.g., postage stamp vs. duct tape).

Acrylic PSAs are typically synthesized through solution polymerization or emulsion polymerization techniques [1,2]. Nowadays, emulsion polymerization is preferred for synthesis of adhesives, paints, paper coatings, and cosmetics due to its reduced environmental impact [5]. The

use of water as a reaction medium provides an inherently safe process by means of facilitating mass transfer and heat dissipation during the course of polymerization. The low viscosity of the reaction medium also allows one to obtain the high molecular weight polymers which are less easily achieved in solution polymerization (i.e., due to chain transfer to solvent). Moreover, the use of water is more environmentally friendly compared to using volatile organic compounds (VOCs) in solution polymerization.

Emulsion polymerization is a heterogeneous polymerization process which involves dispersing relatively hydrophobic monomers (e.g., butyl acrylate) in water using an oil-in-water emulsifier (e.g., sodium dodecyl sulfate) above its critical micelle concentration (CMC) [5,6]. Subsequent to the formation of stabilized monomer droplets and numerous monomer-swollen micelles, the polymerization is initiated with a water-soluble initiator (e.g., potassium persulfate). The reactive free radicals, formed by the dissociation of the initiator in water, will polymerize with the moderately dissolved monomers in the water phase to form primary radicals. The primary radicals add monomer units until they reach a size where they become hydrophobic (typically chain lengths from 6 to 15 monomer units). These oligomeric radicals migrate into the monomer-swollen micelles and initiate polymerization to form polymer particles. Thus, the primary locus of polymerization is within the polymer particles due to their large surface area compared to the monomer droplets. Transport of monomer from the monomer droplets to the growing polymer particles enables the polymerization to continue until the monomer is exhausted. At the end of reaction, a colloidal dispersion of polymer particles in aqueous medium, aka latex, is obtained.

Emulsion polymerization can be carried out using a batch or semi-batch process [5,6]. In the batch process, all components are added to the reactor, and the mixture is heated to the desired temperature under constant agitation. In the semi-batch process, pre-emulsified monomer and

initiator solutions are added continuously to the reaction mixture. Seeded emulsion polymerizations can be employed in either batch or semi-batch mode to ensure batch-to-batch reproducibility of the final particle size. In seeded emulsion polymerization, the polymerization of monomer with a controlled amount of emulsifier and initiator in a previously prepared latex proceeds so that the seed particles grow in size without the generation of new particles.

As suggested above, in copolymerization, two monomers are used to provide a combination of their respective properties. Due to the differing reactivity of each monomer, the copolymer composition can vary during a batch process [7]. In other words, the higher reactivity monomer will be consumed preferentially during the early stages of the polymerization while the less reactive monomer will be consumed at a lower rate; this will invariably result in composition drift and perhaps, a deterioration of properties. To achieve a polymer with homogeneous properties, the copolymer composition must be kept relatively constant. Thus, a seeded semi-batch emulsion copolymerization can be used to synthesize the copolymer with both a narrower particle size distribution and narrow composition distribution.

In spite of the fact that latex-based PSA processes are more environmentally friendly than their solvent-based counterparts, latex-based PSAs are faced with the challenge of achieving sufficient shear strength without compromising tack and peel strength [8–10]. Solvent-based PSAs more easily form a continuous gel network as opposed to the discrete microgels found in latex-based PSAs [11]. In addition, surfactants, commonly added to emulsion-based PSA formulations, may reduce PSA performance due to the migration of ionic surfactant molecules from the bulk latex to the PSA film surface during the drying process [12]. Therefore, in order to improve the adhesion properties and broaden their range of applications, the optimization of latex-based PSA microstructure is considered as an effective way to achieve these goals. As noted, however, the

improvement of one property (e.g., shear strength) often occurs at the cost of declining performance in another (e.g., tack).

Various approaches have been proposed to overcome the above-mentioned challenges [13–17]. These include the synthesis of PSAs with bimodal particle size distributions (PSDs) through miniemulsion polymerization or blending techniques [14,15]. The addition of microstructural modifiers such as crosslinkers (e.g., ally methacrylate) and chain transfer agents (e.g., n-dodecyl mercaptan) simultaneously to regulate the adhesive properties [16]. A post treatment of latex-based PSA films under suitable conditions also has been studied to improve the performance of PSA films [17].

The inclusion of nanofillers in PSA matrix can be considered as a potential avenue towards the improvement of PSA microstructure. Nanofillers are materials with at least one dimension in the range of 1-100 nanometers (nm). There are different types of nanofillers such as nanoplates (e.g., nano-layered silicates), nanofibres (e.g., carbon nano-tubes) and nanoparticles (e.g., nano-TiO_2) [18]. They noticeably enhance different properties of the polymer matrix such as mechanical, thermal, electrical, optical, and barrier properties as compared to conventional fillers due to their extremely high surface to volume ratio and/or their extremely high aspect ratio. A good dispersion of nanofillers within the polymer matrix leads to significant interfacial interactions between the polymer and the nanofiller which imparts superior properties to the nanocomposite material compared to their conventional composite counterparts [19]. The incorporation of nanofillers such as carbon nano-tubes [20] , montmorillonite clay [21], nano-layered silicates [22], and nano-TiO_2 [23] into water-based PSAs has been explored in recent years to modify their adhesive performance.

Cellulose nanocrystals (CNCs) are rod-like nanoparticles extracted from cellulosic resources such as cotton, bleached wood pulp, bacterial cellulose, and microcrystalline cellulose (Figure 1.1) [24]. The preparation of CNCs involves a controlled acid hydrolysis process in which a strong acid such as sulfuric, nitric or hydrochloric acid is utilized to dissolve the amorphous chains from cellulose fibers and release the crystalline domains (Figure 1.2.a) [25]. The physical dimensions of CNCs are controlled by the cellulosic source and acid hydrolysis conditions such as the acid type, acid concentration, and hydrolysis time and temperature. Among the different acids, sulfuric acid appears to be the most effective for hydrolysis due to the incorporation of sulfate ester groups into the surface of the CNCs (Figure 1.2.b) [26]. The sulfate ester groups provide the CNCs with a negative charge and consequently make them dispersible in water.

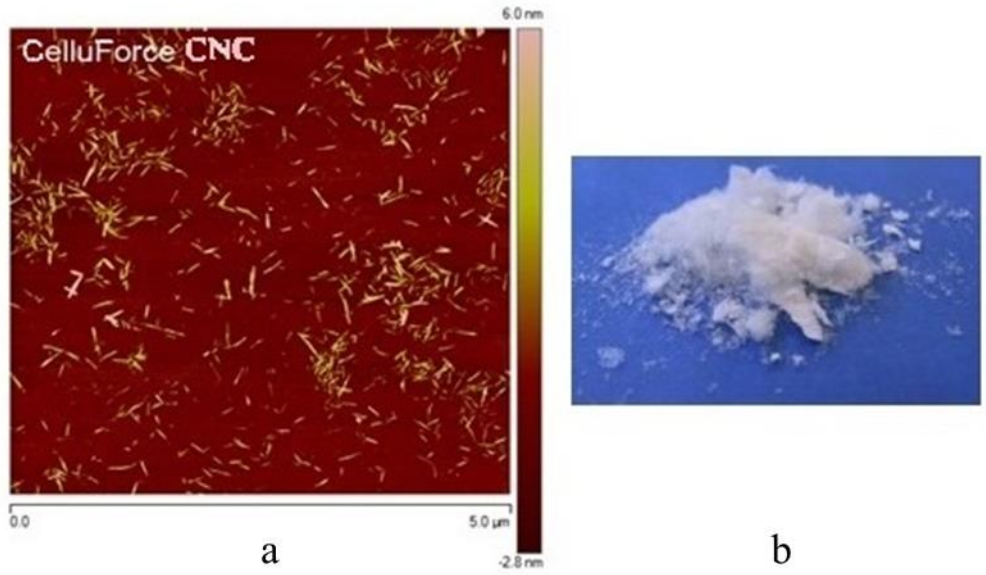

Figure 1.1 a) AFM image of CNCs (Dr. Cranston lab, McMaster University), b) CNC fine powder.

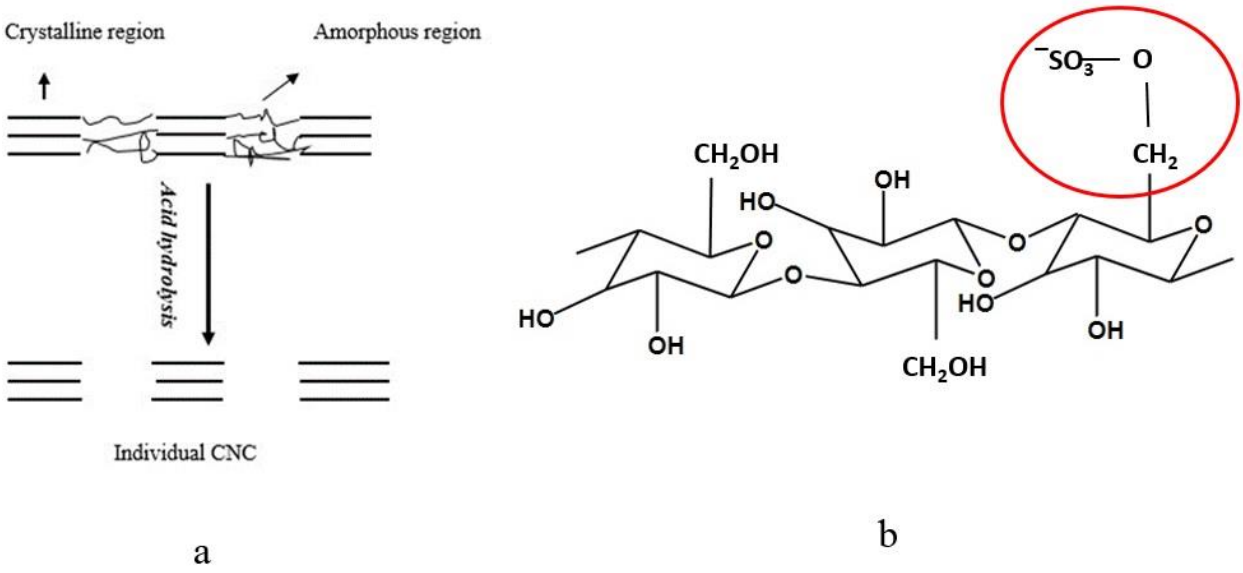

Figure 1.2 a) CNC acid hydrolysis (Chauhan and Chakrabrati, 2012), b) CNC molecular structure (Oke, 2010).

CNCs are highly crystalline (54-88% crystalline regions) [27]. Due to their near perfect crystalline arrangement, they have a greater axial elastic modulus than Kevlar and their mechanical properties are within the range of other reinforcement materials such as steel wire, carbon fiber, and clay nanoplatelets. CNCs have a high aspect ratio (length/diameter: 3-5 nm wide, 50-500 nm in length), high specific surface area (170-533 m^2g^{-1}), and low density (1.6 g cm^{-3}).[1] They have a reactive surface containing –OH side groups which facilitate surface functionalization for surface property modification, and to make them suitable for use as functional fillers. In addition, a few studies on the oral and dermal toxicity of CNCs have shown a lack of adverse health effects [28]. The largest manufacturer of CNCs is located in Canada (CelluForce, Windsor QC). Owing to the attributes noted above, the application of CNCs in composite materials has gained increasing

[1] Note: most nanomaterials tend towards a spherical shape whereas CNCs are rod-like and thus, have an aspect ratio.

attention. It is predicted that CNCs have potential applications in a broad range of fields including paints, packaging, coatings, medicine, biomedical devices, and electronics.

The production of CNCs from various cellulosic sources via different hydrolysis conditions has been studied in recent years, since the shape, size, and surface charge of CNCs have a great influence on its dispersibility and compatibility with the host polymer [29]. The CNC dispersions are mostly incorporated into the matrix through solution casting and *in situ* polymerization techniques. CNC dispersions are prepared depending on the nature of the matrix (aqueous vs. non-aqueous polymer dispersions). CNCs obtained by sulfuric acid hydrolysis exhibit high dispersibility and stability in water due to the presence of negatively charged sulfate groups on their surface. Therefore, aqueous CNC dispersions can be directly employed in the synthesis of CNC/latex via *in situ* emulsion polymerization techniques (polymerization of monomers in the presence of CNCs) and blending techniques (mixing a latex with an aqueous CNC dispersion).

Favier et al. [30] prepared the first composite latex with microcrystalline cellulose via blending technique. The mechanical measurements showed that the storage modulus of a styrene/butyl acrylate (35/65 % w/w) copolymer matrix was significantly improved with CNC loadings as low as 1 wt.%. Subsequent efforts using the same copolymer system investigated the effect of CNCs obtained from wheat straw [31,32] or tunicin [33]. The resulting nanocomposites displayed noticeably enhanced mechanical properties even at low CNC contents. Vatansever et al. [34] reported the synthesis of CNC reinforced poly (BA-co-MMA) via blending technique with different CNC content to a maximum of 3 wt%. The thermal, barrier, and mechanical properties (e.g., tensile strength) of the nanocomposites were enhanced with increasing CNC content. However, in none of the above cases was adhesive performance measured.

The synthesis of stable cellulose nanoparticle/latex dispersions was reported via miniemulsion polymerization by adding a reactive monomer, ϒ-methacryloxypropyl triethoxysilane (MPS), to the polymerization formulation [35,36]. It was reported that the addition of CNCs improved the storage modulus of nanocomposite films in the rubbery state. However, the perfectly homogeneous distribution of cellulose nanoparticles within nanocomposite films was not achieved after film formation. Most recently, nanocellulose fibres were added to a suspension polymerization of 2-ethyl hexyl acrylate for adhesive applications.

Up to date, there are no reports of emulsion polymerization of BA/MMA with CNCs. We hypothesized that CNC, as a nanofiller due to its high aspect ratio or as a crosslinker due to the presence of surface hydroxyl groups, can improve latex-based PSA performance.

1.1 Research objectives

We hypothesize that the addition of CNCs to a latex formulation will modify adhesive properties. The main objective of this research was to investigate the impact of CNCs on the adhesive properties of PSA films. We prepared the PSA films through both *in situ* emulsion polymerization and blending. In addition, we compared the adhesive performance of CNC/PSA films with that of PSA films containing a crosslinker and chain transfer agent. The synthesis of a colloidally stable CNC/latex dispersion as part of an *in situ* emulsion polymerization was the major challenge in this study. In order to achieve our goals, the following experiments were designed:

1. Modification of a standard *in situ* batch emulsion polymerization formulation and polymerization procedure to synthesize a stable CNC/latex and study the polymer properties of the ensuing CNC/latex.

2. Synthesis of CNC/PSA via *in situ* seeded semi-batch emulsion polymerization and evaluation of the adhesive performance of PSA nanocomposite films.
3. Evaluation of the adhesive performance of the PSA nanocomposite films via blending technique.
4. Study on the effect of CNC along with crosslinker and/or chain transfer agent on the PSA nanocomposite adhesive performance.

1.2 Thesis structure

This thesis was written in a journal article format and divided into five chapters. The second chapter provides literature review on "**Polymer Nanocomposites for Emulsion-based Coatings & Adhesives "** and will be submitted to Journal of Nanomaterials. The third chapter **"Synthesis of Poly (n-butyl acrylate/methyl methacrylate)/CNC Latex Nanocomposites via *in situ* Emulsion Polymerization"** was published online in Macromolecular Reaction Engineering Journal. doi/10.1002/mren.201700013. This chapter presents an effective approach for the synthesis of a stable CNC/latex nanocomposite through *in situ* emulsion polymerization. The fourth chapter **"Pressure Sensitive Adhesive Property Modification Using Cellulose Nanocrystals"** was submitted to International Journal of Adhesion and Adhesives. This chapter reports the preparation of PSA nanocomposite films via *in situ* seeded semi-batch emulsion polymerization and compares these to films produced via blending. We conclude in the final chapter with a summative discussion and provide recommendations for future work in this exciting area of research.

1.3 References

[1] Satas D. Handbook of Pressure Sensitive Adhesive Technology. 2nd ed. New York: Van Nostrand Reinhold; 1989.

[2] Benedek I. Pressure-Sensitive Adhesives and Applications. 2nd ed. New York: Marcel Dekker Inc; 2004.

[3] Kendall K. Molecular Adhesion and its Application. Kluwer Academic/ Plenum Publishers; 2001.

[4] Packham DE. Handbook of Adhesion Technology. Berlin: Springer Heidelberg Inc; 2011.

[5] Lovell, PA. ; El-Aasser MS. Emulsion Polymerization and Emulsion Polymers. New York: John Wiley & Sons, Chichester; 1997.

[6] Chern C-S. Principles and Applications of Emulsion Polymerization. New Jersey: John Wiley & Sons; 2008.

[7] Dubé MA, Penlidis A. A Systematic Approach to the Study of Multicomponent Polymerization Kinetics-the bytyl acrylate/methyl methacrylate/vinyl acetate Example: 1. Bulk Copolymerization. Polymer (Guildf) 1995;36:587–98.

[8] Zosel A. Shear Strength of Pressure Sensitive Adhesives and Its Correlation To Mechanical Properties. J Adhes 1994;44:1–16.

[9] Lakrout H, Sergot P, Creton C. Direct Observation of Cavitation and Fibrillation in a Probe Tack Experiment on Model Acrylic Pressure-Sensitive Adhesives. J Adhes 1999;69:307–59.

[10] Deplace F, Carelli C, Mariot S, Retsos H, Chateauminois A, Ouzineb K. Fine Tuning the Adhesive Properties of a Soft Nanostructured Adhesive with Rheological Measurements. J Adhes 2009;85:18–54.

[11] Tobing SD, Klein A. Molecular Parameters and Their Relation to the Adhesive Performance of Emulsion Acrylic Pressure-Sensitive Adhesives. II. Effect of Crosslinking. J Appl Polym Sci 2001;79:2558–64.

[12] Zosel A, Schuler B. The Influence of Surfactants on the Peel Strength of Water-Based Pressure Sensitive Adhesives. J Adhes 1999;70:179–95.

[13] Jovanović R, Ouzineb K, McKenna TF, Dubé MA. Butyl acrylate/methyl methacrylate Latexes: Adhesive Properties. Macromol Symp 2004;206:43–56.

[14] Fonseca GE, McKenna TF, Dubé MA. Miniemulsion vs. Conventional Emulsion Polymerization for Pressure-Sensitive Adhesives Production. Chem Eng Sci 2010;65:2797–810.

[15] Fonseca GE, McKenna TFL, Dubé MA. Effect of Bimodality on the Adhesive Properties of Pressure Sensitive Adhesives: Role of Bimodal Particle Size and Molecular Weight Distributions. Ind Eng Chem Res 2010;49:7303–12.

[16] Qie L, Dubé MA. Manipulation of Chain Transfer Agent and Cross-Linker Concentration to Modify Latex Micro-Structure for Pressure-Sensitive Adhesives. Eur Polym J 2010;46:1225-1236.

[17] Qie L, Dubé MA. Influence of Polymer Microstructure on the Performance of Post-Treated Latex-Based Pressure Sensitive Adhesives. J Appl Polym Sci 2012;124:349–64.

[18] Marquis DM, Guillaume É, Chivas-joly C. Properties of Nano Fillers in Polymer. Nanocomposites Polym with Anal Methods 2005:261-284.

[19] Hanemann T, Szabó DV. Polymer-nanoparticle Composites: From Synthesis to Modern Applications. Materials 2010;3:3468-35170.

[20] Wang T, Lei CH, Dalton AB, Creton C, Lin Y, Fernando KAS. Waterborne, Nanocomposite Pressure-Sensitive Adhesives with High Tack Energy, Optical Transparency, and Electrical Conductivity. Adv Mater 2006;18:2730–4.

[21] Kajtna J,Šebenik U. Microsphere Pressure Sensitive Adhesives-acrylic polymer/montmorillonite Clay Nanocomposite Materials. Int J Adhes Adhes 2009;29:543–50.

[22] Khalina M, Sanei M, Mobarakeh HS, Mahdavian AR. Preparation of Acrylic/silica Nanocomposites Latexes with Potential Application in Pressure Sensitive Adhesive. Int J Adhes Adhes 2015;58:21-27.

[23] Lee SW, Park JW, Park CH, Kwon YE, Kim HJ, Kim EA, et al. Optical Properties and UV-curing Behaviors of Optically Clear PSA-TiO_2 Nano-composites. Int J Adhes Adhes 2013;44:200–8.

[24] Habibi Y, Lucia LA, Rojas OJ. Cellulose Nanocrystals: Chemistry, Self-Assembly, and Applications. Chem Rev 2010;110:3479-3500.

[25] Samir MASA, Alloin AF, Dufresne A. Review of Recent Research into Cellulosic Whisker, Their Properties and Their Application in Nanocomposites Field. Biomacromolecules 2005;6:612–26.

[26] Beck-Candanedo S, Roman M, Gray DG. Effect of Reaction Conditions on the Properties and Behavior of Wood Cellulose Nanocrystal Suspensions. Biomacromolecules 2005.

[27] Moon RJ, Martini A, Nairn J, Simonsen J, Youngblood J. Cellulose Nanomaterials Review: Structure, Properties and Nanocomposites. Chem Soc Rev Chem Soc Rev 2011;40:3941–94.

[28] Roman M. Toxicity of Cellulose Nanocrystals: Review. Ind Biotechnol 2015;11:25-33.

[29] Dufresne A. Nanocellulose: From Nature to High Preformance Tailored Materials. Berlin: Walter de Gruyter GmbH; 2012.

[30] V. Favier, G. R. Canova JYC. Nanocomposite Materials form Latex and Cellulose Whiskers. Polym Adv Technol 1994;6:351–5.

[31] Helbert W, Cavaille JY, Dufresne A, Fourier UJ. Straw Cellulose Whiskers . Part I : Processing and Mechanical Behavior. Polym Compos 1996;17:604–11.

[32] Dufresne A, Cavaillé JY, Helbert W. Thermoplastic Nanocomposites Filled with Wheat Straw Cellulose Whisker. Part 11: Effect of Processing and Modeling. Polym Compos 1997;18:198–210.

[33] Hajji P, Cavaille JY, Favier V, Gauthier C, Vigier G. Tensile Behavior of Nanocomposites From Latex and Cellulose Whiskers. Polym Compos 1996;17:612–9.

[34] Vatansever A, Dogan H, Inan T, Sezer S, Sirkecioglu A. Properties of Na-Montmorillonite and Cellulose Nanocrystal Reinforced Poly(butyl acrylate-co-methyl methacrylate) Nanocomposites. Polym Eng Sci 2015;55:2922–8.

[35] Elmabrouk A Ben, Wim T, Dufresne A, Boufi S. Preparation of Poly(styrene-co-hexylacrylate)/cellulose Whiskers Nanocomposites via Miniemulsion Polymerization. J Appl Polym Sci 2009;114:2946-2955.

[36] Ben Mabrouk A, Kaddami H, Magnin A, Belgacem MN, Dufresne A, Boufi S. Preparation of Nanocomposite Dispersions Based on Cellulose Whiskers and Acrylic Copolymer by Miniemulsion Polymerization: Effect of the Silane Content. Polym Eng Sci 2011;51:62–70.

Chapter 2:

Nanocomposite Emulsion-based Coatings & Adhesives

Polymer Nanocomposites for Emulsion-Based Coatings and Adhesives: A Literature Review

2.1 Introduction

Polymer composites are composed of two distinct phases: a polymer matrix phase and a dispersed phase [1]. The polymer matrix phase is the primary or continuous phase while the dispersed phase is embedded in the matrix in a discontinuous manner. The properties of polymer composites are usually noticeably different from those of its constituent phases. Polymer composites can be designed and manufactured to offer various properties for specific applications. The use of composite materials to resolve technological problems was considered long ago, but in the early 1960s, polymer composites started capturing the attention of industry [2]. Nowadays, composite materials are widely used in in the fabrication of a variety of products ranging from aircraft parts, spacecraft parts, sporting goods, automobile parts, and structural components due to the relative ease in their manufacturing process (low temperature and pressure), their lightness, and their low raw material and fabrication costs [3]. Three classes of polymers, namely thermosets, thermoplastics, and rubbers, are used as the matrix phase; and fillers, mostly fibers and particulates, are used as the dispersed phase in polymer composites. The addition of fibers or particulates to the polymer matrix often improves, for example, stiffness, creep resistance, and fracture toughness. It has been established that the size, shape, aspect ratio, and distribution of the dispersed particles; and the state of the interface between the particles and polymer matrix greatly affect the macroscopic behaviour of polymer composites [4]. In recent decades, polymer composites have been the material of choice for many engineering applications but the

optimization of their performance in some applications still remains a challenge. For instance, in some applications, the use of large amounts of filler in the polymer matrix is required to provide significant improvements in composite properties which may lead to unfavourable properties such as brittleness and opacity [5].

The transition from microscale to nanoscale materials often induces dramatic changes in physical properties [6]. Nanostructured materials are materials with at least one dimension (diameter or thickness) in the range of 1-100 nm. Nanomaterials can be categorized based on their geometries including spheres (e.g., nano-SiO_2, nano-TiO_2), layered (e.g., nanolayered silicate), fibrous materials (e.g., carbon nanotubes, nanofibers), and rods (e.g., cellulose nanocrystals) [7]. They have a very large surface area for a given volume and high aspect ratio in the case of layered and fibrous geometries [6]. Therefore, due to the fact that surface properties are primary determinants in many important chemical and physical interactions [7], nanoscale materials possess noticeably different properties from their microscale counterparts. The use of nanomaterials to alter polymer properties is not a new idea. In the early 1990s, Toyota Central Research Laboratories in Japan reported on a nylon-6 polymer matrix filled with nano-clay, which they called "hybrid" material [8]. It was shown that a very small amount of nano-clay loading resulted in a pronounced improvement in thermal and mechanical properties. The term "nanocomposites" was introduced for the first time in 1994 [9–11]. Afterwards, researchers began investigating the use of different nanomaterials and searching for new applications. In general, nanomaterials can noticeably enhance a broad range of polymer properties such as mechanical, thermal, barrier, scratch/abrasion resistant, fire-retardant, optical, magnetic, and electrical properties compared to conventional fillers [12]. In particular, nanomaterials with high aspect

ratios have the greatest impact on mechanical properties while spherical nanomaterials are best for the improvement of other properties such as barrier, thermal, or optical properties [6,13].

Not surprisingly, polymer nanocomposites have been in increasing demand for many manufactured products. Polymer nanocomposites can be manufactured using the same fabrication process utilized for polymer composites. In addition, only a very small amount of nanomaterial is required to achieve significant property modification. Furthermore, advancements in characterization tools have facilitated the modification of the nanomaterials' surfaces to improve nanomaterial compatibility with the polymer matrix. Therefore, the list of available nanomaterials is expanding rapidly and new engineering applications for these nanocomposites are being developed at a rapid pace [7].

One concern with nanocomposite materials relates to their environmental impact. The production of polymers brings many potential workplace and environmental hazards as does the use of nanomaterials. Efforts towards safer, more sustainable polymer production processes may lead to the use of nanocomposite materials for their energy benefits (e.g., high strength lightweight materials) among others [14]. As for polymer production, one can look at emulsion-based (i.e., water-based) processes for a more sustainable approach [15]. In this review, we will focus on the use of nanomaterials in emulsion-based clearcoats, paints, and adhesive applications.

Clearcoats are commonly used as topcoats in automobile, wood flooring, wood furniture, facades and optical plastic applications [16]. Coatings and paints must usually possess gloss, high adhesion, surface hardness, water-resistance, flame resistance as well as flexibility. Adhesives are substances with capability of holding at least two surfaces together for temporary or permanent applications. There are different classes of adhesives, namely structural adhesives, instant adhesives with industrial applications, and pressure sensitive adhesives (PSAs) with applications

in consumer products such as labels, note pads, and tapes [17,18]. Adhesives must be able to form a bond even on a rough surface and then withstand a minimum level of stress upon debonding [18]. PSAs differ from the other adhesives as they typically stick to the surface upon contact without any required force, chemical reaction, or UV irradiation [17]. Emulsion-based coatings, paints, and adhesives are becoming increasingly commercially important due to the use of water as a synthesis medium instead of organic solvents. Although they are more environmentally friendly, emulsion-based products often need property enhancement in order to broaden their applications and compete with their counterparts manufactured using more hazardous techniques. For instance, solvent-based coatings have better gloss and hardness as opposed to emulsion-based coatings due to their curing mechanism in which the oil reacts with atmospheric oxygen to form very hard crosslinked materials while in emulsion-based coatings, soft films form upon the evaporation of water [19]. Another example is the case of solvent-based PSAs, which have better cohesive strength as they more easily form a continuous gel network compared to the discrete microgels formed in emulsion-based PSAs [20]. As mentioned earlier, the use of nanomaterials is a promising way to enhance or alter the polymer matrix properties.

2.2 Nanocomposite synthesis

To incorporate nanomaterials into polymer matrices, different techniques depending on the nature of the nanomaterial and of the polymer matrix can be utilized. In general, these techniques include template synthesis, melt compounding, *in situ* polymerization, and mixing (blending) [21]. For the template synthesis method, nanomaterials, mostly inorganic nanoparticles, are synthesized simultaneously with the polymer matrix. Because the synthesis of nanoparticles occurs during polymerization, nanoparticle aggregation is reduced. However, the technique is limited because of

the high temperatures usually necessary for nanoparticle production (>130 ^{o}C). The melt compounding technique is commonly used in commercial nanocomposite production. The polymer is melted at high temperature and then mixed with nanoparticles under shear stress. Careful attention to the choice of an appropriate temperature is required to obtain a polymer melt at an optimum viscosity to withstand the shear forces from the compounder as well as to prevent degradation of the polymer and nanoparticles during synthesis. *In situ* polymerization differs from the template synthesis method by the fact that the nanoparticles are prepared *a priori*. Polymerization processes such as dispersion, suspension, emulsion, miniemulsion, and Pickering emulsion have been used. Essentially, in this technique the polymerization of monomers occurs in the presence of the nanomaterial. Except for the dispersion polymerization technique, which uses a solvent as reaction medium, the other polymerization techniques are water-based and present a less hazardous process. Finally, the mixing or blending technique involves mixing of prepared polymers and nanomaterials. In some cases the polymer can be in the form of a suspended latex (i.e., a colloidal dispersion of polymer particles in water) or dissolved in a solvent (i.e., aqueous or non-aqueous depending on the polymer solubility). The blending technique often involves low-shear mixing but in some cases, high shear mixing or sonication are required to improve nanomaterial dispersion in the polymer matrix [22]. Further details on the water-based latex process are provided below.

2.3 Nanoparticle agglomeration

The aggregation and dispersion of nanomaterials are crucial in nanocomposite synthesis as they have influence on the nanocomposite properties [7]. Nanoparticle agglomerates act as defects resulting in a reduction in nanocomposite performance. The agglomeration of particles is intrinsic,

especially in nanoscale processing due to their large surface area and very strong van der Waals interactions [23]. Therefore, the preparation of a homogeneous dispersion remains an important technical challenge. Depending on the synthesis conditions and the surface chemistry, the nanoparticles tend to form soft or hard agglomerates [23]. Hard agglomerates consist of smaller particles which are fused together and form one larger solid particle. These large particles can be destroyed only by high energy milling. Soft agglomerates are accumulations of isolated particles which are connected to each other by attractive physical interactions like van der Waals or hydrogen bridge forces. Soft agglomerates can be disrupted into smaller particles by shear forces generating mechanical stress gradients. Interparticle interactions depend mainly on the particle surface chemistry, the shape, aspect ratio, interparticle distance and the polydispersity [24]. In nanocomposite processes, the main goal is to achieve an interaction between the nanoparticle and the polymer matrix at the nanometric scale. In other words, the nanoparticles should be well-dispersed in the polymer matrix and each nanoparticle should be wetted by the polymer. The inherent incompatibility of hydrophilic nanoparticles with the usually hydrophobic polymer chains is a major challenge to the formation of a strong interfacial polymer –nanoparticle interaction. To overcome this issue, compatibilizers and/or surface treatments can be used to lower the surface energy of the nanoparticles.

2.4 Surface modification

A variety of surface modification techniques can be used to compatibilize the nanoparticles and polymer matrix while keeping bulk material properties more or less intact [25]. Material surfaces (either the nanoparticle, the polymer or both) can be modified and tuned by using physical interactions, adsorption of molecules onto their surface (e.g., surface-active agents), or by using a

chemical treatment [26,27]. The chemical approach involves chemical attachment of polymer (or oligomer) chains to the nanoparticle surface through covalent bonds. For instance, silane coupling agents (i.e., silicon-containing molecules covalently attached to the particle surface) are used to functionalize the surfaces of silicon, aluminum, and titanium. Silane coupling agents may also contain reactive groups that can copolymerize with the monomers. Chemical surface modification, called surface-grafting, consists of two separate steps: activation of the surface followed by grafting. There are two different grafting strategies, namely grafting-from (surface-initiated polymerization) and grafting-to.

2.4.1 Grating-from technique

In the grafting-from technique, an initiator is immobilized on the surface and followed by *in situ* surface-initiated polymerization with monomer [25]. Initiators such as azo-bis-isobutyronitrile [28], and phenyl pyrenyl methyl groups can be immobilized onto surfaces and then radicals formed by oxidizing agents [29,30], ozone [31], and energy sources (e.g., heat, uv light) [32–34]. A variety of *in situ* surface-initiated polymerization reactions can be employed such as radical, controlled radical, carbocationic, anionic, and ring-opening polymerization [35,36]. The chain length and chain density play an important role in tuning the surface chemistry of grafted-polymer. Attempts have been made to improve the control over graft density and chain length. For example, in the atom transfer radical polymerization (ATRP) grafted-from technique, the graft density can be controlled by adding "dummy initiators" containing the same anchoring groups as the initiator but lacking the ability of initiation of the polymerization [37]. The chain length can be controlled by adjusting the rate of termination in polymerization reaction through the use of sacrificial initiator molecules [38].

2.4.2 Grafting-to method

In the grafting-to method, an end-functionalized polymer is synthesized and subsequently adsorbed onto a substrate to form a chemical bond (i.e., chemisorption) [25]. Different polymerization techniques can be employed to synthesize end-functionalized polymers [39–41]. In this technique, the synthesized polymers can be characterized prior to grafting whereas characterization is not straightforward in the grafting-from method. However, grafting-to methods are limited to low grafting densities due to the steric hindrance imposed by the grafted chains. In the grafting-to strategy, high graft chain density can be obtained using self-assembled monolayers (SAMs) [42,43]. SAMs can form spontaneously ordered molecular assemblies onto a substrate. They consist of three main components: the head group, the functional group and the assembling structure. The head group must have a high affinity for the graftable substrate. For instance, head groups containing silanes are appropriate for polymer, and alumina substrates. Head groups with alcohols are used for iron oxide and silicon substrates.

Although the surface modification methods discussed above are useful to design interfaces with a level of control over graft density and chain length, understanding which interface structures are optimal for achieving specific composite properties is still a challenge [25].

2.5 Nanomaterials

2.5.1 Nano-ZnO particles

Nano-ZnO particles are multifunctional inorganic nanoparticles with high luminous transmittance, intensive ultraviolet and infrared absorption. They can be added to polymers to improve heat resistance, and mechanical and optical properties for coating applications [44] . The blend synthesis of poly(styrene-co-butyl acrylate) (poly(Sty/BA)) latex/ZnO nanocomposites was studied for the influence of dispersant type, nanoparticle loadings, nanoparticle size, and dispersing

time on the mechanical, ultraviolet (UV) and near infrared (NIR) shielding properties of the resulting nanocomposites. Three different nano-ZnO particle sizes were studied with mean size of 60 nm (specific area of 30 m^2/g), 100 nm (specific area of 10 m^2/g) and 1 micron at nanoparticle loadings from 3 to 9% (based on polymer weight). The effect of two dispersants, one an ultra-high molecular weight block copolymer with a strong anionic group, and the other, sodium polyacrylate, on the dispersibility of nano-ZnO particles in water was also investigated. The nano-ZnO particles were dispersed in water via ball milling for 4 h. Transmission Electron Microscopy (TEM) micrographs showed that the anionic dispersant resulted in almost complete dispersion of the ZnO nanoparticles to their original size while use of the sodium polyacrylate resulted in significant agglomerates in a non-homogeneous dispersion. This behaviour was attributed to the fact that dispersants with long chains and strong affinity groups improve the dispersibility of nano-ZnO particles due to their steric and static stabilization effects. Agglomeration increased with nano-ZnO loading and particle size. Not surprisingly, increasing the dispersion time from 0.5 to 4 h yielded better homogeneity of the nanoparticle dispersion in the polymer matrices. The tensile strength, and UV and NIR shielding properties of the nanocomposites increased with nano-ZnO loading while the elongation at break did not change significantly. The glass transition temperature (T_g) was also shown to vary with nanoparticle content. The composite polymers with micro-ZnO particles had a lower tensile strength compared to their nano-sized counterparts although the nanocomposites with 100 nm ZnO exhibited higher tensile strength than those containing 60 nm ZnO. The latter could be related to the surface properties of the nanoparticles. FTIR analysis revealed that 100 nm ZnO particles had more OH groups at their surface, leading to stronger interfacial interaction between the nanoparticles and the polymer matrix in comparison to the 60

nm ZnO particles. This indicates that not only size will affect properties but also the surface group interactions should be considered.

The nanocomposites containing 60 nm ZnO particles had better UV shielding properties than those of 100 nm ZnO while the polymer matrices containing micro ZnO had no influence. It was concluded that the more homogeneous nanocomposites had improved scattering and absorbance of UV rays and lower transmittance of UV light, which led to higher absorbance intensity at 365 nm (a blue-shift). Consequently, the nanocomposite coatings were less transparent. The ZnO particle size had no effect on NIR absorbance and transmittance.

Dhoke et al. [45] investigated the effect of nano-ZnO content on the mechanical and heat resistant properties of silicon-modified alkyd-based waterborne coatings subjected to high temperatures for industrial applications. A series of nano-ZnO/silicone-modified alkyd-based waterborne coatings with different nanoparticle loadings (0.05, 0.1, 0.2 and 0.3% based on polymer weight) was synthesized via blending technique. The coatings were blended with nano-ZnO particles with an average size of less than 40 nm and specific area of 29 m^2g^{-1} at several concentrations. The resulting nanocomposites were dip-coated on pretreated cold rolled mild steel panels. The coated panels were cured in an oven at 130 ^oC for 30 min and cooled to room temperature prior to characterization using Fourier Transform Infrared (FTIR) spectroscopy and Differential Scanning Calorimetry (DSC). The FTIR analysis revealed that the peak at 825.7 cm^{-1}, characteristic of Si-O-CH_3, disappeared and a new peak at 897.8 cm^{-1} was formed indicating the complete interaction between the hydrolyzed ZnO nanoparticle surfaces and silicone-modified alkyds. The DSC thermogram of neat and ZnO based coatings indicated that the curing temperature (ΔT_{curing}) of nanocomposite coatings decreases and the heat of curing (ΔH_{curing}) increases compared to that of the neat coating. This observation suggests that the interaction between nano-ZnO and

polymer improves the curing of coatings. The authors noted that the residual crosslinking enthalpy decreased with increasing nano-ZnO concentration suggesting that crosslinking increased. The increased crosslinking also reduced the amount of volume defects and cavities in the nanocomposite, as confirmed by scanning electron microscopy (SEM). The addition of nano-ZnO imparted higher abrasion resistance and resistance to scratching, likely because of the degree of interaction between the nanoparticles and the polymer matrix.

In summary, the addition of nano-ZnO particles to polymers for coatings applications imparts a wide range of interesting properties. These include mechanical and heat-resistance properties, scratch and abrasion resistance, and UV shielding. The use of a dispersant was also shown to help make a homogeneous nanocomposite. Nano-ZnO composite coatings can find application in various automotive industries, smoke stacks, stoves, furnaces, heaters and incinerators, and other instances where exposure to high temperature is a concern.

2.5.2 Nano-TiO_2 particles

Titanium dioxide (TiO_2) pigments are usually employed in paints, inks, and paper to provide opacity and whiteness [46]. TiO_2 pigments have a high refractive index (2.55-2.76), hence they are able to reflect, refract, or scatter light more efficiently than many other pigments. They have a high UV absorption which improves the durability of TiO_2-based paints or coatings for exterior applications. In addition, they are inherently nontoxic and can be applied in a wide range of products without health and safety concerns. He et al. [47] and Zhou et al. [48], synthesized a series of poly (BA-co-methyl methacrylate (MMA))/nano-TiO_2 composite latexes via high shear mixing (SM), ball milling mixing (BM), and *in situ* polymerization (IS) techniques. They used nano-TiO2 with a mean size of 40 nm and micro-TiO_2 with a mean size of 0.22 μm. With the SM

method, the nanoparticles were dispersed into water via high-shear stirring at 2000 rpm for 1 h followed by ultrasonic irradiation for 0.5 h to obtain a water dispersion of nano-TiO_2 particles. For the BM method, the nanoparticles were dispersed into water via ball milling for 1 h, followed by ultrasonication for 0.5 h. The aqueous nano-TiO_2 dispersions obtained from the SM and BM methods were blended with prepared acrylic latexes. For the IS method, a particle seed stage was used without TiO_2, followed by a batch feed of the remaining components including monomer, water, emulsifier, and initiator, pre-emulsified with nano-TiO_2 particles. The three synthesis methods were compared at a 3% nano-TiO_2 content and the SM method was selected for further study at nanoparticle loadings of 3, 5, 7, and 9 wt% (based on polymer).

According to TEM, the nano-TiO_2 latex obtained from the IS technique had the best nanoparticle dispersion but surprisingly, the coatings prepared from the IS technique had the lowest tensile strength. In fact, even the tensile strength of the IS nanocomposite was lower than the base acrylic coating without filler or blended with micro-TiO_2. This observation was attributed to effects on the polymerization kinetics due to the presence of the TiO_2. The nanocomposite prepared according to the SM method showed the highest tensile strength. Increases in tensile strength were noted up to a loading of 7% TiO_2, but decreased at 9% loading. These observations were consistent with TEM results, which showed the presence of TiO_2 agglomerates at 9% loading. UV-VIS absorbance and transmittance were highly dependent on dispersion. As a result, the IS technique provided the highest UV absorbance and the lowest UV transmittance among the three techniques.

Stable poly(BA/MMA) core/nano-TiO_2-shell latexes have also been synthesized through *in situ* emulsion polymerization for coating applications [49]. A detailed process was described though the mechanical and thermal properties of the nanocomposite coatings were not reported.

Cetyl trimethyl ammonium bromide (CTAB), a cationic surfactant, was used in all polymerizations with different initiator types from anionic, to non-ionic and cationic ones. Their *in situ* polymerization containing an anionic initiator (ammonium persulfate, APS) proved most effective to maintain the nanocomposite latex stability in face of the negatively charged nano-TiO_2 particles.

To improve the mechanical properties of nano-TiO_2 latex composite coatings without diminishing their optical properties, the nanoparticles must be very well-dispersed. Although the preparation of stable nano-TiO_2/latexes via blending or *in situ* polymerization has been reported, achieving the right balance between the mechanical and optical properties remains a challenge. Furthermore, in most studies, mechanical property measurements were limited to a narrow range of measurement types. A more complete evaluation of the effect of nano-TiO_2 on other coatings properties such as scratch/abrasion resistance, adhesion strength, and solvent resistant are needed.

2.5.3 Nano-Al_2O_3 particles

Nano-aluminum oxide (nano-Al_2O_3) particles are used in many industrial products such as abrasive agents, insulators, and coatings due to their high hardness (hardness on Mohs's scale is 9). They are mostly employed to modify coatings to improve scratch and abrasion properties [50].

Polyurethane acrylates (PUA) are used as basic building blocks in UV-waterborne applications due to their excellent properties such as adhesion on substrates, flexibility, and durability. Sow et al. [51] investigated the effect of nano-Al_2O_3 on mechanical, optical, and thermal properties of UV-waterborne nanocomposite coatings. Al_2O_3 nanoparticles with a particle size of 13 nm and a specific surface area of 100 m^2/g were dispersed directly into a PUA resin at loadings of 1, 3, and 5 wt%, and then mixed under high shear for 20 min. The resulting nanocomposite coatings were applied to sugar maple wood as a substrate. The addition of nano-

Al_2O_3 decreased the gloss and hardness of the coatings due to nanoparticle aggregation as confirmed by TEM micrographs. Nanoparticle aggregation was a result of the nano-Al_2O_3 surface hydroxyl groups, which make their dispersion difficult in non-aqueous media. The aggregates increased the surface roughness of nanocomposites and consequently decreased hardness and gloss. The inclusion of nano-Al_2O_3 improved the scratch resistance but did not significantly improve adhesion strength.

Emulsion-based poly(vinyl acetate) poly(VAc) is used as an adhesive in the wood industry. The addition of well-dispersed nano-Al_2O_3 particles to a poly(VAc) matrix can significantly improve the bonding strength of water-based poly(VAc) in dry and wet conditions as well as at elevated temperatures [50]. Using nano-Al_2O_3 contents ranging from 1 to 4 wt% in water via ultrasonication, nanocomposite blends with a poly(VAc) matrix were prepared. Increasing the nanoparticle loading enhanced the mechanical properties of poly(VAc) adhesive. At 4 wt% loading, the nano-Al_2O_3 particles could not be well-dispersed and consequently, the agglomerated particles lowered the adhesive bond strength. The thermal stability of the poly(VAc) matrix was positively affected by the inclusion of nano-Al_2O_3 loading. The poly(VAc) nanocomposite latexes showed greater stability and provided an improved barrier to water loss compared to the base poly(VAc) coating.

As noted above, a good dispersion of nano-Al_2O_3 particles in a polymer matrix is highly dependent on the nanocomposite processing method (direct addition of nano-Al_2O_3 powder into coating dispersion or blending of aqueous nano-Al_2O_3 dispersions with latex) as well as its loading in the polymer matrix.

2.5.4 Nano-SiO_2 particles

The inclusion of nano silica (nano-SiO_2) into a polymer matrix can enhance thermal and mechanical properties of a polymer where transparency is a basic requirement. Nano-SiO_2 particles, with a hardness of 7 on Mohs's scale, can be employed in coatings to improve their abrasion and scratch resistance. Xiong et al. [52] investigated the synthesis of acrylic/nano-SiO_2 composite latexes through *in situ* seeded emulsion polymerization and blending techniques (high shear mixing (SS) and ball milling (BM)). They used nano-SiO_2 with a mean size of 20 nm and specific area of 640 m^2g^{-1} in a poly(BA-co-Sty) (53:39 w:w) polymer matrix. The standard polymerization formulation with an anionic/non-ionic emulsifier mixture along with glycidyl methacrylate (GMA), as a functional monomer, also was used. The blend methods used were the same as He et al.[47], and described in the nano-TiO_2 section. For their *in situ* technique, after completion of the polymerization seed stage, the remaining monomer charge was pre-emulsified in the presence of nano-SiO_2 particles and fed to the reaction vessel. The high shear blending method proved better than the *in situ* technique and other blend techniques. Agglomerates in the nanocomposites decreased both tensile strength and elongation at break; those from the *in situ* technique displayed poorer mechanical properties than the base latex. Nano-SiO_2 loadings beyond 3 wt% resulted in decreasing mechanical properties. Up to 3 wt%, a homogeneous dispersion of nano-SiO_2 in the polymer led to strong interfacial interactions between the nanoparticles and the polymer. In addition, optical property measurements revealed that the nano-SiO_2 composites provided a barrier to UV light whereas micro-silica composites did not.

One-pot synthesis of acrylate polymer/silica nanocomposite particles with high silica encapsulation efficiency through miniemulsion polymerization was reported by [53]. Commercial MMA/nano-SiO_2 and BA/nano-SiO_2 dispersions were used in this study. Surface modification of

the nano-SiO_2 particles was performed using a coupling agent, 3-(trimethoxysilyl) propyl methacrylate (MPS) prior to polymerization. A monomer mixture containing MMA:BA 3:1 (w/w) with standard miniemulsion polymerization reagents was used. The surface modification led to an improved encapsulation efficiency (up to 95%) and degree of grafting of polymer onto the nano-SiO_2.

Mizutani et al. [54,55] prepared nano-SiO_2/poly(BA:MMA, 65:35 w/w) latexes via blending and *in situ* emulsion polymerization techniques for wall paint applications. They used nano-SiO_2 with a diameter of 20-30 nm. The resulting paint films were evaluated for gloss, surface hardness, adhesion and solvent resistance. For the *in situ* technique, prior to polymerization, an aqueous mixture containing initiator and reactive non-ionic surfactant (poly(ethylene oxide)) was added dropwise to a nano-SiO_2 aqueous dispersion with vigorous stirring at 60 ^oC. Next, the seed stage monomer mixture was added dropwise to the reaction mixture. This was followed by the usual semi-batch polymerization procedure. In this case, a substantial loading (50 wt% based on polymer) of nano-SiO_2 was used to prepare each nanocomposite for each technique. For the *in situ* technique, a core-shell structure for the nano-SiO_2 latexes was obtained. The resulting paint films were superior to that from the blending technique in terms of gloss, solvent resistance, and water resistance, while the surface hardness of the paint films were inferior to that of the blended films. These differences could be explained by the latex shells covering the nano-SiO_2 cores for the *in situ* case. However, the neat paint films (without nano-SiO_2) displayed higher gloss and surface hardness than the nanocomposite films prepared via the *in situ* technique. Furthermore, the nano-SiO_2 composite paints showed lower adhesion compared to the neat paint film as their lower organic content weakened the film's adhesion power. However, some reduction in adhesion is acceptable as it can be modified by adding an appropriate primer (undercoat).

Sow et al. [51] demonstrated the effect of surface-modified nano-SiO_2 particles on the mechanical, optical, and thermal properties of UV-waterborne nanocomposite coatings. Hydrophobic fumed nano-SiO_2 (surface-modified by methacryloxypropyl groups) with a particle size of 12 nm and a specific surface area of 150 m^2/g was dispersed into polyurethane acrylate resins at loadings of 1, 3, and 5 wt%, then mixed at high shear for 20 min. The resulting nanocomposite coatings were applied on sugar maple wood as substrate. The addition of surface-modified nano-SiO_2 decreased the coating hardness, which was attributed to nanoparticle aggregation. On the other hand, the inclusion of surface-modified nano-SiO_2 significantly increased scratch resistance and adhesion strength even at low loadings (1 wt%). These coatings were compared to nano-Al_2O_3 coatings. The surface-modified nano-SiO_2 composite coatings were superior in terms of scratch resistance and adhesion strength, while inferior in terms of gloss. Due to their excellent scratch resistance and high adhesion strength, these nano-SiO_2 coatings could be used for wooden furniture and kitchen cabinets.

Zhang et al., [56] reported the synthesis of poly(Sty–BA–acrylic acid (AA))/SiO_2 using different polymerizable emulsifiers such as hydroxypropyl methacrylate sodium sulfate (HPMAS), sodium vinyl sulfate, and vinyl alkylphenol polyether sulfates (NRS-10), in the presence of nano-SiO_2 particles. They employed seeded semi-continuous emulsion polymerization. The mechanical properties of the nanocomposite films at nano-SiO_2 contents from 1 to 10 wt% were evaluated. Nano-SiO_2 dispersions with a mean particle size of 96 nm were added to the reaction mixture at the seed stage along with a pre-emulsified monomer mixture. The emulsions prepared from a mixture of two polymerizable emulsifiers NRS-10 and HPMAS (1:1, w/w) yielded high monomer conversions, low coagulum, and small particle sizes. The nano-SiO_2 particles displayed some surface activity during the polymerization and led to increased monomer

conversion in most cases. The nanocomposite films prepared at 2 wt% nano-SiO_2 (based on monomer) demonstrated remarkable hardness and adhesion, whereas gloss and water resistance were slightly diminished. Overall, increasing nano-SiO_2 loading showed little influence on coating properties.

Wang et al. [57] reported the use of surface-modified nano-SiO_2 in the synthesis of poly(n-BA-co-AA, 97:3 w/w) nanocomposites for PSA applications. Semi-batch emulsion polymerization was used to prepare latexes with a core-shell structure. Prior to polymerization, the nano-SiO_2 particles were functionalized with MPS and pre-emulsified under vigorous stirring and sonication for 1 h. They were then added to the reactor with the initiator solution at the seed stage and followed by a typical emulsion polymerization procedure. The MPS-functionalized nano-SiO_2 particles (6 wt% based on polymer) were added as particle cores and compared to cases with the same poly(BA-co-AA) shell but with poly(BA) and poly(MMA) cores. The inclusion of the MPS-nano-SiO_2 in the polymer matrix improved thermal stability and storage modulus of the resulting PSAs. The shear strength of the nano-SiO_2 PSA films were a factor of five higher than those with the acrylic cores. The nano-SiO_2/PSA films also yielded tack between that of the poly(BA) cored and poly(MMA) cored PSA films. However, the peel strength of the nano-SiO_2 PSA films was inferior to the others. Thus, an improved shear strength was achieved at the cost of diminishing peel strength, which is a typical conundrum faced in emulsion-based PSA formulations.

The synthesis of nano-SiO_2/poly(EHA/AA/MMA) nanocomposites via miniemulsion polymerization was reported by [58] for PSA applications. A standard miniemulsion polymerization formulation and procedure were employed to prepare nano-SiO_2/latexes. Nano-SiO_2 dispersions with a mean particle size of 12 nm at concentrations from 0 to 4 wt% (based on

total monomer) were used. The nano-SiO_2 particles reportedly were mostly incorporated in the polymer particles with the majority located in the particle shells due to their hydrophilic nature. The elastic and loss modulus as well as the latex viscosity increased with nano-SiO_2 content. Increases in tack of 250 and 300% were achieved for nano-SiO_2 loadings of 2 and 4 wt%, respectively. The nanocomposite films at 4 wt% nano-SiO_2 loading, displayed the highest shear strength whereas their peel strength was the lowest among all samples.

The use of soft polymer-silica nanocomposites as nanofiller in PSAs was investigated by [59]. Colloidal aqueous dispersions of poly(BA)/nano-SiO_2 silica (with 40 wt% nano-SiO_2), were synthesized through *in situ* free radical polymerization and poly(N-vinyl pyrrolidone) colloidal stabilizer, PNVP, using a cationic radical initiator. Latex particles with a soft core-hard shell structure were obtained. PSA films also were prepared from blends of the nanocomposite particles and poly(BA) homopolymer particles at various weight ratios. Probe tack tests resulted in tack adhesion improvements up to 2.36 times and adhesion energy improvement up to 1.39 times compared to neat poly(BA) homopolymer films. The nano-scale mechanical deformation and energy dissipation ability of the 'soft-hard' nanocomposite particles was expected to increase adhesion energy.

Czech et al. [60] studied the effect of amorphous silica nanoparticles on the adhesive properties of commercial PSAs. Amorphous nano-SiO_2 particles were mixed at concentrations between 1 and 5 wt% with commercial PSAs at 7000 rpm for 15 min. It was found that the addition of amorphous nano-SiO_2 particles had a negative influence on tack even at 1 wt% while the shear strength increased significantly with nano-SiO_2 content. The peel strength increased at 1 wt% nano-SiO_2 loading but decreased sharply at higher nanoparticle contents.

In summary, in most cases the inclusion of nano-SiO_2 improved adhesion strength in coatings and shear strength in PSAs. However, coating and adhesive properties such as surface hardness and gloss for coatings and peel strength and tack for adhesives, were not improved.

2.5.5 Nanoplatelet fillers

Nano-clays are layered alumino-silicates bound by ions [61]. They possess a naturally closed structure. In order to enhance mechanical, thermal and barrier properties, as well as fire resistance [62,63], their structure must be altered to an intercalated or exfoliated form throughout nanocomposite processing. Intercalated nanocomposites are generally obtained via *in situ* polymerization in which a nano-clay treatment or the use of a monomer is required. Exfoliated nanocomposites can be achieved via blending. The final structures of clay nanocomposites have wide ranges of variations, depending on the degree of intercalation and exfoliation. However, exfoliated nanocomposites exhibit superior improvements compared to intercalated nanocomposites. The organically modified montmorillonite (OMMT) and natural sodium montmorillonite (Na-MMT) clays can be employed in emulsion polymerization to prepare nanocomposites. Although Na-MMT clays are easy to disperse in water due to their highly hydrophilic nature, their insufficient interaction with hydrophobic polymer tends to form an intercalated structure [62,64,65]. However, the synthesis of stable Na-MMT clay/poly(acrylate) latexes through seeded emulsion polymerization was reported by Yilmaz et al. [66], and the resulting nanocomposites displayed a mostly exfoliated structure. The use of OMMT clays in emulsion polymerization can be beneficial when the stability of the latex is not important for the final application. OMMT clays may not be the best choice for preparation of nanocomposites for coating and adhesive applications as the stability of the latex in direct usage is crucial. Therefore,

the use of lightly modified clay [67,68] or the preparation of nanocomposites via miniemulsion polymerization [69] can be used to overcome the stability issues.

Yilmaz et al. [67] synthesized stable OMMT/poly(BA-co-MMA) latexes as aqueous binders for leather coatings. The inclusion of OMMT in poly(acrylate) matrices resulted in an improved surface properties of the leathers compared to the base latex. Diaconu et al. [69] synthesized stable and partially exfoliated poly(MMA-co-BA)/clay nanocomposites via miniemulsion polymerization. The resulting nanocomposites demonstrated remarkable improvement in storage modulus, mild improvement in tensile strength and a loss in elongation at break compared to the base polymer. The thermal stability of the nanocomposites was also improved and the flammability decreased. Nanocomposite preparations via blending led to unstable clay/latexes due to aggregation of the clays. Subsequently, Diaconu et al. [70] reported the preparation of poly(MMA-co-BA)/Na-MMT clay nanocomposites through seeded semi-batch emulsion polymerization. As expected, the inclusion of Na-MMT clay in the formulation resulted in substantial improvement in mechanical and thermal properties. Blends using these compounds resulted in similar property improvement except for a significant reduction in elongation at break. Vatansever et al. [71] explored the same system using identical conditions except that they heated the blended Na-MMT/latex at 60 ^{o}C for 1h while stirring at 500 rpm. For both techniques, the addition of Na-MMT in the polymer matrix resulted in an enhancement of tensile strength and elongation at break (87 and 800%, respectively). At the same time, the elastic modulus of the nanocomposite films was reduced by 45% compared to that of the base film. The thermal property of the nanocomposite films was slightly improved with the addition of Na-MMT. Moreover, there was little difference in mechanical and thermal properties of the nanocomposite films prepared via the in situ polymerization technique and the blending technique.

The use of Na-MMT clay as a nanofiller in emulsion-based poly(BA/MMA) PSAs was reported by Li et al. [72]. The clay (0-5 wt% based on monomer) along with a small amount of sodium diphosphate (SDP) were dispersed in water and sonicated to obtain a stable aqueous clay dispersion. Polar co-monomers such as AA and 2-acrylamido-2-methyl-1-propane sulfonic acid (AMPS) were also employed in the polymerization formulation as it was assumed that strong interaction of carboxyl and amido moieties with MMT might make the polymer end-tethered on silicate layers [73–75]. It was expected that the ionic monomer, AMPS, could further separate the clay layers and facilitate insertion of monomers [73,76,77]. It was revealed that both intercalated and exfoliated structures of MMT co-existed in the nanocomposites. Substantial improvements in storage modulus and cohesive strength were achieved by incorporation of MMT. Tack did not change with increasing MMT loading whereas peel strength slightly decreased. A 3 wt% MMT loading was considered optimal to achieve a good balance of holding strength, peel strength and tack properties.

Loftan [78] reported on (Na-MMT) clay nanocomposites with an undisclosed emulsion polymer for use as PSAs. The modified nanocomposite PSA films containing 2 wt% clay demonstrated a significant improvement in shear strength without overly compromising tack and peel strength. They also displayed an excellent tackifier response, improving tack and peel strength relative to the base PSA, with better retention of shear strength.

Synthesis of acrylic polymer/MMT clay nanocomposite PSA films was investigated by Kajtna et al. [79]. Different types and amounts of modified and unmodified montmorillonite clays were dispersed in ethyl acrylate (EA)/EHA monomer mixtures, which were then polymerized via suspension polymerization. The MMT loading varied from 0-2 wt%. For the case of OMMT clay, both tack and peel strength gradually decreased with increasing OMMT clay content, while shear

strength significantly increased. A maximal value of shear strength was observed at1 wt% OMMT clay loadings. On the other hand, the unmodified MMT clay had a moderate effect on adhesion. Tack, peel strength and shear strength remained unchanged regardless of the unmodified clay content.

The synthesis and use of Laponite clay armored latex particles with a soft polymer core, i.e., poly(n-lauryl acrylate), as a nanocomposite filler in a poly(BA-co-AA) waterborne PSA was reported by Wang et al. [80]. Polymer particles having Laponite clay armor were prepared using a Pickering miniemulsion polymerization of n-lauryl acrylate. The resulting ‘‘soft–hard’’ poly(n-lauryl acrylate)–Laponite hybrid particles were blended at various low concentrations (1.5 and 2.7 wt%) with the poly(BA-co-AA) latex. The inclusion of the “soft–hard’’ hybrid particles led to increases in tack energy, by raising the plateau stress and increasing the strain at failure. A 70% increase in tack energy, comparing to the base PSA, was achieved at 2.7 wt% hybrid particle concentration. This significant tack energy enhancement was attributed to the soft PLA core ensuring that the adhesives were not stiffened by the nano-sized Laponite clays. Slippage at the interface between the nano-clay platelets and the polymer matrix introduced an additional energy dissipation mechanism during deformation.

The impact of hydrophilic clay on wood adhesive properties was evaluated by Kaboorani & Riedl [81]. Commercial PVAc in liquid form was used as the polymer matrix. Two different clays (Na+ activated surface and unmodified surface) at loadings between 1 and 4 wt% were directly blended with the PVAc at 1500 rpm for 15 min. Increased nano-clay loadings led to an increased shear strength of wood joints in both the wet and dry states as well as at elevated temperatures. Inclusion of nano-clay improved the thermal stability of PVAc to different degrees depending on nano-clay loading and type. TEM micrographs revealed that there is a direct link

between the quality of dispersion and properties of nano-composites. At low loadings, nano-clay was dispersed well in the matrix and the exfoliated structure was obtained. But at higher loadings (4 wt%) a coexistence of exfoliated and intercalated structures was observed. As, Na+ activated surface clay was generally better dispersed in the PVAc matrix than the unmodified surface clay, the adhesive properties were better for the former case.

Bonnefond et al. [82] reported on the preparation of poly(BA:MMA 90:10 w/w)/ MMT latexes via miniemulsion polymerization for PSA applications. A regular OMMT clay and a reactive one were used. The shear adhesion failure temperature (SAFT) and shear resistance of the hybrid latex films synthesized with reactive OMMT were better than those prepared with the regular OMMT clay, but presented a liquid-like probe-tack performance. When allyl methacrylate (AMA) was added to the formulation, SAFT and shear resistance improved, but the film had a very low energy of adhesion due to the excessively cross-linked matrix. In order to reduce cross-link density and thus improve the adhesion energy, small amounts of chain transfer agent (n-dodecyl mercaptan, n-DDM) were used. Adhesive films made from these waterborne hybrid dispersions showed excellent SAFT and shear resistance, and good energy of adhesion. Cryo-TEM results showed that the hybrid latex particles presented a substantial number of dumbbell-like particles in which the clay platelets were embedded, presenting an encapsulated morphology, and some platelets were also located at the polymer/water interface.

The impact of molybdenum disulfide (MoS_2) nano-platelets as a reinforcing filler on adhesive properties of polyurethane (PU)/acrylate PSAs was investigated by Daniloska et al. [83]. Bulk MoS_2 has a layered structure, with each layer consisting of a covalently bonded S− Mo−S hexagonal quasi two-dimensional network [84,85] and connected to other layers by weak attractive van der Waals forces. MoS_2 is employed to improve tribology properties [86] and stabilize the

polymer matrix [87]. The hybrid PU/acrylate latexes were synthesized via miniemulsion polymerization using a photo-initiator in a tubular reactor. MoS_2 was dispersed in a poly(vinyl-pyrrolidone) (PVP) solution then sonicated to prepare stable aqueous MoS_2 dispersions. Subsequently, the resulting latexes were blended with aqueous MoS_2 dispersions at concentrations from 0.1 to 0.75 wt% (based on polymer weight) to obtain MoS_2-nanocomposite latexes. The mechanical and adhesive properties (i.e., adhesion energy) of the resulting nanocomposites films were compared with those of the base PSA. The addition of a very low amount of nano-platelets (0.1 − 0.25 wt%) led to a significant improvement of PSA tack adhesion. This observation was ascribed to the good dispersion of exfoliated MoS_2 using PVP which acts as an interfacial bridge between the inorganic and polymer phases in the final film. The PVP might also provide an additional energy dissipation mechanism when the MoS_2 slides along the interface under deformation of the nanocomposite. However, MoS_2 content greater than 0.25 wt. % resulted in a decrease in adhesive properties because the adhesive became too stiff and lost some dissipative properties.

In summary, the exfoliated structure in clay nanocomposites is required to improve the mechanical, thermal, and barrier properties of a polymer matrix. The exfoliated form can be achievable using emulsion or miniemulsion polymerization depending on the type of clay. The exfoliated form also can be obtained via blending if the MMT clay layer is separated and distributed very well in an aqueous medium using ultrasonication. Furthermore, the stability of clay/latexes are also important factor when nanocomposite latexes are used directly for coating and adhesive applications.

2.5.6 Carbon nanotubes (CNTs)

Carbon nanotubes (CNTs) are inert, cylindrical and are further classified as single-walled (SWNT) or multi-walled nanotubes (MWNT). CNTs are reportedly stronger than steel and can conduct heat and electricity far better than copper. Owing to their unique properties, the addition of small amounts of CNTs can improve mechanical, thermal, and barrier properties as well as the electrical conductivity of polymer matrices while retaining the optical clarity of nanocomposites.

The impact of MWNTs on thermal and mechanical properties of poly(Sty/BA/AA/acrylamide 64:34:1:1 w/w) was studied by Dufresne et al. [88]. The latex was prepared via emulsion polymerization, and MWNTs were suspended in a distilled water solution of 1 wt% sodium dodecyl sulfate (SDS) surfactant via sonication. Afterwards, the stable MWNT dispersions at various loading (0- 15 wt%) were mixed with the latex to prepare nanocomposite films. The thermal stability of the resulting nanocomposites was strongly enhanced by MWNT loading. Their mechanical properties were also improved by increasing the MWNT loading without lowering the elongation at break up to 3 wt%. A low percolation threshold concentration (1.5 wt%) with a good load transfer to the matrix was achieved due to a good interfacial interaction between the MWNT and the polymer.

Vandervorst et al. [89] investigated the dispersion of two different functionalized CNTs in acrylate latexes. Poly(EHA/BA/EA/MMA) and poly(BA-MMA-MAA) were prepared through semi-batch emulsion polymerization for PSA and coating applications, respectively. SWNTs were functionalized with poly(vinyl alcohol) (PVA) and carboxylic acid, and applied to the acrylate latex at concentrations from 1 to 3 wt% .The PVA-CNT dispersion was directly blended with acrylate latex whereas the COOH-CNTs were dispersed in dimethyl formamide (DMF) with ultrasonication prior to mixing. It was found that the PVA-CNTs were finely dispersed in the latex

whereas the COOH-CNTs were not and consequently, the resulting PVA-CNT films exhibited lower optical absorption coefficients than that of the COOH-CNTs. Furthermore, it was revealed that all nanocomposite PSA films had good film integrity and noticeable tack. The COOH-CNT coatings were crack-free while the base coating films showed micro-cracking and were opaque. The PVA-CNT coatings were heated at 90 ^{o}C for 30 min to achieve good film formation. This observation was attributed to the plasticizing effect of DMF on the acrylic latex.

The influence of modified CNTs on the adhesive properties of a semi-batch emulsion polymerized poly(BA/AA 99:1 w/w) was investigated by Wang et al. [90]. SWNTs were functionalized with hydrophilic PVA through esterification and subsequently blended with poly(BA) using sonication. The nanofiller loading varied from 0 to 1 wt% (based on monomer weight). The mechanical properties of poly(BA)/PVA–SWNT nanocomposite adhesives including Young's modulus (Y), yield stress (δ_y), and storage and loss moduli were increased with PVA-SWNT loadings. The probe tack at two different debonding speeds of 10 and 100 μms^{-1} were measured and key tack properties including critical stress (δ_0), maximum in the stress (δ_{max}), as well as adhesion energy were obtained from probe-tack curves. It was found that tack properties increased up to 0.3 wt% then decreased with increasing nanofiller content. This behavior was attributed to the PVA-SWNT percolation threshold concentration, at which a continuous network of SWNT was formed. The electrical conductivity of nanocomposite PSAs reached a maximum at 0.3 wt% and remained at a plateau with increasing PVA-SWNT content. The inclusion of PVA-SWNT made PSAs stiffer, and more dissipative due to the polymer grafted on the surface of the SWNTs, which is an ideal but unusual combination. It is worth mentioning that the nanocomposite adhesives preserved their optical properties. The resulting nanocomposite PSAs are well-suited for interconnects in electronic assemblies.

In order to improve the dispersion of CNTs in latex/CNT nanocomposite processing, surfactant (SDS) as a dispersing agent and chemically functionalized CNTs (e.g., PVA-CNTs and COOH-CNTs) were used. The PVA-CNTs was dispersed very well in the latex nanocomposites. The lowest threshold concentration of CNTs was reported for PVA-CNTs as 0.3 wt.%.

2.5.7 Cellulose nanocrystals

Cellulose nanocrystals (CNCs) are rod-like nanoparticles with a high aspect ratio (length/diameter: 3-5 nm wide, 50-500 nm in length), high specific surface area (170-533 m^2g^{-1}), and low density (1.6 g cm^{-3}) [91] . They are extracted from bulk cellulose using mechanical or chemical treatments such as grinding, homogenization, as well as oxidation and acid hydrolysis [92]. The physical dimensions of CNCs are highly dependent on their source (e.g., hemp, bacteria, green algae, tunicin) and synthesis conditions [91] . Due to the near perfect crystalline structure of CNCs (54-88% crystalline regions), their axial Young's modulus is theoretically higher than Kevlar and their mechanical properties are within the range of other reinforcement materials such as steel wire, carbon fiber, and clay nanoplatelets [91]. CNCs also have a reactive surface containing –OH side groups facilitating surface functionalization and consequently enhancing CNC dispersion in a wide range of polymer matrices. Owing to CNCs' desirable mechanical and chemical properties as well as their nontoxicity and sustainability, they are recognized as reinforcing nanofillers with great potential for a more sustainable polymer production.

The first reported use of CNCs in a poly(St-co-BA 35:65 w/w) matrix was investigated two decades ago [93]. Aqueous CNC dispersions ranging up to 6 wt% (based on polymer) were homogeneously mixed with polymer matrices to prepare CNC/latex nanocomposites. The resulting films exhibited a significant improvement in composite modulus at the rubbery state

(above T_g) of the polymer. The composite modulus of the nanocomposite at 6 wt% was 300 times higher than that of the base latex. CNC loadings of 3 wt% or higher improved the thermal stability of the polymer matrix. This work was followed by studies of different mechanical models to predict the mechanical properties of the polymer nanocomposites as a function of CNC loading [94][95]. Consequently, the large and unusual reinforcement effect of CNCs was attributed to the formation of a rigid network resulting from hydrogen bonding between the CNCs. The impact of nanocomposite processing methods on the mechanical properties of the nanocomposite films was investigated by Hajji et al. [96], Helbert et al. [97], and Dufresne et al. [98]. Aqueous CNC dispersions were blended with poly(St-co-BA) and dried under a range of conditions to obtain several nanocomposite films. Three methods were used: casting by direct evaporation, freeze drying followed by hot pressing, and freeze drying followed by extrusion then hot pressing. It was revealed that direct evaporation gave the most efficient reinforcement results likely due to less damage and forced orientation of the CNCs as compared to the other processing methods.

Stable nanocomposite dispersions based on poly(St-co-EHA) (65:35 w/w) and CNCs were synthesized via batch miniemulsion polymerization [99]. A coupling agent, MPS, was added to the formulations in low amounts (2 wt% based on total monomer) to enhance the stability of the polymer/CNC dispersions. It was assumed that polymer particles bearing polar groups on their surfaces were able to anchor onto the CNCs through hydrogen bonding and consequently prevent agglomeration and coagulation. TEM observations showed a homogeneous distribution of CNCs within the nanocomposites and it was suggested that physical interactions between silanol-functionalized latex particles and the CNC particles were responsible. The evaluation of mechanical properties of the nanocomposites films indicated that both tensile strength and yield stress increased considerably with CNC loadings from 0 to 4 wt% (based on monomer). This

significant enhancement in film strength was ascribed to the relatively high aspect ratio (~20:1) of the CNCs. DMA analysis revealed reduced chain mobility and suggested potential crosslinking whereas DSC analysis showed a quasi-constant value of T_g for all films, which suggested a crosslink free nanocomposite. This discrepancy between DMA and DSC observations may be related to the localization of the CNCs on the particle surfaces in the miniemulsion which prevented their even dispersion in the polymer matrix after film formation [99]. Further study by the same group examined the effect of CNC content (1 to 5 wt%) and MPS concentrations (1 to 3 wt%) on the thermal and mechanical properties of nanocomposite dispersions [100]. DSC analysis displayed the same trends as observed in the previous study. DMA analysis showed that the storage modulus in the rubbery state of the matrix was remarkably enhanced upon addition of the CNCs, which was in agreement with the well-known reinforcing effect of cellulose. However, above 3 wt% CNC loadings, the reinforcing effect was due mostly to the MPS content. Furthermore, the reinforcing effect of the CNCs at 1 wt% MPS was much higher than that at 3 wt% MPS. At such a level, the presence of MPS prevented the formation of a rigid percolating CNC network through strong hydrogen bonding interactions between adjacent CNCs.

CNC/waterborne epoxies [101–103] and CNC/waterborne PU nanocomposites [104,105] were prepared via blending for coating applications. The CNCs derived from different cellulosic origins including tunicin, wood, flax, and cotton linter were respectively compared in the films. The nanocomposite films demonstrated a remarkable increase in Young's modulus and tensile strength with CNC loading. For instance, an increase from 0.51 to 344 MPa and 4.27 to 14.86 MPa for Young's modulus and tensile strength , respectively, were observed with increasing CNC loading from 0 to 30 wt% [104]. The enhanced mechanical properties were ascribed to the synergistic interaction between fillers and between the filler and PU matrix. Scanning electron

microscopy (SEM) showed that the CNCs were well dispersed within the PU matrix and suggested strong interaction between the CNCs and PU matrix due to hydrogen bonding.

CNCs derived from acacia pulp and commercial bacterial cellulose were respectively used as reinforcements in a commercial acrylic polymer [106] and commercial BA-co-MMA resins [107]. The mechanical properties, including Young's modulus and tensile strength, considerably improved with increased CNC loadings.

Poaty et al. [108] reported the surface chemical modifications of CNC using alkyl quaternary amines or acryloyl chloride to prepare waterborne acrylic wood nanocomposite coatings. The freeze dried CNC derivatives at 2 wt% loading (base on polymer) were mixed with waterborne coatings then applied to sugar maple wood for further characterization. The surface modified CNCs were shown to be better dispersed in aqueous acrylic coating as confirmed by AFM results. Accordingly, the abrasion resistance of the nanocomposite coatings increased by up to 38% due to the addition of 2 wt% surface modified CNCs. Additionally, the surface modified CNCs did not degrade the optical properties of the nanocomposites.

The influence of cellulose nanofibers and carboxylated CNCs on the mechanical properties of waterborne coatings for wood applications was investigated by Veigel et al. [109]. Nanocomposite coatings containing up to 5 wt% CNC were prepared by high-shear mixing and applied to wood substrates. The authors concluded that for practical reasons, a 2 wt% loading of nanocellulose was appropriate. This was because of significantly increasing viscosity with nanocellulose loadings and the need to add water to compensate. In any case, the mechanical properties including elastic modulus, tensile strength, and scratch resistance of the nanocomposite coatings increased with nanocellulose loading. Abrasion resistance and nanocomposite hardness were not significantly affected. The optical properties of the nanocomposite coatings were

degraded compared to that of the base coating. This was attributed to the higher surface roughness of the nanocomposite coatings. Overall, better mechanical coating properties were achieved with the addition of cellulose nanofibers compared to carboxylated CNCs.

The influence of different surface modified CNCs on the mechanical properties of UV-waterborne PU coatings was investigated by Vardanyan et al. [110]. They carried out the surface modification of CNCs using three different cationic surfactants. Fairly concentrated modified CNC gels (14 wt% in water) were blended with a base PU coating via high shear mixing. A 2 wt% CNC loading gave the best performance. The roughness of each nanocomposite coating was similar to that of the base coating, suggesting a good dispersion of CNCs within the PU matrix. The abrasion and scratch resistance of the CNC nanocomposites improved by 30-40% without any loss of appearance.

The influence of CNC on the mechanical properties of poly(BA-co-MMA 50:50 w/w) nanocomposites was reported by Vatansever et al. [71]. The base latex was mixed with CNC (ranging from 1-3 wt% based on total monomer) at 60 ^{o}C, 500 rpm for 1h to prepare CNC/latexes. As expected, the elastic modulus and tensile strength increased with CNC loading while the elongation at break decreased. The thermal resistance slightly increased compared to that of the base film. The water vapor permeability was reduced by increasing the CNC loading.

More recently, partially disintegrated nanocellulose fibres (different from the well-defined CNCs used here) were incorporated in a poly(EHA) matrix via suspension polymerization for PSA applications [111]. The aqueous nanocellulose dispersions were varied from 0 to 5 wt% (based on monomer) in reinforced microsphere adhesives. All three adhesive properties including shear strength, tack, and peel strength were increased by increasing the nanocellulose content. As noted,

there is limited information about the synthesis of CNC/PSA nanocomposites via *in situ* emulsion polymerization and the evaluation of their mechanical performance.

2.6 Conclusion

The use of nanoparticles may lead to improved properties such as mechanical, thermal, barrier, and optical properties in emulsion-based coatings and adhesives. The extent of improvement in these properties depends on nanoparticle size and shape, and degree of dispersion.

Proper dispersion of nanoparticles in polymer matrices is very important to achieve the maximum possible impact on performance. One of the main challenges of using nanoparticles is that they tend to agglomerate due to their high specific surface area. In order to overcome agglomeration, dispersion time or dispersion method can be altered to obtain a homogeneous nanoparticle dispersion. The surface modification of nanoparticles has been reported to improve their dispersion and interaction within the polymer matrix. The surface modification can be carried out using surfactants (non-covalently modification) or functionalization of the surface of the nanoparticles (covalently modification).

Nanoparticles with a high aspect ratio such as nanoclays, CNTs, and CNCs are ideal candidates to enhance the mechanical properties of a polymer matrix. Among them, the surface modification of CNTs is required to improve their dispersions in the polymer matrix as they are naturally inert. However, surface functionalization can introduce defects on the CNT surfaces and negatively affect their dispersibility. Regarding nanoclays, their surface functionalization leads mostly to edge modification and is therefore less effective. Intercalation via *in situ* polymerization is preferred. CNCs present interesting versatility in that they can undergo surface functionalization such as esterification, acetylation, and silylation to tune their compatibility with the polymer

matrix; this is due to their abundant and accessible surface hydroxyl groups. Considering CNCs' nontoxicity, sustainability, and surface functionality, makes them one of the most promising candidates among other reinforcing nanoparticles.

2.7 References

1. Jose, J. P.; Malhotra, S. K.; Thomas, S.; Joseph, K.; Goda, K.; Sreekala, M. S. Advances in polymer composites: Macro- and microcomposites – state of the art, new challenges, and opportunities. In *Polymer Composites*; Thomas, S., Joseph, K., Malhotra, S. K., Goda, K., Sreekala, M. S., Eds.; Walter de Gruyter GmbH & Co.KGaA, 2012; Vol. 1, pp. 1–16.

2. Mazumdar, S. K. *Composites Manufacturing Material, product, and Process Engineering*; CRC Press LLC: Boca Raton, 2002.

3. Taha, M. A.; El-Sabbagh, A. M.; Taha, I. M. *Trends in Composite Materials and their Design*; Trans Tech Publications Ltd: Stafa-Zurich, 2010.

4. Ahmed, S.; Jones, F. R. A review of particulate reinforcing theories for polymer composites. *J. Mater. Sci.* **1990**, *25*, 4933–4942.

5. Zhang, Z.; Friedrich, K. Artificial neural networks applied to polymer composites: a review. *Compos. Sci. Technol.* **2003**, *63*, 2029–2044.

6. Luo, J. J.; Daniel, I. M. Characterization and modeling of mechanical behavior of polymer/clay nanocomposites. *Compos. Sci. Technol.* **2003**, *63*, 1607–1616.

7. Hussain, F. Review article: Polymer-matrix Nanocomposites, Processing, Manufacturing, and Application: An Overview. *J. Compos. Mater.* **2006**, *40*, 1511–1575,

8. Usuki, A.; Kawasumi, M.; Kojima, Y.; Okada, A.; Kurauchi, T.; Kamigaito, O. Swelling behavior of montmorillonite cation exchanged for ω-amino acids by -caprolactam. *J. Mater. Res.*

1993, *8*, 1174–1178.

9. Lan, T. Clay-Reinforced Epoxy. *Chem. Mater.* **1994**, 2216–2219.

10. Lan, T.; Kaviratna, P. D.; Pinnavaia, T. J. Mechanism of Clay Tactoid Exfoliation in Epoxy-Clay Nanocomposites. *Chem. Mater.* **1995**, *7*, 2144–2150.

11. Giannelis, E. Polymer layered silicate nanocomposites. *Adv. Mater.* **1996**, 29–35.

12. Marquis, D. M.; Guillaume, É.; Chivas-joly, C. Properties of Nanofillers in Polymer. In *Nanocomposites and Polymers with Analytical Methods*; Cuppoletti, J., Ed.; In Tech Europe: Rijeka, 2011; pp. 261–284.

13. Marti´Nez-Marti´Nez, D. Nanocomposite coatings. In *Encyclopedia of tribology*; Wang, Ed.; 2013; pp. 2359--2364.

14. Dube, M. A.; Salehpour, S. Applying the Principles of Green Chemistry to Polymer Production Technology. *Macromol. React. Eng.* **2014**, *8*, 7–28.

15. Zhang, Y.; Dube, M. A. Green Emulsion Polymerization Technology. In *Advances in Polymer Science*; Springer International Publishing AG, 2017.

16. Zhou, Shuxue and Wu, L. Transparent Organic – Inorganic Nanocomposite Coatings. *Funct. Polym. Coatings Princ. Methods, Appl.* **2015**, *1*, 1–71.

17. Kellar, E. J. C. Key issues in selecting the right adhesive. In *Advances in structural adhesive bonding*; Dillard, D., Ed.; Woodhead Publishing Limited: Boca Raton, 2010; pp. 3–19.

18. Satas, D. *Handbook of Pressure Sensitive Adhesive Technology*; 2nd ed.; Van Nostrand Reinhold: New York, 1989.

19. Gumfekar, S. P.; Kunte, K. J.; Ramjee, L.; Kate, K. H.; Sonawane, S. H. Synthesis of CaCO3-P(MMA-BA) nanocomposite and its application in water based alkyd emulsion coating. *Prog. Org. Coatings* **2011**, *72*, 632–637.

20. Tobing, S. D.; Klein, A. Molecular parameters and their relation to the adhesive performance of emulsion acrylic pressure-sensitive adhesives. II. Effect of crosslinking. *J. Appl. Polym. Sci.* **2001**, *79*, 2558–2564.

21. Mittal, V. Polymer Nanocomposites in Emulsion and Suspension: an Overview. In *Polymer Nanocomposites by Emulsion and Suspension Polymerization: an Overview*; Mittal, V., Ed.; Royal Society of Chemistry, 2011; pp. 1–31.

22. Taylor, A. C. Advances in nanoparticle reinforcement in structural adhesives. In *Advances in Structural Adhesive Bonding*; Dillard, D., Ed.; Woodhead Publishing Limited: Boca Raton, 2010; pp. 151–182.

23. Hanemann, T.; Szabó, D. V. *Polymer-nanoparticle composites: From synthesis to modern applications*; 2010; Vol. 3.

24. Krishnamoorti, R. Strategies for Dispersing Nanoparticles in Polymers. *MRS Bull.* **2007**, *32*, 341–347.

25. Rufin, M. A.; Grunlan, M. A. Surface - Grafted Polymer Coatings : Preparation , Characterization , and Antifouling Behavior. In *Functional Polymer Coatings: Principles, Methods, and Applications*; Wu, L., Baghdachi, J., Eds.; John Wiley & Sons, Inc, 2015; pp. 218–238.

26. Uyama, Y.; Kato, K.; Ikada, Y. *Surface Modification of Polymers by Grafting*; Galina, H., Ed.; Springer International Publishing AG: Berlin/Heidelberg, 1998; Vol. 137.

27. Zhou, F.; Huck, W. T. S. Surface grafted polymer brushes as ideal building blocks for "smart" surfaces. *Phys. Chem. Chem. Phys.* **2006**, *8*, 3815–3823.

28. Bergbreiter, D. E.; Caraway, J. W. Thermoresponsive Polymer-Bound Substrates. *Am. Chem. Soc.* **1996**, *118*, 6092–6093.

29. Bergbreiter, D. E.; Zhou, J. New grafting chemistry for functionalized polyethylene films. *J. Polym. Sci. Part A Polym. Chem.* **1992**, *30*, 2049–2053.

30. Bamford, C. .; Al-Lamee, K. . Studies in polymer surface functionalization and grafting for biomedical and other applications. *Polymer (Guildf).* **1994**, *35*, 2844–2852.

31. Loh, F. C.; Tan, K. L.; Kang, E. T.; Neoh, K. G.; Pun, M. Y. Near-u.v. radiation induced surface graft copolymerization of some O3-pretreated conventional polymer films. *Eur. Polym. J.* **1995**, *31*, 481–488.

32. Svarfvar, B. L.; Ekman, K. B.; Sundell, M. J.; Nasman, J. H. Electron-beam graft-modified membranes with externally controlled flux. *Polym. Adv. Technol.* **1996**, *7*, 839–846.

33. Sheu, M. S.; Hoffman, A. S.; Ratner, B. D.; Feijen, J.; Harris, J. M. Immobilization of polyethylene oxide surfactants for non-fouling biomaterial surfaces using an argon glow discharge treatment. *J. Adhes. Sci. Technol.* **1993**, *7*, 1065–1076.

34. Tian, J.; Lin, X.; Huang, B.; Xu, J. Plasma induced grafting of styrene onto nascent polyethylene powder. *Eur. Polym. J.* **1995**, *31*, 755–760.

35. Brittain, W. J.; Minko, S. A structural definition of polymer brushes. *J. Polym. Sci. Part A Polym. Chem.* **2007**, *45*, 3505–3512.

36. Edmondson, S.; Osborne, V. L.; Huck, W. T. S. Polymer brushes via surface-initiated polymerizations. *Chem. Soc. Rev.* **2004**, *33*, 14.

37. Matyjaszewski, K.; Tsarevsky, N. V. Nanostructured functional materials prepared by atom transfer radical polymerization. *Nat. Chem.* **2009**, *1*, 276–288.

38. Matyjaszewski, K.; Miller, P. J.; Shukla, N.; Immaraporn, B.; Gelman, A.; Luokala, B. B.; Siclovan, T. M.; Kickelbick, G.; Vallant, T.; Hoffmann, H.; Pakula, T. Polymers at Interfaces: Using Atom Transfer Radical Polymerization in the Controlled Growth of

Homopolymers and Block Copolymers from Silicon Surfaces in the Absence of Untethered Sacrificial Initiator. *Macromolecules* **1999**, *32*, 8716–8724.

39. Zhao, B.; Brittain, W. J. Polymer brushes: Surface-immobilized macromolecules. *Prog. Polym. Sci.* **2000**, *25*, 677–710.

40. Hilf, S.; Kilbinger, A. F. M. Functional end groups for polymers prepared using ring-opening metathesis polymerization. *Nat. Chem.* **2009**, *1*, 537–546.

41. Tasdelen, M. A.; Kahveci, M. U.; Yagci, Y. Telechelic polymers by living and controlled/living polymerization methods. *Prog. Polym. Sci.* **2011**, *36*, 455–567.

42. Vericat, C.; Vela, M. E.; Salvarezza, R. C. Self-assembled monolayers of alkanethiols on Au(111): surface structures, defects and dynamics. *Phys. Chem. Chem. Phys.* **2005**, *7*, 3258–3268.

43. Love, J. C.; Estroff, L. a.; Kriebel, J. K.; Nuzzo, R. G.; Whitesides, G. M. *Self-Assembled Monolayers of Thiolates on Methals as a Form of Nanotechnology*; 2005.

44. Xiong, M.; Gu, G.; You, B.; Wu, L. Preparation and Characterization of Poly (styrene butylacrylate) Latex / Nano-ZnO Nanocomposites. *J. Appl. Polym. Sci.* **2003**, *90*, 1923–1931.

45. Dhoke, S. K.; Bhandari, R.; Khanna, A. S. Effect of nano-ZnO addition on the silicone-modified alkyd-based waterborne coatings on its mechanical and heat-resistance properties. *Prog. Org. Coatings* **2009**, *64*, 39–46.

46. Allen, N. S.; Edge, M.; Verran, J.; Stratton, J.; Maltby, J.; Bygott, C. Photocatalytic titania based surfaces: Environmental benefits. *Polym. Degrad. Stab.* **2008**, *93*, 1632–1646.

47. He, Q.; Wu, L.; Gu, G.; You, B. Preparation and Characterization of Acrylic/Nano-TiO2 Composite Latex. *High Perform. Polym.* **2002**, *14*, 383–396.

48. Zhou, S.; Wu, L.; Xiong, M.; He, Q.; Chen, G. Dispersion and UV-VIS Properties of Nanoparticles in Coatings. *J. Dispers. Sci. Technol.* **2005**, *25*, 417–433.

49. Ai, Z.; Sun, G.; Zhou, Q.; Xie, C. Polyacrylate-core/TiO2-shell nanocomposite particles prepared byin situ emulsion polymerization. *J. Appl. Polym. Sci.* **2006**, *102*, 1466–1470.

50. Kaboorani, A.; Riedl, B. Nano-aluminum oxide as a reinforcing material for thermoplastic adhesives. *J. Ind. Eng. Chem.* **2012**, *18*, 1076–1081.

51. Sow, C.; Riedl, B.; Blanchet, P. UV-waterborne polyurethane-acrylate nanocomposite coatings containing alumina and silica nanoparticles for wood: Mechanical, optical, and thermal properties assessment. *J. Coatings Technol. Res.* **2011**, *8*, 211–221.

52. Xiong, M.; Wu, L.; Zhou, S.; You, B. Preparation and characterization of acrylic latex/nano-SiO2 composites. *Polym. Int.* **2002**, *51*, 693–698.

53. Qi, D. ming; Bao, Y. zhong; Weng, Z. x.; Huang, Z. ming Preparation of acrylate polymer/silica nanocomposite particles with high silica encapsulation efficiency via miniemulsion polymerization. *Polymer (Guildf).* **2006**, *47*, 4622–4629.

54. Mizutani, T.; Arai, K.; Miyamoto, M.; Kimura, Y. Application of silica-containing nano-composite emulsion to wall paint: A new environmentally safe paint of high performance. *Prog. Org. Coatings* **2006**, *55*, 276–283.

55. Mizutani, T.; Arai, K.; Miyamoto, M.; Kimura, Y. Preparation of spherical nanocomposites consisting of silica core and polyacrylate shell by emulsion polymerization. *J. Appl. Polym. Sci.* **2006**, *99*, 659–669.

56. Zhang, F. A.; Kang, J. S.; Luo, M.; Yu, C. L. Preparation and properties of soapless poly(styrene-butyl acrylate-acrylic acid)/SiO_2 composite emulsion. *Iran. Polym. J. (English Ed.* **2012**, *21*, 289–296.

57. Wang, N.; Guo, Y.; Xu, H.; Liu, X.; Zhang, L.; Qu, X.; Zhang, L. Preparation of a silica/poly(n-butyl acrylate-co-acrylic acid) composite latex and its pressure-sensitive properties. *J. Appl.*

Polym. Sci. **2009**.

58. Khalina, M.; Sanei, M.; Mobarakeh, H. S.; Mahdavian, A. R. Preparation of acrylic/silica nanocomposites latexes with potential application in pressure sensitive adhesive. *Int. J. Adhes. Adhes.* **2015**.

59. Yamamoto, Y.; Fujii, S.; Shitajima, K.; Fujiwara, K.; Hikasa, S.; Nakamura, Y. Soft polymer-silica nanocomposite particles as filler for pressure-sensitive adhesives. *Polymer (Guildf).* **2015**, *70*, 77–87.

60. Czech, Z.; MacIejewski, Z.; Kondratowicz-Maciejewska, K. Water-borne pressure-sensitive adhesives acrylics modified using amorphous silica nanoparticles. *Polish J. Chem. Technol.* **2016**, *18*, 124–128.

61. Dodiuk, H.; Belinski, I.; Dotan, a.; Kenig, S. Polyurethane adhesives containing functionalized nanoclays. *J. Adhes. Sci. Technol.* **2006**, *20*, 1345–1355.

62. Yano, K.; Usuki, A.; Okada, A.; Kurauchi, T.; Kamigaito, O. Synthesis and properties of polyimide-clay hybrid Films. *Am. Chem. Soc. Polym. Prepr. Div. Polym. Chem.* **1997**, *35*, 2289–2294.

63. Ray, S. S.; Okamoto, K.; Okamoto, M. Structure - property relationship in biodegradable Poly (butylene succinate)/ layered silicate nanocomposites. *Macromolecules* **2003**, *36*, 2355–2367.

64. Lee, D. C.; Jang, L. W. Preparation and Characterization of PMMA-Clay Hybrid Composite by Emulsion Polymerization. *J. Appl. Polym. Sci.* **1996**, *61*, 1117–1122.

65. Lai, M. C.; Chang, K. C.; Yeh, J. M.; Liou, S. J.; Hsieh, M. F.; Chang, H. S. Advanced environmentally friendly anticorrosive materials prepared from water-based polyacrylate/Na+-MMT clay nanocomposite latexes. *Eur. Polym. J.* **2007**, *43*, 4219–4228.

66. Yilmaz, O.; Cheaburu, C. N.; Gülümser, G.; Vasile, C. On the stability and properties of the

polyacrylate/Na-MMT nanocomposite obtained by seeded emulsion polymerization. *Eur. Polym. J.* **2012**, *48*, 1683–1695.

67. Yilmaz, O.; Chiriac, A. P.; Cheaburu, C. N.; Nita, L. E.; Gülümser, G.; Duraccio, D.; Cimmino, S.; Vasile, C. Nanocomposites based on montmorillonite/acrylic copolymer for aqueous coating of soft surfaces. *Solid State Phenom.* **2009**, *151*, 129–134.

68. Yilmaz, O.; Cheaburu, C. N.; Durraccio, D.; Gulumser, G.; Vasile, C. Preparation of stable acrylate/montmorillonite nanocomposite latex via in situ batch emulsion polymerization: Effect of clay types. *Appl. Clay Sci.* **2010**, *49*, 288–297.

69. Diaconu, G.; Paulis, M.; Leiza, J. R. High solids content waterborne acrylic/montmorillonite nanocomposites by miniemulsion polymerization. *Macromol. React. Eng.* **2008**, *2*, 80–89.

70. Diaconu, G.; Paulis, M.; Leiza, J. R. Towards the synthesis of high solids content waterborne poly(methyl methacrylate-co-butyl acrylate)/montmorillonite nanocomposites. *Polymer (Guildf).* **2008**, *49*, 2444–2454.

71. Vatansever, A.; Dogan, H.; Inan, T.; Sezer, S.; Sirkecioglu, A. Properties of Na-Montmorillonite and Cellulose Nanocrystal Reinforced Poly(butyl acrylate-co-methyl methacrylate) Nanocomposites. *Polym. Eng. Sci.* **2015**, 2922–2928.

72. Li, H. A. O.; Yang, Y.; Yu, Y. Acrylic emulsion pressure-sensitive adhesives (PSAS) reinforced with layered silicate. *J. Adhes. Sci. Technol.* **2004**, *18*, 1759–1770.

73. Xu, M.; Choi, Y. S.; Kim, Y. K.; Wang, K. H.; Chung, I. J. Synthesis and characterization of exfoliated poly(styrene-co-methyl methacrylate)/clay nanocomposites via emulsion polymerization with AMPS. *Polymer (Guildf).* **2003**, *44*, 6387–6395.

74. Hasegawa, N.; Kawasumi, M.; Kato, M.; Usuki, A.; Okada, A. Preparation and mechanical properties of polypropylene-clay hybrids using a maleic anhydride-modified polypropylene

oligomer. *J. Appl. Polym. Sci.* **1998**, *67*, 87–92.

75. Kato, M.; Usuki, A.; Okada, A. Synthesis of polypropylene oligomer/clay intercalation compounds. *J. Appl. Polym. Sci.* **1997**, *66*, 1781–1785.

76. Choi, Y. S.; Wang, K. H.; Xu, M.; Chung, I. J. Synthesis of Exfoliated Polyacrylonitrile / Na-MMT Nanocomposites via Emulsion Polymerization. *Polymer (Guildf).* **2002**, 2936–2939.

77. Kim, Y. K.; Choi, Y. S.; Wang, K. H.; Chung, I. J. Synthesis of Exfoliated PS / Na - MMT Nanocomposites via Emulsion Polymerization. *Chem. Mater.* **2002**, *14*, 4990–4995.

78. Loftan, L. *Adhesives & Sealants Industry*. 2004, pp. 31–36.

79. Kajtna, J.; Šebenik, U. Microsphere pressure sensitive adhesives-acrylic polymer/montmorillonite clay nanocomposite materials. *Int. J. Adhes. Adhes.* **2009**, *29*, 543–550.

80. Wang, T.; Colver, P. J.; Bon, S. A. F.; Keddie, J. L. Soft polymer and nano-clay supracolloidal particles in adhesives : synergistic effects on mechanical properties. *Soft Matter* **2009**, *5*, 3842–3849.

81. Kaboorani, A.; Riedl, B. Effects of adding nano-clay on performance of polyvinyl acetate (PVA) as a wood adhesive. *Compos. Part A Appl. Sci. Manuf.* **2011**, *42*, 1031–1039.

82. Bonnefond, A.; Mičušík, M.; Paulis, M.; Leiza, J. R.; Teixeira, R. F. A.; Bon, S. A. F. Morphology and properties of waterborne adhesives made from hybrid polyacrylic/montmorillonite clay colloidal dispersions showing improved tack and shear resistance. *Colloid Polym. Sci.* **2013**, *291*, 167–180.

83. Daniloska, V.; Keddie, J. L.; Asua, J. M.; Tomovska, R. MoS2 nanoplatelet fillers for enhancement of the properties of waterborne pressure-sensitive adhesives. *ACS Appl. Mater. Interfaces* **2014**, *6*, 22640–22648.

84. Helveg, S.; Lauritsen, J.; Laegsgaard, E.; Stensgaard, I.; Norskov, J.; Clausen, B.; Topsoe, H.;

Besenbacher, F. Atomic-scale structure of single-layer MoS2 nanoclusters. *Phys. Rev. Lett.* **2000**, *84*, 951–4.

85. Lauritsen, J. V.; Kibsgaard, J.; Helveg, S.; Topsøe, H.; Clausen, B. S.; Lægsgaard, E.; Besenbacher, F. Size-dependent structure of MoS2 nanocrystals. *Nat. Nanotechnol.* **2007**, *2*, 53–58.

86. Hou, X.; Shan, C. X.; Choy, K. L. Microstructures and tribological properties of PEEK-based nanocomposite coatings incorporating inorganic fullerene-like nanoparticles. *Surf. Coatings Technol.* **2008**, *202*, 2287–2291.

87. Matusinovic, Z.; Shukla, R.; Manias, E.; Hogshead, C. G.; Wilkie, C. A. Polystyrene/molybdenum disulfide and poly(methyl methacrylate)/molybdenum disulfide nanocomposites with enhanced thermal stability. *Polym. Degrad. Stab.* **2012**, *97*, 2481–2486.

88. Dufresne, A.; Paillet, M.; Putaux, J. L.; Schweitzer, A. A. Processing and characterization of carbon nanotube / poly (styrene-co-butyl acrylate) nanocomposites. *J. Mater. Sci.* **2002**, *37*, 3915–3923.

89. Vandervorst, P.; Lei, C. H.; Lin, Y.; Dupont, O.; Dalton, A. B.; Sun, Y. P.; Keddie, J. L. The fine dispersion of functionalized carbon nanotubes in acrylic latex coatings. *Prog. Org. Coatings* **2006**, *57*, 91–97.

90. Wang, T.; Lei, C. H.; Dalton, A. B.; Creton, C.; Lin, Y.; Fernando, K. A. S.; Sun, Y. P.; Manea, M.; Asua, J. M.; Keddie, J. L. Waterborne, nanocomposite pressure-sensitive adhesives with high tack energy, optical transparency, and electrical conductivity. *Adv. Mater.* **2006**, *18*, 2730–2734.

91. Moon, R. J.; Martini, A.; Nairn, J.; Simonsen, J.; Youngblood, J. *Cellulose nanomaterials review: structure, properties and nanocomposites*; 2011; Vol. 40.

92. Dufresne, A. Preparation of cellulose nanocrystals. In *Nanocellulose From Nature to High*

Performance Tailored Materials; Walter de Gruyter GmbH: Berlin/ Boston, 2012; pp. 83–124.

93. Favier, V.; Canova, G. R.; Cavaillé, J. Y.; Chanzy, H.; Dufresne, A.; Gauthier, C. Nanocomposite materials form latex and cellulose whiskers. *Polym. Adv. Technol.* **1994**, *6*, 351–355.

94. Favier, V.; Chanzy, H.; Cavaille, J. Y. Polymer Nanocomposites Reinforced by Cellulose Whiskers. *Macromolecules* **1995**, *28*, 6365–6367.

95. Favier, V.; Cavaille, J. Y.; Canova, G. R.; Shrivastava, S. C. Mechanical percolation in cellulose whisker nanocomposites. *Polym. Eng. Sci.* **1997**, *37*, 1732–1739.

96. Hajji, P.; Cavaillé, J. Y.; FAVIER, V.; Gauthier, C.; Vigier, G. Tensile Behavior of Nanocomposites From Latex and Cellulose Whiskers. *Polym. Compos.* **1996**, *17*, 612–619.

97. Helbert, W.; Cavaille, J. Y.; Dufresne, a; Fourier, U. J. Straw Cellulose Whiskers . Part I : Processing and mechanical behavior. *Polym. Compos.* **1996**, *17*, 604–611.

98. Dufresne, A.; Cavaillé, J. Y.; Helbert, W. Thermoplastic Nanocomposites Filled with Wheat Straw Cellulose Whisker. Part 11: Effect of Processing and Modeling. *Polym. Compos.* **1997**, *18*, 198–210.

99. Elmabrouk, A. Ben; Wim, T.; Dufresne, A.; Boufi, S. Preparation of poly(styrene- co -hexylacrylate)/cellulose whiskers nanocomposites via miniemulsion polymerization. *J. Appl. Polym. Sci.* **2009**, *114*, 2946–2955.

100. Ben Mabrouk, A.; Kaddami, H.; Magnin, A.; Belgacem, M. N.; Dufresne, A.; Boufi, S. Preparation of nanocomposite dispersions based on cellulose whiskers and acrylic copolymer by miniemulsion polymerization: Effect of the silane content. *Polym. Eng. Sci.* **2011**, *51*, 62–70.

101. Matos Ruiz, M.; Cavaillé, J. Y.; Dufresne, A.; Gérard, J. F.; Graillat, C. Processing and characterization of new thermoset nanocomposites based on cellulose whiskers. *Compos.*

Interfaces **2000**, *7*, 117–131.

102. Ruiz, M. M.; Cavaille, J. Y.; Dufresne, A.; Graillat, C.; Gerard, J.-F. New waterborne epoxy coatings based on cellulose nanofillers. *Macromol. Symp.* **2001**, *169*, 211–222.

103. Xu, S.; Girouard, N.; Schueneman, G.; Shofner, M. L.; Meredith, J. C. Mechanical and thermal properties of waterborne epoxy composites containing cellulose nanocrystals. *Polymer (Guildf).* **2013**, *54*, 6589–6598.

104. Cao, X.; Dong, H.; Li, C. M. New nanocomposite materials reinforced with cellulose nanocrystals in Waterborne Polyurethane. *Biomacromolecules* **2007**, *8*, 899–904.

105. Wang, Y.; Tian, H.; Zhang, L. Role of starch nanocrystals and cellulose whiskers in synergistic reinforcement of waterborne polyurethane. *Carbohydr. Polym.* **2010**, *80*, 665–671.

106. Pu, Y.; Zhang, J.; Elder, T.; Deng, Y.; Gatenholm, P.; Ragauskas, A. J. Investigation into nanocellulosics versus acacia reinforced acrylic films. *Compos. Part B Eng.* **2007**, *38*, 360–366.

107. Trovatti, E.; Oliveira, L.; Freire, C. S. R.; Silvestre, A. J. D.; Pascoal Neto, C.; Cruz Pinto, J. J. C.; Gandini, A. Novel bacterial cellulose-acrylic resin nanocomposites. *Compos. Sci. Technol.* **2010**, *70*, 1148–1153.

108. Poaty, B.; Vardanyan, V.; Wilczak, L.; Chauve, G.; Riedl, B. Modification of cellulose nanocrystals as reinforcement derivatives for wood coatings. *Prog. Org. Coatings* **2014**, *77*, 813–820.

109. Veigel, S.; Grull, G.; Pinkl, S.; Obersriebnig, M.; M??ller, U.; Gindl-Altmutter, W. Improving the mechanical resistance of waterborne wood coatings by adding cellulose nanofibres. *React. Funct. Polym.* **2014**, *85*, 214–220.

110. Vardanyan, V.; Poaty, B.; Chauve, G.; Landry, V.; Galstian, T.; Riedl, B. Mechanical properties of UV-waterborne varnishes reinforced by cellulose nanocrystals. *J. Coatings Technol.*

Res. **2014**, *11*, 841–852.

111. Kajtna, J.; Šebenik, U. Novel acrylic/nanocellulose microsphere with improved adhesive properties. *Int. J. Adhes. Adhes.* **2017**, *74*, 100–106.

Chapter 3:

Latex/CNC Nanocomposites via Emulsion Polymerization

Synthesis of Poly(n-butyl acrylate/methyl methacrylate)/CNC Latex Nanocomposites via *in situ* Emulsion Polymerization

Zahra Dastjerdi, Emily D. Cranston, Marc A. Dubé*

***Abstract*:** Cellulose nanocrystals (CNCs) are renewable, non-toxic and naturally available organic nanoparticles derived from cellulosic resources such as cotton and wood pulp. Poly(n-butyl acrylate-co-methyl methacrylate)/CNC latexes are successfully synthesized via *in situ* emulsion polymerization. The effect of CNC loading on overall conversion, polymer particle size, glass transition temperature (T_g), gel content, latex viscosity, and storage and loss moduli of dried latex are studied. While the effect of CNC content on overall conversion, polymer particle size, and T_g of the resulting latexes is negligible, significant increase in gel content, latex viscosity, and storage and loss moduli are observed.

3.1 Introduction

Nanoparticles such as nanoclays, nano-layered silicate, nano SiO_2, nano TiO_2, and carbon nanotubes have been incorporated into polymer matrices to modify polymers for mechanical, thermal, optical, electrical, barrier and fire retardant properties. Given their potential as a polymer property modifier, cellulose nanocrystals (CNCs) are being increasingly used as reinforcement materials.[1] CNCs are rod-like nanoparticles extracted from cellulosic resources such as cotton, wood pulp, and microcrystalline cellulose through an acid hydrolysis process.[2] The acid hydrolysis process employs a strong acid such as sulfuric, nitric or hydrochloric acid to dissolve

the amorphous chains from cellulose fibers and release the crystalline domains.[3] Among the different acids, sulfuric acid appears to be the most effective for hydrolysis due to the grafting of negatively charged sulfate half-ester groups onto the surface of the CNCs [4] which make the CNCs dispersible in water.[2] Due to the near perfect crystalline arrangement of cellulose polymer chains in the particles, CNCs have a greater specific axial elastic modulus than Kevlar and steel wire.[1] CNCs also have a high aspect ratio (L/D: 50-500 nm in length/3-5 nm in width), low density (1.6 g cm^{-3}),[1] and high specific surface area (170-533 m^2 g^{-1}).[5] In addition, a few studies on the oral and dermal toxicity of CNCs have shown a lack of adverse health effects.[6]

In nanocomposites, improved material properties arise when a high interfacial area between the nanoparticles and polymer matrix is present; this often results in strong interaction forces. This interaction is enhanced when the nanoparticles are well dispersed; this also leads to homogeneous and consistent material properties. Different dispersion techniques such as solution mixing, melt mixing and *in situ* polymerization can be employed to incorporate nanoparticles into a polymer matrix. The appropriate technique is determined by the nature of the polymer, the inherent properties of the nanoparticles and the final product application. *In situ* polymerization techniques include bulk, suspension, dispersion, solution, and emulsion polymerization. These *in situ* techniques are preferred as they employ a more cost-effective one-pot synthesis method and generally achieve more effective dispersion of the nanoparticles because these avoid solution viscosity constraints. In this study, we have chosen an *in situ* emulsion polymerization technique to synthesize latex/CNC nanocomposites, water being the common medium for the preparation of both CNC dispersions and emulsion polymerizations.

A wide range of products from commodity rubbers, coatings, paints, and adhesives to more exotic biomaterials and high-tech products are synthesized by emulsion polymerization.

Advantages of emulsion polymerization compared to other free radical polymerizations such as bulk and solution polymerization include a relatively high reaction rate and excellent heat transfer rates. In addition, the water-based reaction medium makes emulsion polymerization a less toxic process. It follows that we are witnessing more growth in the production of emulsion-based adhesives and water-borne coatings compared to their solvent-based counterparts. However, in many cases, transition from a solution-based to a water-based process results in modification of product properties. For example, adhesives often lack the cohesive/shear strength which is necessary for some applications. Hence, producing latex-based adhesives with very high mechanical performance is essential to broaden their range of applications.

The incorporation of cellulose-based nanomaterials in emulsion polymerization has been reported for a batch miniemulsion polymerization [7,8] For this case, stable dispersions of CNCs (4 wt.%), in poly(styrene-co-ethylhexyl acrylate) were synthesized via *in situ* batch miniemulsion polymerization. These were completed up to a 25% solids content and used high affinity silane coupling agents to compatibilize their formulation.[9] The tensile strength and yield stress of the resulting nanocomposite films showed 1.6 and two-fold increases, respectively, compared to the neat copolymer latex.

In this study, we developed an approach for the synthesis of stable polymer-CNC latex nanocomposites to solids contents of 34 wt.% without the use of a coupling agent. The effect of CNC loading on overall conversion, polymer particle size, glass transition temperature (T_g), gel content, latex viscosity, and loss and storage moduli was investigated.

3.2 Experimental Part

3.2.1 Materials

All materials were used as supplied by manufacturer. Butyl acrylate (BA) and methyl methacrylate (MMA) monomers, sodium dodecyl sulfate (SDS) anionic surfactant, potassium persulfate (KPS) initiator, cetrimonium bromide (CTAB) cationic surfactant**,** and the inhibitor hydroquinone (HQ) were all obtained from Sigma Aldrich. Aerosol® EF-800 anionic surfactant (49-51 wt% aqueous solution) was purchased from CYTEC. Disponil A 3065 *nonionic surfactant* was obtained from BASF. For gel content measurement, tetrahydrofuran (THF, HPLC grade, EMD Chemicals) was utilized as supplied. Poly (vinylidene fluoride) (PVDF) membrane filters with a pore size of 5.0 µm, for use in gel content measurements, were purchased from EMD Millipore. Distilled deionized (DDI) water was used throughout all experiments. CNCs were obtained from CelluForce (Windsor, QC, Canada). Ashless Whatman filter paper (grade 542) was used for filtration of CNC dispersions. Nitrogen gas (Linde Canada) was used to purge the reactor during polymerization.

3.2.2 Aqueous CNC dispersion preparation

A specified amount of dry CNC (0.5, 1 and 2 wt.% based on total monomer weight) was dispersed into the required amount of DDI water to prepare a 1 to 1.5 wt.% aqueous CNC dispersion. Thus, 0.75 g CNC in 75 g DDI water, 1.5 g CNC in 150 g DDI water, and 3 g CNC in 200 g DDI water, were used to prepare CNC loadings of 0.5, 1 and 2 wt.%, respectively. The CNC concentration was changed to maintain a constant percent solids from run to run. The CNC dispersion was first stirred with a magnetic bar for 2-4 h depending on the CNC concentration until it appeared to be well-dispersed according to visual inspection. Afterwards, the dispersion was

sonicated using a Sonic Dismembrator Ultrasonic processor (500 W with 65% amplitude) for 15 min in an ice bath to avoid overheating. Finally, the CNC dispersion was filtered through ashless Whatman 542 filter paper by vacuum filtration.

3.2.3 CNC-polymer latex nanocomposite preparation

BA/MMA-CNC latex nanocomposites were produced via *in situ* emulsion polymerization. In all runs, the BA/MMA ratio, and surfactant, initiator and water concentrations were kept constant while the CNC loading was varied from 0.5 to 2 wt.% based on monomer weight (Table 1). The polymerizations were conducted in a jacketed 1 L stainless steel LabMax^{TM} reactor (Mettler Toledo) equipped with a reflux condenser and nitrogen inlet (Figure 3.1). To start, the SDS solution and monomer mixture were charged to the reactor at room temperature. The stirring speed was increased and then maintained at 300 rpm throughout the polymerization process. The reactor was purged with N_2 and the reactor temperature was increased to 60 ^{o}C (within 30 min). During the reactor heating period, the CNC dispersion was fed to the reactor using a metering pump at a constant rate. Completion of the CNC dispersion feed coincided with the reactor temperature reaching 60 ^{o}C. At that point, the initiator solution was injected into the reaction mixture. The polymerization was conducted for 4 h.

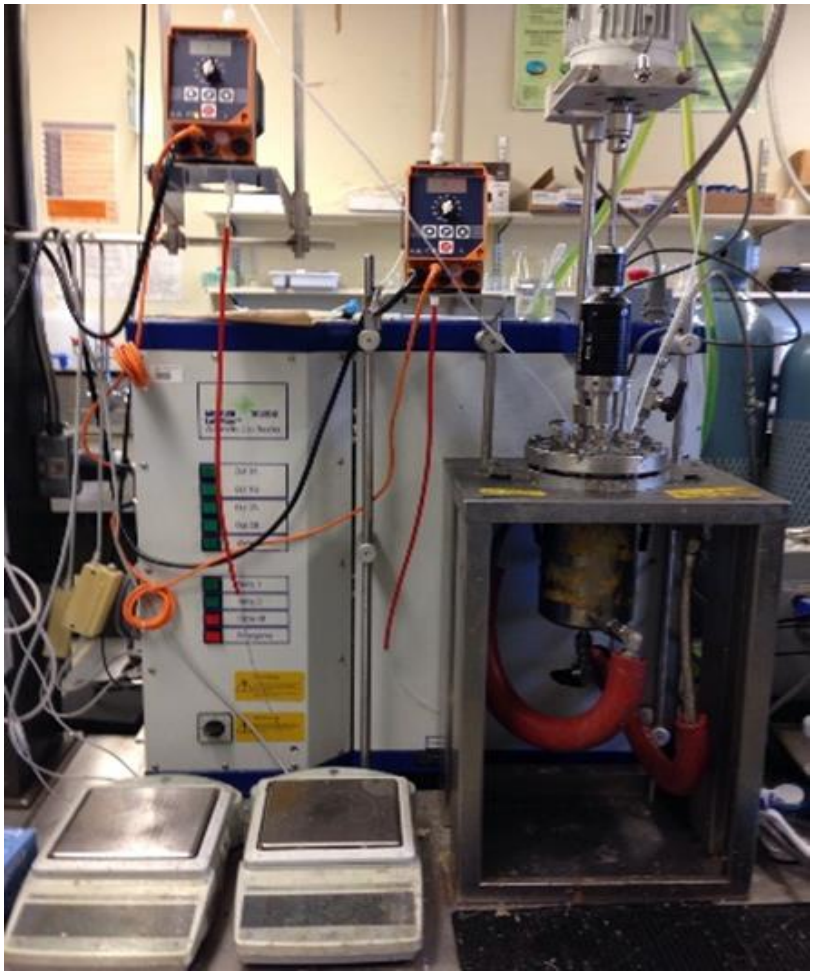

Figure 3.1 Stainless steel LabMax^{TM} reactor (Mettler Toledo).

Table 3.1 *In situ* emulsion polymerization formulation.

Component	**Amount**	
	(g)	(phm)*
Butyl acrylate (BA)	135	90
Methyl methacrylate (MMA)	15	10
Sodium dodecyl sulfate (SDS)	3	2
Potassium persulfate (KPS)	0.15	0.1
Cellulose nanocrystals (CNC)	0-3	0-2
Deionized distilled water (DDI H_2O)	300	200

*phm = parts per hundred parts monomer

3.2.4 Characterization

The CNC average particle size in the initial CNC dispersions in water and the average diameter of the latex/CNC nanocomposite particles were measured using a Malvern NanoS Zetasizer DLS. For the CNC dispersions, 0.1 mL of CNC dispersion was diluted in 5 mL DDI water in a poly(styrene) cuvette. For the CNC latex nanocomposites, 0.1 mL of each sample was diluted with 2 mL DDI water. The reported diameters are intensity-weighted average particle sizes. We note that for CNCs which are rod-like nanoparticles, the DLS measurement gives only an "apparent" particle size assuming spherical geometry. Additional characterization of these CNCs was reported elsewhere.[10]

A standard gravimetric method was applied to calculate the latex solids content. 1 g latex was weighed into an aluminum dish, then dried in a vacuum oven at 30 °C until constant weight was achieved (typically, for 2 days). The solids content (*SC*) was calculated with:

$$SC = \frac{W_{DS}}{W_{LS}} \quad (1)$$

where, W_{DS} is the weight of dried latex sample; W_{LS} is the weight of the latex sample. Subsequently, the overall monomer conversion, X_t, was calculated using:

$$X_t = \frac{SC - W_I - W_{Surf} - W_{CNC}}{W_{TM}} \quad (2)$$

where *SC* is the solids content (see Equation 1), and W_I, W_{Surf} ,W_{CNC} refer to the weight fractions of initiator, surfactant, and CNC in the reactor, respectively. W_{TM} refers to the weight fraction of total monomer in the formulation. Thus, X_t, represents the overall monomer conversion.

For gel content measurement, 0.05 g dry polymer was weighed and sealed in PVDF membranes to form a pouch. The pouch was then placed in 20 mL THF in a 100 mL glass jar. The jar was gently, mechanically shaken for 24 h. Finally, the membrane was removed from the jar and dried in a fume hood until reaching a constant weight. The gel content was calculated using:

$$Gel\ content = \frac{mass\ of\ dry\ gel}{mass\ of\ initial\ dry\ polymer} \quad (3)$$

A differential scanning calorimeter (DSC) Model Q1000 from TA Instruments was used to measure glass transition temperature (T_g). The DSC was equipped with an autosampler, a refrigerated cooling system and nitrogen as the purge gas. Around 7 mg of dried polymer was weighed into a standard DSC hermetic aluminum sample pan. The analysis was performed using a modulated DSC method with modulation amplitude of ±1 ^oC every 60 s. The sample was cooled to -80 ^oC, held isothermally for 3 min, and followed by a heating ramp of 10 ^oC/min until the sample reached 130 ^oC. The cooling and heating cycle was repeated two times. The T_g was calculated from the inflection point in the reversed heat flow curve from the second cycle using the software provided.

The viscosity of a 200 mL sample of each latex was measured using a Thermo Scientific HAAKE Viscotester^{TM} (Model D) at room temperature with a standard spindle (R#2 or R#3, respectively) at 100 and 200 rpm. Viscosity values were recorded after 1 min stabilization.

Dynamic mechanical analysis (DMA) was performed using a RDA III rheometer (TA Instruments). A specified amount of polymer was cast on a circular silicon release paper (diameter = 25 mm). The sample was put under fume hood until dry. The sample thickness was 1.7 ± 0.2 mm. The DMA measurements were done at room temperature in frequency sweep mode from 0.1 - 80 Hz; measured values had a 10% uncertainty.

3.3 Results and Discussion

Several batch emulsion polymerizations were conducted to achieve a final stable polymerization formulation (Table 3.1). In preliminary experiments, a previously devised

formulation [11] with a relatively high KPS concentration (0.38 phm), along with a sodium bicarbonate buffer was selected and resulted in latex coagulation for a range of CNC contents (from 0.1 - 2 phm) (Table A.1-A.6). Because of these results, the interaction of each reactant with CNC was studied in the same proportions in the formulation noted above. Particle sizes were measured for various mixtures of CNC dispersed in water with each component at room temperature (Figure 3.2). Initially, KPS was omitted from these tests. Measurements were taken at 30 and 180 min for the mixtures, which were stirred constantly using a magnetic stir bar. It appeared that the buffer and emulsifier both interacted with the CNC under these conditions, leading to the formation of aggregates. All of the mixtures remained transparent throughout the procedure except for mixture #7, which became turbid. It was then decided to eliminate the buffer from future formulations and modify the way in which CNCs were charged to the reactor (Table A.7). Thus, each CNC dispersion was gradually charged to the reactor by a feed pump during the heating and mixing period, rather than fully charging all reaction components at the beginning.

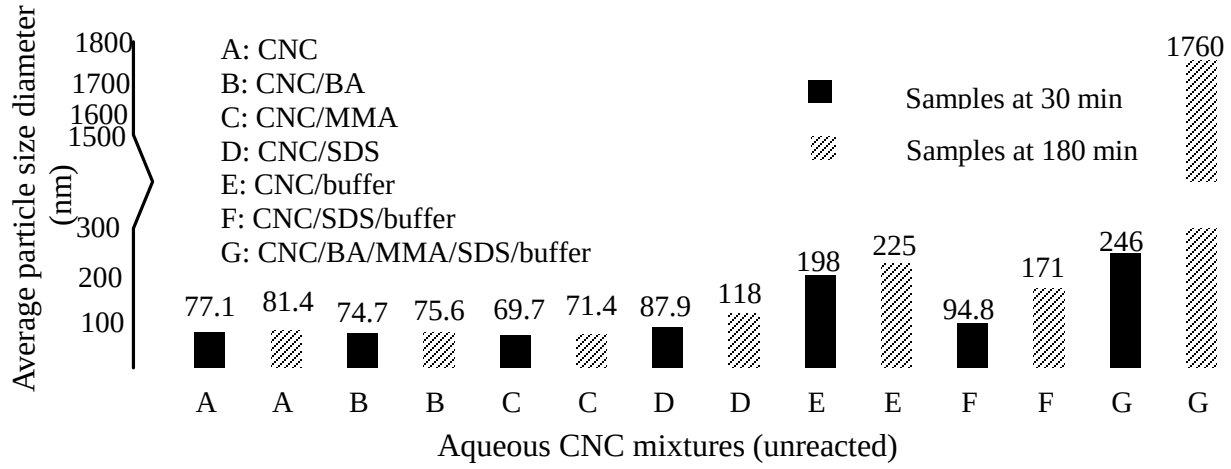

Figure 3.2 Interaction of CNC dispersions with component in reaction mixture.

The effect of initiator concentration on emulsion polymer latex coagulation is well understood.[12] KPS is an anionic initiator which can be considered as an electrolyte. Increased KPS concentration leads to increased ionic strength and subsequently, decreases the thickness of the electrical double layer surrounding the polymer particle surface, which results in particle coagulation. KPS is known to strongly interact with CNC through ionic interactions, which leads to a significant increase in mixture viscosity even at the early stages of polymerization.[13] This often rapid and strong increase in viscosity was noted in several of our experiments that resulted in coagulation (Table A.2-A.6). Because of concerns for destabilization of the emulsion polymerizations, we decreased the initiator content of our starting formulation from 0.38 to 0.1 phm (Table A.7). Further experiments showed that the maximum KPS concentration to achieve a stable emulsion under our conditions was 0.27 phm (Table A.15).

Surfactants common in emulsion polymerization, including anionic (EF-800 & SDS), cationic (CTAB), and combinations of ionic/non-ionic (EF-800/Disponil & CTAB/Disponil) were selected to study their effect on latex stability in the presence of CNC. The KPS content was kept constant (0.1 phm) while the amount of total surfactant was varied from 1 to 1.5 to 2 phm (Table A.9-A.12). All attempts led to coagulation except for the runs using SDS at 1.5 and 2 phm. The latex coagulation can be attributed to the complex ionic interaction of the emulsifiers with CNCs in the reaction mixture; which extends beyond the present study. In summary, at 2 phm CNC loading, the maximum solids content was 34 wt.% and the SDS concentration was 2 phm; at 1 phm CNC loading, the maximum solids content was 41 wt.% at SDS concentration of 1.5 phm (Table A.13 and A.14).

The remaining discussion reports on batch emulsion polymerization formulations with CNC loadings ranging from 0 to 2 phm. In these formulations (Table 1), the KPS and SDS concentrations were kept constant.

3.3.1 Latex particle size and monomer conversion profile

The particle size of the CNCs in the initial aqueous CNC dispersions was measured (78 ±3 nm, PDI = 0.135) prior to the polymerization. DLS characterization for all CNC dispersions confirmed the absence of agglomerates, thus the CNC was well dispersed in all cases (Figure 3.3). The latex particle size was also monitored during polymerization. Particle size tracking at the early stages in the polymerization revealed potential coagulation issues. The final polymer particles in the latexes varied between 88 and 92 (±3) nm (PDI = 0.045-0.053), essentially showing that CNC incorporation during polymerization did not affect the latex particle size (e.g., Figure 3.4). This is not surprising given the low amounts of CNC in the formulations. Particle size distribution was narrow for all cases, essentially monodisperse, which indicates that the resulting latexes were coagulum free. Because the particle size did not vary with CNC loading, the monomer conversion was also insensitive to CNC content (Figure 3.5). Final conversions between 94 and 96 wt.% were achieved. Attempts to identify the location of the CNC relative to the particles was attempted using TEM. Because of the low CNC loadings and further dilution required of the TEM method, it was not possible to identify a precise location of the CNCs. However, it is unlikely that the CNCs would be found at the particle cores.

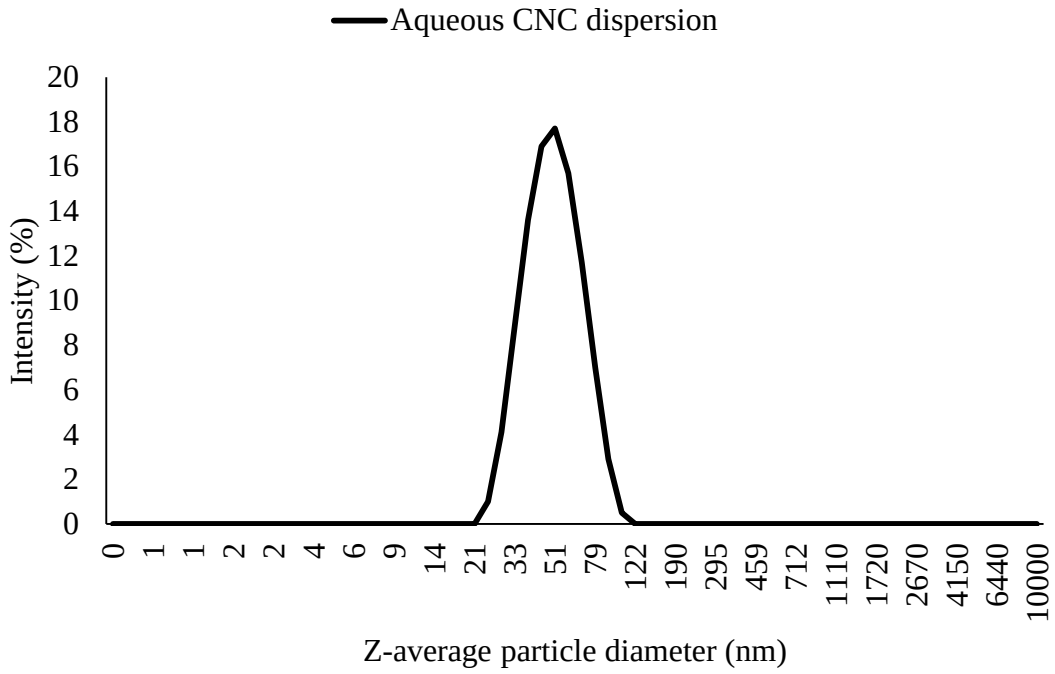

Figure 3.3 Particle size of CNC aqueous dispersion.

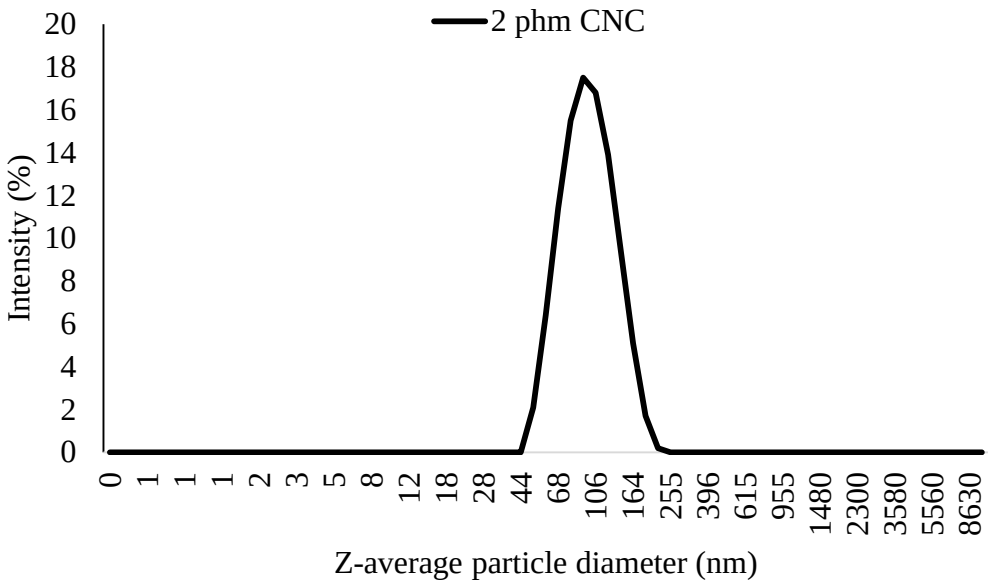

Figure 3.4 Particle size of CNC latex for 2 phm CNC loading.

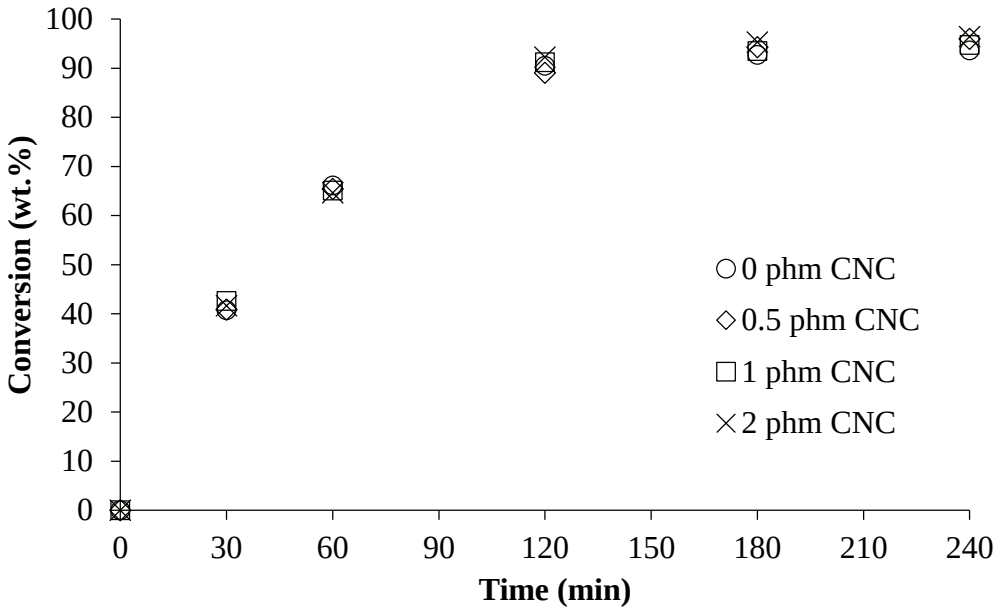

Figure 3.5 Overall monomer conversion vs. time for emulsion polymerizations with different CNC loadings.

3.3.2 Gel content and glass transition temperature

The gel content represents the insoluble, cross-linked portion of the polymer. As shown in Table 3.2, the gel content of the latexes increased with increasing CNC content. This provides some evidence for crosslinking of the CNC with the polymer matrix which can be induced by graft copolymerization. The formation of radicals on cellulose surfaces by KPS has been reported.[14–16] Ghosh *et al.* [14] proposed a mechanism for graft copolymerization on cellulose through its hydroxyl groups:

$$S_2O_8^{2-} \rightarrow 2\ SO_4^{\bullet -} \quad (1)$$

$$S_2O_8^{2-} + \text{Cellulose-OH} \rightarrow \text{Cellulose-O}^{\bullet} + SO_4^{\bullet -} + HSO_4^{-} \quad (2)$$

They reported that although the primary free radical $SO_4^{\cdot-}$ (Reaction 1) initiated the polymerization, the lower active radicals $S_2O_8^{2-}$ could abstract hydrogen from the hydroxyl group and create active sites on the cellulose surface for graft copolymerization as shown in reaction (2).

Mirsa *et al.* [15] proposed two different pathways for $SO_4^{\cdot-}$ reactivity with cellulose:

$$SO_4^{\bullet-} + \text{Cellulose-OH} \rightarrow \text{Cellulose-O}^{\bullet} + HSO_4^{-} \quad (3)$$

$$SO_4^{\bullet-} + H_2O \rightarrow HSO_4^{-} + OH^{\bullet} \quad (4)$$

$$OH^{\bullet} + \text{Cellulose-OH} \rightarrow H_2O + \text{Cellulose-O}^{\bullet} \quad (5)$$

$SO_4^{\cdot-}$ can directly react with hydroxyl groups on cellulose (Reaction 3) to generate free radicals which may initiate graft polymerization from the cellulose. Alternatively, they can react with water (Reaction 4) to form $OH^{\cdot-}$ which could also initiate graft polymerization on the cellulose backbone (Reaction 5). Zhou *et al.* [16] recently reported the multifunctional crosslinking activity of CNCs with polymers which they attributed to the participation of surface hydroxyl groups in the polymerization reaction *via* the above mechanisms.

Table 3.2 Gel content of poly(BA/MMA) latexes with different CNC loadings.

CNC loading (phm)	Gel content (wt.%)
0	28.4±1.9
0.5	53.3±2.3
1	62.1±1.7
2	68.5±2.5

DSC measurements of the base latex (i.e., CNC loading of 0 phm) and CNC latex nanocomposites were performed (Table 3.3). Only a single transition was detected for each case. The addition of CNC to the formulation shows a slight tendency towards increasing T_g. No significant differences between the T_g of the base latex and that of the CNC latex nanocomposites were observed. Similar T_g results for CNCs from bacterial cellulose, wheat straw, and tunicin in polymer composites were reported.[1,3,7] It is possible that increased crosslinking due to the CNCs restricts polymer chain mobility, thus resulting in increased T_g. Given the low amounts of CNC in the latexes, it is not surprising that the results show only minor differences.

Table 3.3 T_g of poly(BA/MMA) latexes with different CNC loadings.

CNC loading (phm)	**T_g (^OC)**
0	-42.2
0.5	-41.7
1	-41.4
2	-40.1

3.3.1 Dynamic mechanical analysis

According to the DMA results, increasing CNC content caused an increase in the storage modulus (G', Figure 3.6) and loss modulus (G", Figure 3.7) while the tan δ (G"/G', Figure 3.8) decreased slightly (data exhibited a 10% uncertainty). Generally, an increase in G' is related to an increase in a polymer's elastic properties with frequency. As the molecular motion of the polymer chains was more restricted due to the CNC in the polymer matrix, the polymer showed a more elastic response with increasing CNC content. As discussed earlier, there is evidence of

crosslinking of CNC with the polymer and this supports the increased restrictions to motion observed in the DMA results. G" results, which correlate to a polymer's viscous behaviour or capacity for energy dissipation, were similar to that for G'. For all samples in the entire frequency range tested, G' was greater than G"; this indicates that the polymer's elastic behaviour prevailed over its viscous behaviour. This observation is consistent with the formation of three-dimensional networks by intermolecular interaction forces within stable dispersions, emulsions, and gels [17]. The ratio G"/G' (or tan δ) quantifies the balance between energy loss and storage. As expected in nanocomposite materials, adding the stiff filler (i.e., CNC) to the soft polymer matrix appears to decrease tan δ.[18] However, the decrease appears to be only significant at the highest CNC loading of 2 wt.%.

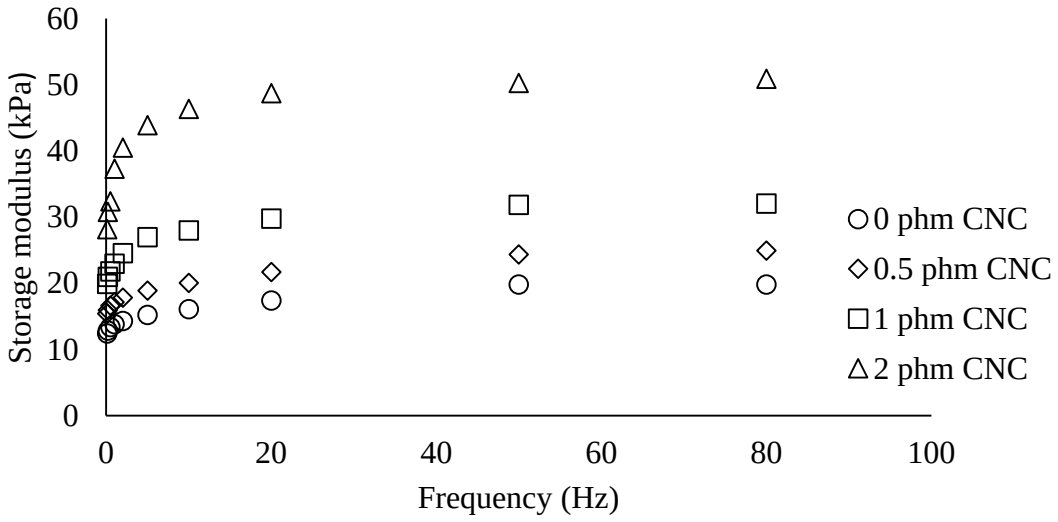

Figure 3.6 Storage modulus vs. frequency for poly(BA/MMA) latexes with different CNC loadings.

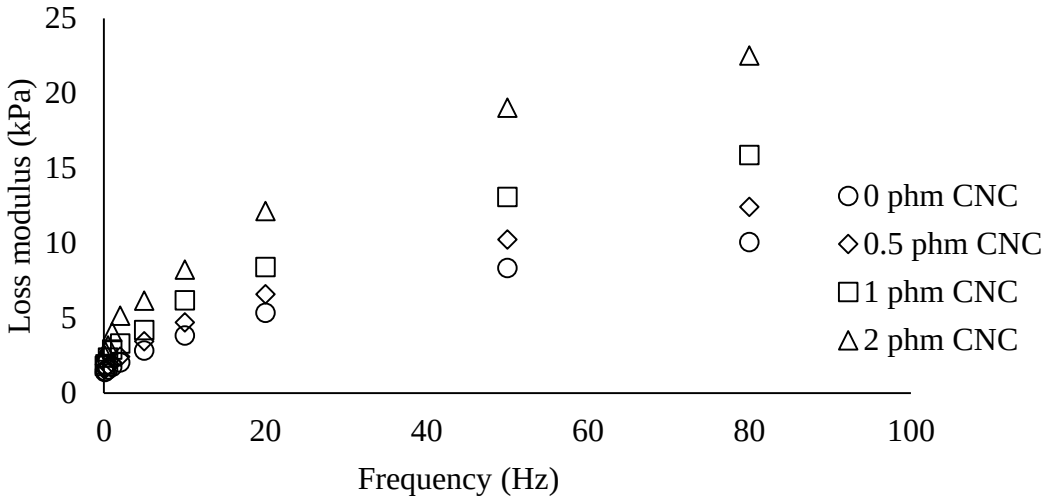

Figure 3.7 Loss modulus vs. frequency for poly(BA/MMA) latexes with different CNC loadings.

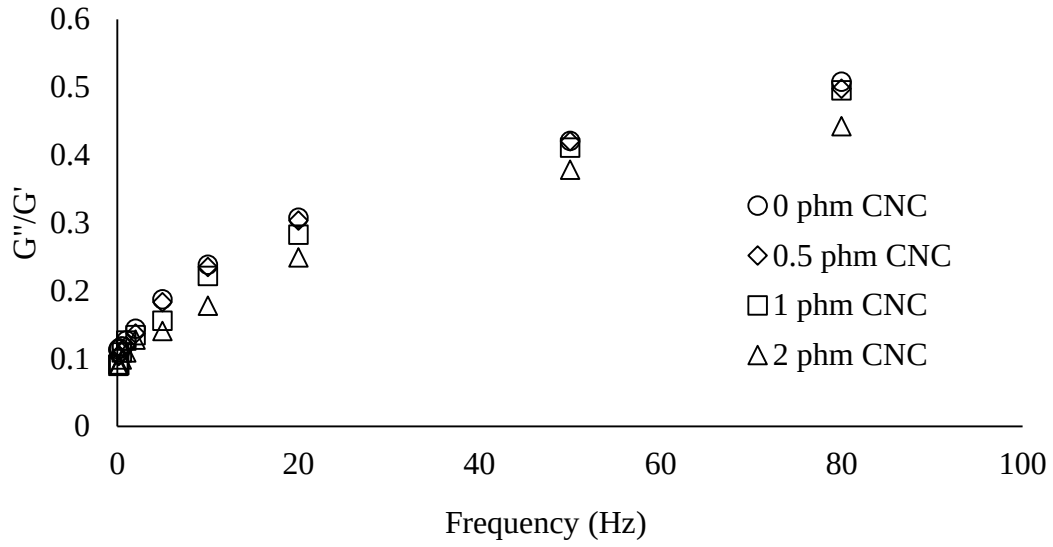

Figure 3.8 *Tan* δ vs. frequency for poly(BA/MMA) latexes with different CNC loadings.

The 2 phm CNC latex nanocomposite showed a 2.7-fold increase in G' compared to the base latex at a shear rate of 1 Hz. This is a significantly larger increase than that reported for silica latex nanocomposites.[19,20] Wang et al. [19] synthesized a MPS-silica/acrylate composite latex via semicontinuous emulsion polymerization. The G' of the composite latex containing 6.75 wt.% silica showed a 1.7-fold increase compared to their base latex without silica. Khalina et al. [20]

reported on the synthesis of acrylic/silica latex nanocomposites through miniemulsion polymerization. The G' of the nanocomposite containing 2 wt.% silica was 1.4 times that of the base latex. This indicates that the high crystallinity and aspect ratio of CNCs leads to improved mechanical reinforcement, even at low loadings, compared with other nanoparticles.

The influence of CNC loading on the flexibility or stiffness of the resulting latex nanocomposites can also be quantified with the complex modulus:

$$\text{Complex modulus} = \sqrt{(G'^2 + G''^2)} \quad (6)$$

The complex modulus was calculated for the frequency range of 0.1 to 10 Hz (Table 3.4). As expected, increasing the CNC loading resulted in stiffer nanocomposites due to the interaction (i.e., crosslinking) of the CNC with the polymer matrix.

Table 3.4 G', G", and complex modulus of nanocomposites with different CNC loadings at different frequencies. Data showed a 10% experimental error.

	Storage modulus (kPa)			Loss modulus (kPa)			Complex modulus (kPa)		
Frequency (Hz)	0.1	1	10	0.1	1	10	0.1	1	10
0 phm CNC	12.4	13.8	16.1	1.4	1.8	3.8	12.5	13.9	16.6
0.5 phm CNC	15.4	17.2	20.1	1.6	2.0	4.7	15.5	17.3	20.6
1 phm CNC	19.9	23.0	28.0	1.8	3.1	6.2	20.0	23.2	28.7
2 phm CNC	28.2	37.4	46.4	2.5	4.1	8.2	28.3	37.6	47.1

3.3.2 Viscosity

The latex viscosity increased with CNC content (Table 3.5). CNC aqueous dispersions on their own can lead to high viscosity, but this is at CNC loadings well above that used in this study. The addition of CNC to the base case latex as a blend at the levels used in this study showed no increase in viscosity. It was only when the CNC was included in the polymerization in situ that the viscosity increase was observed. Thus, the increased viscosity was likely a result of a thickening effect arising from intermolecular interactions between the hydroxyl groups on the CNC surface and the carbonyl groups of the acrylic polymer. A similar effect of nanofillers, such as nanosilica and nanosized alumina, on nanocomposite viscosity was reported by Khalinia *et al*. [20] and Hanemann.[21] Hanemann [21] compared the flow behaviour of microsized versus nanosized polyester resin/alumina composites. He showed that filler size, and particularly its specific surface area, had a significant impact on the viscosity of the composite material. As such, with increasing specific surface area for the microsized polyester resin (34 m^2/g) to its nanosized counterpart (107 m^2/g), the viscosity increased significantly and the maximum attainable nanofiller load was greatly decreased. Not surprisingly, the large specific surface area of CNC (ca. 533 m^2/g) [1] resulted in very high latex viscosity at low loading (i.e., 1 and 2 phm; Table 3.5). In addition, inter-particle crosslinking in latex polymer systems is known to increase polymer viscosity.[22] Thus, the crosslinking of CNC with the polymer could also be a contributing factor to the viscosity increase. In summary, the intermolecular interactions between the CNC and the polymer, the high specific

surface area of the CNC, and the increased crosslinking may all contribute to the significant viscosity increase.

Table 3.5 Nanocomposite viscosity of poly(BA/MMA) latexes with different CNC loadings.

CNC loading (phm)	Viscosity (mPa.s)
0	56
0.5	63
1	167
2	339

The complex viscosity of the dried nanocomposite films was calculated from DMA data using the complex modulus divided by the frequency. The complex viscosity profiles (Figure 3.9) show that nanocomposite viscosity increased with CNC loading, particularly at lower frequencies. A shear thinning behaviour was also observed, as would be expected for most polymers and anisotropic particles.[23]

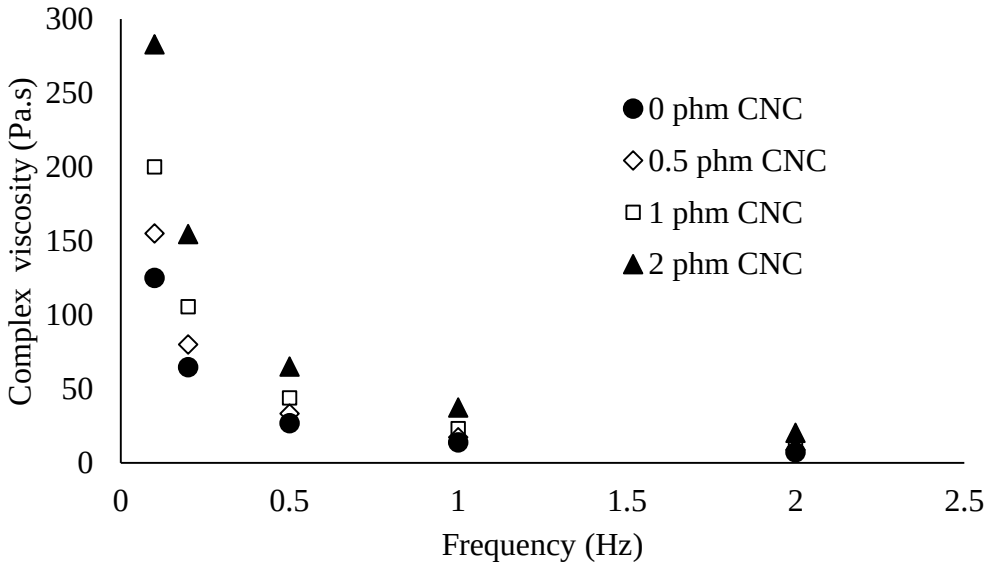

Figure 3.9 Complex viscosity vs. frequency of the dried nanocomposite films for different CNC loadings.

3.3.3 Conclusion

A stable *in situ* nanocomposite emulsion polymerization formulation was achieved, after several modifications on a preliminary polymerization formulation, with CNC loadings ranging from 0.1 to 2 phm. Modifications to the formulation included the removal of buffer, decreasing the KPS amount from 0.38 to 0.1 phm, and varying the SDS concentration associated with CNC loadings and solids content. Furthermore, unlike typical *in situ* emulsion polymerization procedures, the CNC dispersions were gradually charged to the reactor by a feed pump during the heating and mixing period rather than fully charging, which is done for the other components.

The gel content and viscosity increased significantly with CNC loadings. The gel content of latex nanocomposite at 2 phm CNC loading was 2.4 times that of the base latex (0 phm CNC), and the latex nanocomposite at 2 phm was almost 6 times more viscous than the base latex. Furthermore, DMA results showed that adding CNC to the polymer matrix increased the

nanocomposite material's elasticity. These observations were attributed to the crosslinking ability of the CNC surface hydroxyl groups due to KPS activation, intermolecular interaction between the CNC and polymer, and the high specific surface area of CNC.

It is evident that only small amounts of CNC are needed to significantly influence the latex mechanical properties. Given its non-toxic nature, CNCs appear to be an ideal component to influence latex properties as part of a more sustainable approach to polymer reaction engineering.

Acknowledgements: The authors gratefully acknowledge the financial support of CelluForce Inc. and the Natural Science and Engineering Research Council (NSERC) of Canada.

3.4 References

[1] R. J. Moon, A. Martini, J. Nairn, J. Simonsen, J. Youngblood, *Chem. Soc. Rev* **2011**, *40*, 3941.

[2] Y. Habibi, L. A. Lucia, O. J. Rojas, *Chem. Rev.* **2010**, *110*, 3479.

[3] M. A. S. Azizi Samir, F. Alloin, A. Dufresne, *Biomacromolecules* **2005**, *6*, 612.

[4] S. Beck-Candanedo, M. Roman, D. G. Gray, *Biomacromolecules* **2005**, *6*, 1048.

[5] A. Dufresne, *Nanocellulose: From Nature to High Performance Tailored Material*, Walter de Gruyter GmbH, Berlin, **2012**.

[6] Roman M. Toxicity of Cellulose Nanocrystals: Review. Ind Biotechnol 2015;11:25-33.

[7] A. Ben Elmabrouk, T. Wim, A. Dufresne, S. Boufi, *J. Appl. Polym. Sci.* **2009**, *114*, 2946.

[8] A. Ben Mabrouk *et al.*, *Polym. Eng. Sci.* **2011**, *51*, 62.

[9] S. W. Zhang, S. X. Zhou, Y. M. Weng, L. M. Wu, *Langmuir*. **2006**, *22*, 4674.

[10] M. S. Reid, M. Villalobos, E. D. Cranston, *Langmuir*., DOI:10.1021/acs.langmuir.6b03765.

[11] M. A. Qie, L. Dubé, *Eur. Polym. J.* **2010**, *46*, 1225.

[12] B. Liu, Y. Wang, M. Zhang, H. Zhang, *Polymers (Basel).* **2016**, *8*, 55.

[13] J. Yang *et al.*, *J. Mater. Chem.* **2012**, *22*, 22467.

[14] P. Ghosh, D. Dev, A. K. Samanta, *J. Appl. Polym. Sci.* **1995**, *58*, 1727.

[15] B. N. Misra, I. K. Mehta, R. C. Khetarpal, *J. Polym. Sci. A Polym. Chem*. **1984**, *22*, 2767.

[16] C. Zhou, Q. Wu, Y. Yue, Q. Zhang, *J. Colloid Interface Sci.* **2011**, *353*, 116.

[17] O. Yilmaz, C. N. Cheaburu, G. Gülümser, C. Vasile, *Eur. Polym. J.* **2012**, *48*, 1683.

[18] V. G. Gregoriou, G. Kandilioti, S. T. Bollas, *Polymer (Guildf).* **2005**, *46*, 11 .

[19] N. Wang *et al.*, *J. Appl. Polym. Sci.* **2009**, *113*, 3113.

[20] M. Khalina, M. Sanei, H. S. Mobarakeh, A. R. Mahdavian, *Int. J. Adhes. Adhes.* **2015**, *58*, 21.

[21] T. Hanemann, *Ceram. Int.* **2008**, *34*, 2099.

[22] B. Gebben, H. W. A. van den Berg, D. Bargeman, C. A. Smolders, *Polymer (Guildf).* **1985**, *26*, 1737.

[23] L.A. Utracki, in Rheological Fundamentals of Polymer Processing, (Eds: J.A Covas, J.F. Agassant, A.C. Diogo, and K. Walters), Kluwer, Academic Publishers, Dordrecht **1995**, 113.

Chapter 4:

PSAs Property Modification Using CNC

Pressure Sensitive Adhesive Property Modification Using Cellulose Nanocrystals

Zahra Dastjerdi, Emily D. Cranston, Marc A. Dubé*

Abstract: The impact of cellulose nanocrystals (CNCs) as a property modifier for pressure sensitive adhesives (PSAs) was investigated. Stable CNC/poly(n-butyl acrylate-co-methyl methacrylate) latex nanocomposites with different CNC loadings ranging from 0.25 to 1 wt.% (based on monomer weight) were synthesized by both an *in situ* seeded semi-batch polymerization and a blending technique. The PSA films obtained from both techniques demonstrated a concurrent enhancement of shear strength, tack, and peel strength with increasing CNC content. However, the performance enhancement for the PSAs prepared via the *in situ* technique were substantially greater: increases of up to 3.8x for tack, 6x for peel strength and 20x for shear strength for the *in situ* technique compared to increases of up to 2.4x for tack, 1.5x for peel strength and 6.4x for shear strength for the blending technique. The difference in mechanical performance of the CNC/PSA films synthesized via the *in situ* technique vs. blending was a result of better interaction of CNCs with the polymer matrix during both latex synthesis and film formation.

4.1 Introduction

Pressure sensitive adhesives (PSAs) are viscoelastic materials which adhere instantly to a substrate with light pressure and are easily removed without leaving an adhesive residue [1]. PSAs find application in a wide range of products such as tapes, labels, protective films and medical products. PSA performance depends on the polymer's microstructural properties such as molecular weight distribution, glass transition temperature (T_g) and gel content which are mainly influenced by monomer composition and reaction conditions [2,3]. Acrylic-based PSAs typically consist of a low T_g monomer such as butyl acrylate (BA, T_g = -54 ^oC) and a high T_g monomer such as methyl methacrylate (MMA, T_g = 115 ^oC). The low T_g monomer provides adhesive strength to the PSA while the high T_g monomer imparts cohesive strength [1].

The performance required of PSAs is determined by the desired application. The mechanical performance of PSAs is usually evaluated by tack, peel strength, and shear strength. Tack is greatly influenced by the wetting capability of the PSA to the substrate, and it reflects how quickly a PSA sticks to a substrate under short contact. Peel strength measures the bond strength between a PSA and a substrate after applying the pressure necessary to wet the substrate. Shear strength is a measure of the internal or cohesive strength of the PSA. A balanced combination of tack, peel strength, and shear strength is required for optimal mechanical performance. [1]

PSAs are produced through hot melt, solution, and emulsion polymerization techniques [4]. Emulsion polymerization is preferred to solution polymerization due to the use of water in the reaction medium instead of organic solvents, for environmental reasons [5]. Higher molecular weight polymers are more easily achievable by emulsion polymerization compared to solution-based methods due to the high polymer concentration at the locus of polymerization (i.e., the polymer particles). The solvent-based polymers are often limited to lower molecular weights due

to the presence of unwanted chain transfer reactions as well as a lower local polymer concentration throughout the polymerization.

Although water-based PSA production is more environmentally friendly, the adhesive performance, particularly shear strength, is typically inferior to that of its solvent-based counterpart. Surfactants, commonly added to emulsion-based PSA formulations, reduce PSA performance due to the migration of ionic surfactant molecules from the bulk latex to the PSA film surface during the drying process [6–8]. In addition, during the drying process, a discrete gel network is formed by coalescence of the latex particles whereas, a continuous gel network occurs through improved chain entanglements in solvent-based PSAs, which leads to better mechanical performance [9,10].

In order to modify the mechanical performance of PSA films produced by emulsion polymerization, one can, for example, add microstructural modifiers such as crosslinkers and chain transfer agents to the reaction formulation. However, the improvement of one property (e.g., shear strength) often occurs at the cost of declining performance in another (e.g., tack). Nonetheless, various approaches have been undertaken to overcome this performance conundrum [11–14].

Fillers, including inert and reinforcing types, are usually added to a polymer matrix to reduce cost, and perhaps improve chemical resistance, and mechanical performance [15]. For PSA films, a number of nanofillers such as carbon nanotubes, nanoclay, nanosilica, and nanoTiO_2 have been shown to positively influence composite material properties [16–23]. For instance, the addition of surface modified carbon nanotubes at small amounts (0.3 wt.%) greatly improved the viscoelastic properties and adhesion energy of emulsion-based PSAs by 65 and 85%, respectively [16]. Attempts to improve the adhesive properties of emulsion-based PSAs using nanosilica have also been reported [22]. Increased nanosilica content resulted in increases to tack of 250 and 300%

at 2 and 4 wt.% nanosilica loadings, respectively. However, the peel strength showed a maximum at 2 wt.% nanosilica loading and worse performance at 4 wt.% loading compared to the base case, while shear strength worsened at 2 wt.% loading and increased at 4 wt.% loading.

One interesting nanomaterial is cellulose nanocrystals (CNCs). CNCs are rod-like nanoparticles most commonly extracted from plant-based products (e.g., wood pulp) via controlled acid hydrolysis [24]. Strong acids, such as sulfuric acid and hydrochloric acid, readily break down the more accessible disordered regions in the cellulose microfibrils while the crystalline domains remain largely intact. When sulfuric acid is used, some of the hydroxyl groups on the CNC surface are substituted with anionic sulfate half-ester groups and this consequently makes the CNCs colloidally stable as dispersions in water. In addition, the presence of hydroxyl groups on the CNC surface offers reactive "handles" for further surface functionalization such as esterification, etherification, silylation, or polymer grafting, which can improve CNCs' compatibility and dispersibility, and facilitate their incorporation into different polymer matrices [25]. High axial elastic modulus, high aspect ratio, low density, renewability and non-toxicity of CNCs make them ideal candidates as nano-reinforcing materials for polymer matrices [26].

The use of CNCs as a property modifier has been investigated in a wide range of natural or synthetic polymers such as natural rubber (NR) [27,28], cellulose acetate butyrate (CAB) [29], poly(lactic acid) (PLA) [30,31], polyurethane [32,33], acrylic films [34–36], and epoxy emulsions [37]. There are different processing techniques to incorporate CNCs into polymer matrices such as blending, *in situ* reaction (e.g., grafting), melt mixing, and in aqueous or non-aqueous media. The appropriate processing technique is determined by the nature of the polymer and the final application [38,39].

For aqueous polymer systems, aqueous CNC dispersions can be added to water-soluble polymers (e.g., polyvinyl alcohol (PVA)), hydro-dispersible polymers (e.g., carboxymethyl cellulose (CMC)) or polymer latexes through blending and *in situ* reaction techniques [40–42]. Favier et al. [34] prepared the first CNC nanocomposite over 20 years ago, spurring an entirely new research thrust. In their seminal work, CNCs and latex were combined via the blending technique. The mechanical measurements showed that the storage modulus of the styrene/butyl acrylate (35/65 % w/w) copolymer matrix was significantly improved with CNC loadings as low as 1 wt.%. Subsequent efforts using the same copolymer system investigated the effect of CNCs obtained from wheat straw [35,43] or tunicin [43]. The resulting nanocomposites displayed noticeably enhanced mechanical properties even at low CNC contents. The strong hydrogen bonding ability between CNCs (and mechanical percolation) was proposed as the governing mechanism behind the formation of a rigid network in the nanocomposite films. More recently, Vatansever et al. [44] reported the synthesis of CNC reinforced poly(BA-co-MMA) via blending with different CNC contents up to a maximum of 3 wt.%. The thermal, barrier, and mechanical properties (e.g., tensile strength) of the nanocomposites were enhanced with increasing CNC content. However, in none of the above cases was adhesive performance measured.

Aqueous CNC dispersions can be incorporated in a polymer composite through *in situ* emulsion polymerization, which is also economically favourable. The synthesis of stable CNC/latex dispersions was reported via miniemulsion polymerization by adding a reactive monomer, ϒ-methacryloxypropyl triethoxysilane (MPS), to the polymerization formulation [45,46] or by tailoring CNC-surfactant interactions [47]. It was reported that the addition of CNCs improved the storage modulus of nanocomposite films in the rubbery state [45,46] and could be used to tailor the polymer molecular weight and the latex size and surface charge [47], respectively.

Most recently, partially disintegrated nanocellulose fibres (different from the well-defined CNCs used here) were added to a suspension polymerization of 2-ethyl hexyl acrylate for adhesive applications [48].

We recently reported on an *in situ* batch emulsion polymerization technique for the incorporation of CNCs into a latex polymer [49]. Having overcome a number of stability challenges, an approach using CNCs in a seed formulation is proposed. In this study, we successfully synthesized CNC/latex nanocomposites via *in situ* seeded semi-batch emulsion polymerization for application as PSAs. The impact of CNC loading on the mechanical and adhesive performance of the PSA films is evaluated and compared to CNC nanocomposite films obtained via blending.

4.2 Experimental methods

4.2.1 Materials

n-Butyl acrylate (BA) and methyl methacrylate (MMA) monomers, sodium dodecyl sulfate (SDS) anionic surfactant, potassium persulfate (KPS) initiator, allyl methacrylate (AMA) crosslinking agent, 1-dodecanethiol (NDM) chain transfer agent, and hydroquinone (HQ) inhibitor were all purchased from Sigma Aldrich. All the above chemicals were reagent grade and were used as received. Tetrahydrofuran (THF, HPLC grade) was obtained from EMD Chemicals. Poly (vinylidene fluoride) (PVDF) membrane filters with a pore size of 5.0 µm were purchased from EMD Millipore. Distilled deionized (DDI) water was used throughout all experiments. CNCs were obtained from CelluForce (Windsor, QC, Canada). Ashless Whatman filter paper (grade 542) was purchased from Fisher Scientific. Nitrogen gas was purchased from Linde Canada. Melinex$^{@}$ 453 polyethylene terephthalate (PET) films were obtained from Tekra.

4.2.2 Aqueous CNC dispersion preparation

A specified amount of spray dried CNC (0.25-1 wt.% based on total monomer weight) was dispersed into the required amount of DDI water and stirred with a magnetic stir bar for 2-4 h depending on the CNC concentration until it appeared to be well-dispersed according to visual inspection. Afterwards, the dispersion was sonicated using a Sonic Dismembrator Ultrasonic processor (500 W with 65% amplitude) for 15 min in an ice bath to avoid overheating. Finally, the CNC dispersion was filtered through ashless Whatman 542 filter paper by vacuum filtration.

4.2.3 CNC latex nanocomposite preparation

CNC latex nanocomposites were prepared via both blending and *in situ* seeded semi-batch emulsion polymerization. All polymerization reactions were performed in a jacketed 1 L stainless steel LabMax™ (Mettler Toledo) reactor. The reactor was equipped with a nitrogen purge line, an anchor stirrer, a sampling line, a reflux condenser with a vent line, and two separate feed pumps. The reaction temperature (65 ^{o}C) and stirring speed (250 rpm) were controlled by iControl LabMax software during polymerization.

A seeded, semi-batch emulsion polymerization approach was employed to produce base latex (0 phm CNC) for blending and all CNC latex nanocomposites. The polymerization process included three stages: a batch stage to produce seed latex particles, a continuous feeding stage to grow the latex particles, and a cook stage to react any remaining monomer. A stable latex formulation reported previously [49] for batch polymerization was modified for the seeded semi-batch approach used here. The BA/MMA weight ratio (90/10 w/w), and initiator amount were kept constant for all runs (Table 4.1). The SDS concentration in the seed stage was varied due to the changing amount of water (the amount of water in turn varied with CNC concentration) to achieve a more or less constant seed particle size from run to run. As a result, different final latex solids

contents ranging from 40 (for 1 wt.% CNC loading) to 50 wt.% (for 0 wt.% CNC loading – base case) were achieved.

Table 4.1 *In situ* semi-batch polymerization formulation.

Component	**Latex seed (g)**	**Monomer emulsion feed (g)**	**Initiator feed (g)**	**Total (g)**	**Total (phm)***
n-Butyl acrylate (BA)	19.8	178.2	-	**198**	**90**
Methyl methacrylate (MMA)	2.2	19.8	-	**22**	**10**
Potassium persulfate (KPS)	0.06	-	0.54	**0.6**	**0.27**
Sodium dodecyl sulfate (SDS)	0.36-0.7	2.6	-	**2.96 - 3.3**	**1.35-1.5**
Cellulose nanocrystals (CNCs)	0-2.2	-	-	**0, 0.55 1.1, 1.65, 2.2**	**0, 0.25, 0.5, 0.75, 1**
Distilled de-ionized (DDI) water	40-95[a]/ 0-165[b]/3[c]	68	54	**220-330**	**100-150**

[a]Water used for SDS solution in seed production stage
[b]Water used for aqueous CNC dispersion
[c]Water used for initiator solution in seed production stage
*phm= parts per hundred parts monomer

To begin, a SDS solution and aqueous CNC dispersion were charged to the reactor at room temperature (Latex seed, Table 4.1). The stirring speed was set to 250 rpm and maintained throughout the run. The reactor was then purged with nitrogen and the reactor temperature increased to 60^{o}C (within 30 min). Next, the monomer mixture and initiator solution were charged to the reactor (Latex seed, Table 4.1). The temperature was then increased to 65^{o}C within 5 min, and the seed stage was continued for 30 min. After completion of the seed stage, the monomer emulsion feed and initiator feed (Table 4.1) were charged separately to the reactor using two feed pumps at constant rates and feeding times of 3.5 and 4 h, respectively. At the completion of the feed stage, the polymerization was allowed to proceed for an additional 60 min to increase the

monomer conversion (cooking stage). Additional runs containing a crosslinker and chain transfer agent without CNC were also prepared for comparative purposes. In those cases, the base case polymerization formulations (Table 1) had 0.44 g of AMA and/or 0.44 g of NDM in the monomer emulsion feed.

To prepare CNC latex nanocomposites via blending, 3 g of aqueous CNC dispersion (with different CNC concentration) were added to 12 g of base latex (Table 4.2); the resulting mixture was mixed vigorously with a magnetic stir bar for 30 min.

Table 4.2 Blend formulation.

CNC content in blended sample (phm)	BA/MMA latex (g)	CNC dispersion (g)	CNC dispersion (wt.%)
0.25	12	3	0.5
0.5	12	3	1
0.75	12	3	1.5
1	12	3	2

4.2.4 Latex and PSA Film Characterization

The monomer conversion was determined using a gravimetric method. The average particle sizes in the aqueous CNC dispersion and in the CNC/latex nanocomposites were measured using a Malvern NanoS Zetasizer dynamic light scatterer (DLS). The DLS measurement provides an *apparent* particle size for CNCs as they have a rod-like shape instead of a spherical one (and is only used to show relative changes in CNC size or degree of aggregation). Further characterization of CNC particles used in this work (i.e., sulfuric acid hydrolyzed CNCs from Celluforce) was reported by Reid et al. [50]. More details on the monomer conversion and DLS measurements are available in [49].

Samples of 0.05 g of dry polymer were sealed in PVDF membranes and immersed in 20 mL of THF. The samples in their pouches were left to swell under gentle shaking for 24 h at room temperature. The sample pouches were then dried in a fume hood until a constant weight was reached. The gel content was calculated as the ratio between the mass of dried sample after removing the soluble components and the mass of the initial polymer. The reported values were average of five samples with (±SD).

8-10 g of each *in situ* or blended latex was cast onto a 50 µm Melinex$^{@}$ sheet with a #30 Meyer rod. The cast films were dried at a controlled temperature (23 ± 1 ^{o}C) and relative humidity (50% ± 5) for 24 h prior to testing. The PSA film thickness was 36 ± 2 µm.

Dynamic mechanical analysis (DMA) was carried out using a RDA III rheometer (TA Instruments) with parallel plate geometry. Polymer samples were cast on circular silicon release paper (diameter = 25 mm, dry thickness = 1.7 ± 0.2 mm) and dried at room temperature (~1 week). All tests were performed at room temperature in the frequency sweep mode from 0.1-80 Hz; measured values had 10% uncertainty.

A VCA Optima Surface Analysis System (AST Products) was used to measure the static contact angle of the latex films. DDI water was used as the probe liquid. A micro syringe was set to automatically dispense a 1 µL liquid droplet on each film. The VCA software calculated right and left contact angles. For each sample, five different spots were measured with a measurement error of ±2.5^{o}.

Loop tack, 180^{o} peel strength and shear strength were measured at 23 ± 1^{o}C and relative humidity of 50% ± 5 according to the Pressure Sensitive Tape Council standards PSTC-6, PSTC-1 and PSTC-7, respectively [51]. A Universal Instron tester was used to measure the loop tack and peel strength of the PSA films, and home-built shear tester was used to measure the shear strength

of the PSA films. The average of five measurements with (±SD) was used in the analysis of adhesive performance.

A 1″ × 6″ strip was cut from the PSA film and formed into a loop with the adhesive side facing out-ward. Approximately 1″ at both ends of the strip was masked with tape and inserted into the upper grip of the Instron tester. The instrument moved the upper grip downward at a speed of 1 mm/s until an area of 1 $inch^2$ came into contact with the stainless steel substrate mounted into the lower grip. Next, the tester moved the upper grip upward at the same speed while recording the force needed to de-bond the loop from the substrate. The maximum force per meter necessary to remove the adhesive was reported as loop tack in N/m.

A 1″ × 5″ strip of the PSA film was used to measure peel strength. The strip was laminated onto a stainless steel substrate with the help of a 2040 g roll coater. The roll coater was passed through the film front-to-back twice (i.e., along the length of the film). The substrate and the strip were immediately inserted into the grips and the upper grip was set to move upward at a speed of 1 mm/s. The average force (N) per m required to peel the strip from the substrate was recorded and reported as peel strength at a peel angle of 180^o.

A 1" x 5" strip of the PSA film was laminated onto a stainless steel substrate with a contact area of 1/2" x 1/2" and then placed in the shear tester using a C-clamp. A 500 g weight was suspended at the end of the strip. The time needed for the PSA film to fall off the testing panel was recorded automatically as the shear strength using Labview™ software.

4.3 Results and Discussion

Overall monomer conversion vs. time data were similar for all runs with final conversions of 97 wt.% for all polymerizations (Fig. 4.1). The addition of CNCs had no impact on monomer conversion and rate of polymerization.

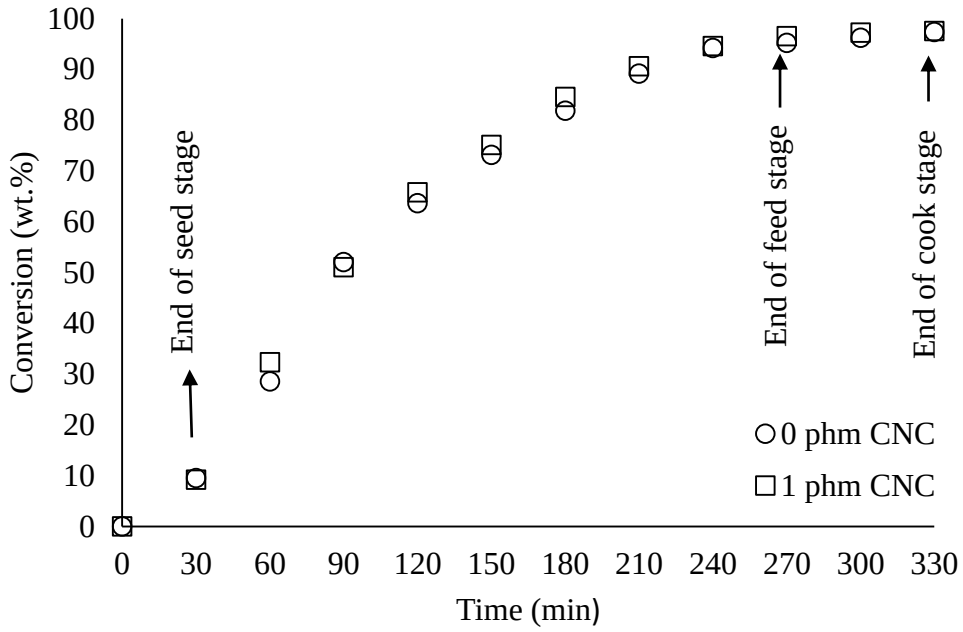

Figure 4.1 Overall monomer conversion vs. time for in situ semi-batch emulsion polymerization with no CNC compared to the highest CNC loading.

The latex particle size was measured during the course of the polymerization. The final latex particle size ranged from 153 (± 3) nm for the base latex (0 phm CNCs) to 167 (± 3) nm for the latex containing 1 phm CNCs. No latexes showed any visible coagulum and this was further confirmed by the monomodal nature and narrow particle size distribution measured by DLS for all latexes (see Appendix A). Thus, the CNC content had a negligible impact on latex particle size.

We believe that in the final CNC/latex dispersion that the majority of the CNCs remain colloidally stable in the water phase (as opposed to being localized at the latex interface or inside

the latex particles). The CNC particle size in dispersion was measured by DLS to be 78 (± 3) nm prior to polymerization and the rigid rod-shaped nanoparticles are known to be on average 100-300 nm long as measured by atomic force microscopy [50]. As the DLS output is heavily skewed by larger scatterers and the amount of CNCs is small compared to the latex, we assume that the DLS signal of the synthesized latexes is dominated by the latex particles and we do not expect to see a bimodal size distribution. As such, the 167 (± 3) nm size measured for the latex with 1 phm CNCs is not influenced by "free" CNCs in the dispersion. Furthermore, due to the relative size of the CNCs compared to the latex particles it is unlikely that CNCs are present at the latex interface because geometric constraints would dictate larger latex particles. This has been shown previously where oil-in-water emulsions stabilized by CNCs display oil droplet sizes that are 2-20 microns at the smallest [52,53]. Similarly, miniemulsion polymerization with CNCs and surfactants give PMMA particles that are microns in size when stabilized by CNCs and nanometers in size when stabilized by surfactant (with the CNCs dispersed in the water phase) [47]. Finally, due to the incompatibility of hydrophilic CNCs with the acrylate monomers and again, the fact that the length of most CNCs is larger than the latex particle diameter, we infer that CNCs are not incorporated *within* the latex particles. We do note however, that the measured latex dimensions do not rule out the possibility that a fraction of the CNCs may be loosely tethered to the latex particles.

A significant increase in gel content was observed with increasing CNC loading for the *in situ* latexes (Table 4.3). The gel content increase provides an indication of the degree of crosslinking of the latexes and may imply that some graft copolymerization of CNCs with polymers occurred through the CNC surface hydroxyl groups [49]. Various mechanisms for the initiation of a graft copolymerization reaction starting from the formation of free radicals on the cellulose backbone due to the KPS initiator have been presented previously [54–56].

Table 4.3 Gel content of poly (BA/MMA) latexes with different CNC loadings.

CNC loading (phm)	Gel content (wt.%)
0	33.3
0.25	45.6
0.5	56.4
0.75	57.6
1	61.6

DSC results for the base latex (0 phm CNC) and the CNC *in situ* latex nanocomposites are shown in Table 4.4. DSC thermograms showed one single transition for all samples with different CNC loadings (see Appendix A). The T_g increased slightly with increasing CNC content. The upward tendency of T_g suggests a restricted mobility of polymer chains which can be attributed to enhanced polymer crosslinking potentially via CNC graft copolymerization. Despite the consistent trend in the results, the changes are within experimental error.

Table 4.4 T_g of poly (BA/MMA) latexes with different CNC loadings.

CNC loading (phm)	T_g (ºC)
0	-40.4
0.25	-39.3
0.5	-39.1
0.75	-38.7
1	-38.3

The effect of CNC loading on the PSA film viscoelastic properties was investigated using DMA (Fig. 4.2). The storage modulus (G') represents the solid (elasticity) characteristic of the

PSAs while the loss modulus (G") represents the liquid (viscous flow) characteristics of the PSAs. PSA elasticity increased with increasing CNC loading due to the chain mobility restriction imposed by CNCs and possible related crosslinking. The G" also increased with increasing CNC content. For all samples, G" was lower than G' which revealed that the polymer elasticity dominated over viscous flow behavior. Furthermore, G' was below 0.3 MPa for all samples and this is consistent with high tack adhesion according to the Dahlquist criterion [57].

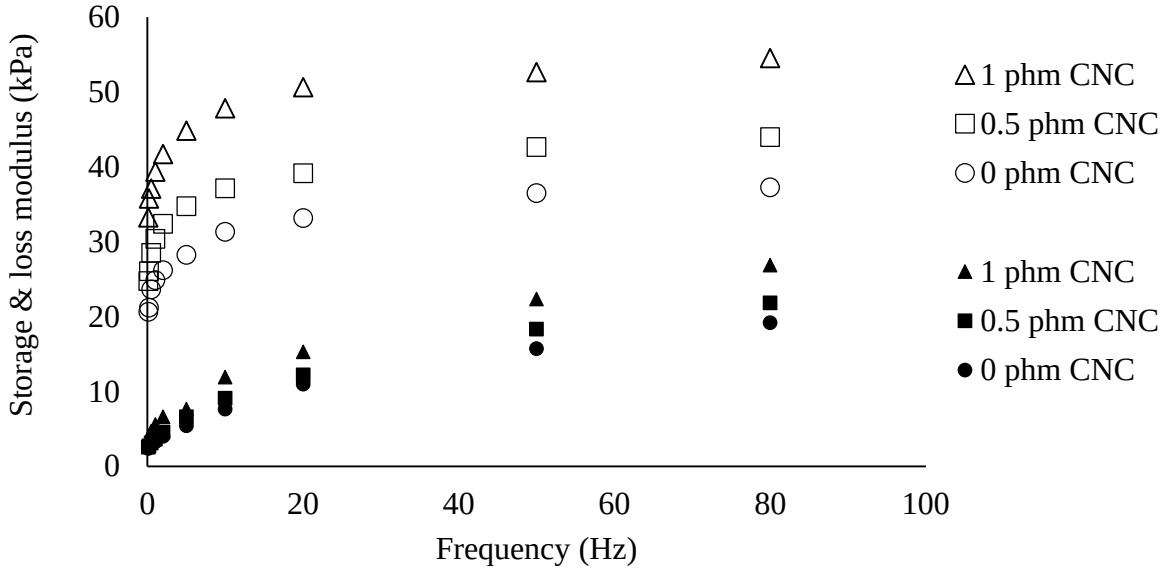

Figure 4.2 Storage modulus (open symbols) & loss modulus (closed symbols) vs. frequency for poly(BA/MMA) latexes with different CNC loadings.

The PSA performance of the dried films obtained via the *in situ* polymerization technique was evaluated using shear strength, loop tack, and peel strength. All three of these properties of the PSA films were noticeably improved with increasing CNC content (Fig. 4.3). The shear strength increased from 3 h for the base latex (0 phm CNC content) to 59 h for the CNC/latex (1 phm CNC content). The loop tack and peel strength results also showed four and six times increase, respectively, from 0 to 1 phm CNC loadings.

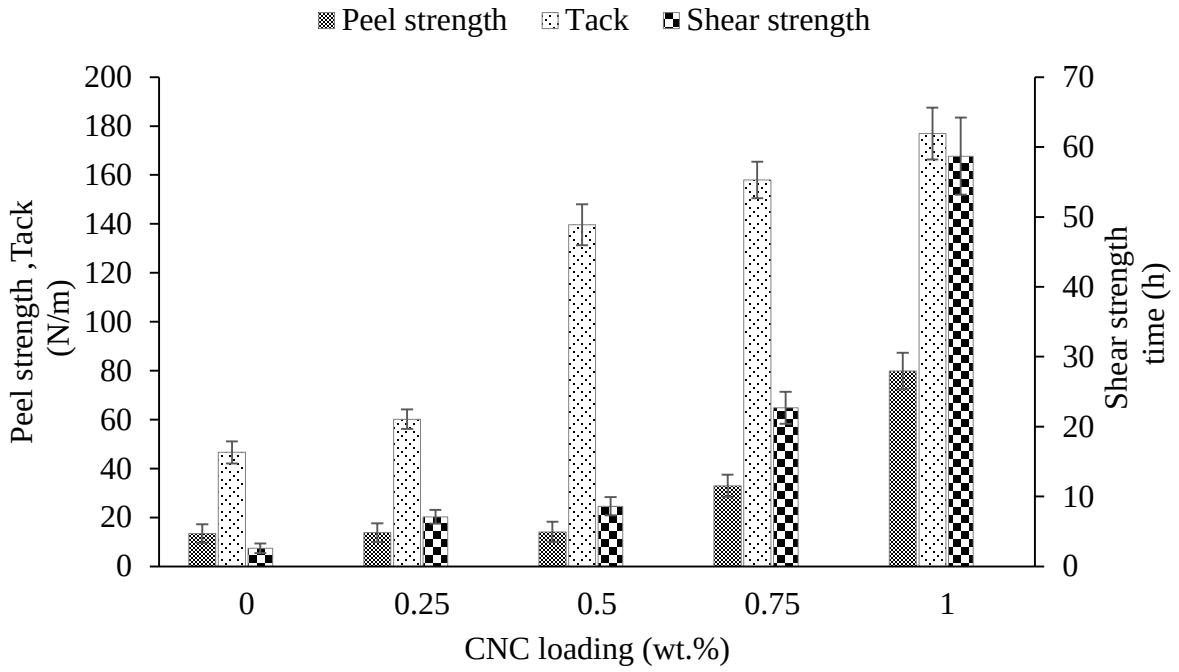

Figure 4.3 The effect of CNC loading in poly(BA/MMA) latexes on shear strength, tack, and peel strength.

The shear strength is an intrinsic property of PSAs and is influenced by the bulk properties of the polymer such as molecular weight, T_g, and crosslinking [2,3]. In particular, an increase in the number of polymer entanglements and/or crosslinking will increase the cohesive strength of the PSA, which is reflected in the shear strength measurement. The increase in shear strength is consistent with increased crosslinking, though not perfectly correlated, and could also be attributed to graft copolymerization with the CNCs (Fig. 4.4). A noticeable increase in shear strength at higher CNC loadings (> 0.5 phm) could also be related to hydrogen bond formation between CNCs at higher loadings in dried films [48].

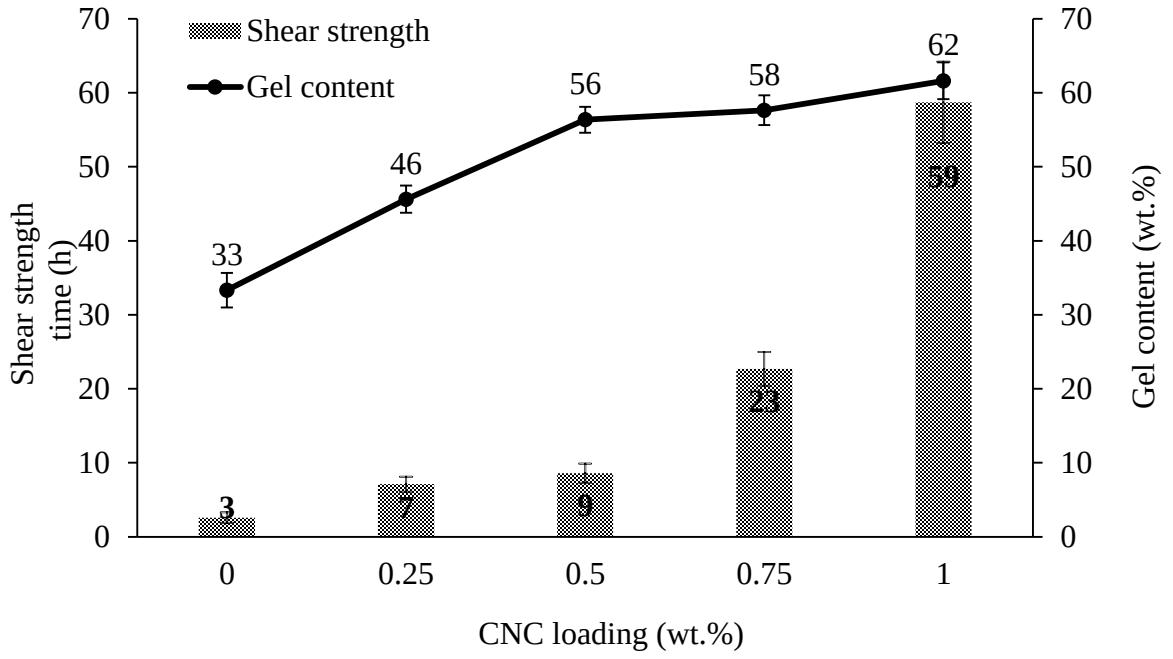

Figure 4.4 The effect of CNC loading in poly(BA/MMA) latexes on gel content.

Increases in both tack and peel strength were observed with increasing CNC loading (Fig. 4.3). Since the interfacial properties of the PSA films can influence tack and peel strength [2,3], contact angle measurements were performed to investigate the effect of CNCs on the surface tension of PSAs with the substrate. Contact angle measurements on all PSA films indicated that the CNCs increased the PSA films' hydrophilicity (because of the CNC surface hydroxyl groups) and thus improved the surface interaction of PSA films with the stainless steel test panel (Fig. 4.5). In most cases, improvement to peel strength and/or tack is achieved at the cost of diminishing shear strength [58]. In this work, adding CNCs to PSA latexes improved all three PSA properties. Kajtna & Sebenik [48] also reported the simultaneous enhancement of these three PSA properties when adding nanocellulose fibres to acrylic microspheres.

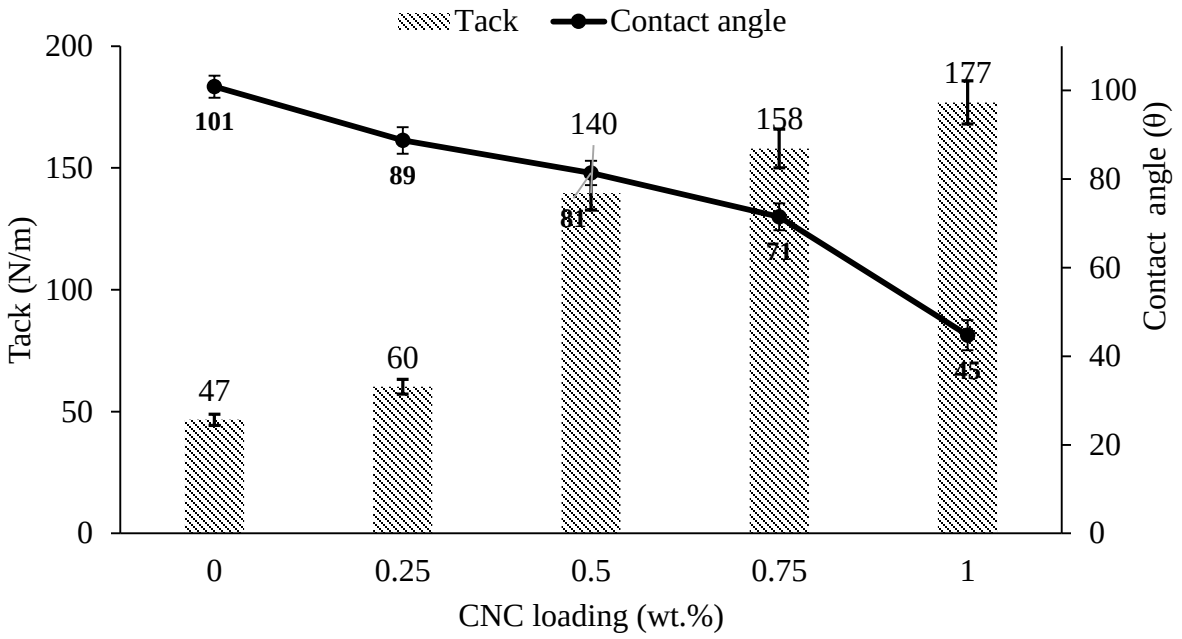

Figure 4.5 The effect of CNC loading in poly(BA/MMA) latexes on contact angle.

Because the adhesive performance of PSA films is a function of the PSAs' bulk properties, different approaches have been applied to modify adhesive properties by manipulating the microstructural properties of the polymer [11–14]. For example, the simultaneous manipulation of CTA and crosslinker has been used to affect PSA properties. We modified the base latex formulation with CTA (0.2 phm) and/or crosslinker (0.2 phm), to compare their adhesive performance with that of the CNC/latexes obtained by the *in situ* technique. The base latex modified with crosslinker only (no CNC) showed the lowest peel strength (8 N/m) and the base latex modified with CTA only (no CNC) exhibited the lowest shear strength (26 s) and unnecessarily high peel strength and tack (Table 4.5). The modified base latex with both CTA and crosslinker displayed a more balanced combination of these three properties. In comparison to the PSA film using the latex with the high CNC loading (1 phm), the peel strength and tack were close but the shear strength was far from adequate. One should keep in mind that the end use of a PSA

determines the required combination of shear strength, tack, and peel strength. For example, protective films, labels, and tapes often require a peel strength between 72-240 (N/m), tack in the range 60-160 (N/m), and shear strength between 0.1-35 (h) with a stainless steel substrate [1]. Thus, depending on the application target, it is evident that CNC/latex nanocomposites can achieve properties similar to other, more complex approaches but without the use of more hazardous additives such as NDM and AMA.

Table 4.5 PSA performance of latex films containing CTA/crosslinker and CNC/latex.

CNC content (phm)	Peel strength (N/m)	Tack (N/m)	Shear strength (h)
0	13	48	2.6
0.25	14	60	7.1
0.5	14	140	8.6
0.75	33	158	22.7
1	80	177	58.7
0 (+ 0.2 phm crosslinker)	9	41	4
0 (+ 0.2 phm CTA)	475	612	26 (s)
0 (+ 0.2 phm CTA and 0.2 phm crosslinker)	52	164	3.1

The adhesive performance of CNC/latexes obtained through a blending technique was also evaluated at different CNC loadings for comparison to the *in situ* polymerized latexes (Table 4.2, Fig. 4.6). As shown in Figure 4.6, the peel strength, tack, and shear strength for blends increased with increased CNC loading. Peel strength and tack were not greatly affected at low CNC loadings while significant changes were observed at CNC loadings greater than 0.5 phm. The adhesive performance of CNC/latex films obtained via blending showed less improvement compared to those synthesized via the *in situ* technique. This could be a result of the higher degree of interaction between the CNCs and the latex due to the longer contact time (5 h) at an elevated temperature (65

°C). This is in contrast to the preparation of the CNC/latex blends that were at room temperature for 30 min. CNCs are expected to agglomerate during film formation if they are not well distributed in the polymer matrix and/or have low compatibility with the hydrophobic polymer, however if CNCs are anchored to the polymer matrix they may remain more uniformly dispersed [46]. This supports the notion that grafting from CNCs occurred during the *in situ* polymerization, which may have served to anchor the CNCs to the polymer. Thus, a stronger effect of CNC loading would be expected in the PSA films produced from the *in situ* technique compared to the blend technique.

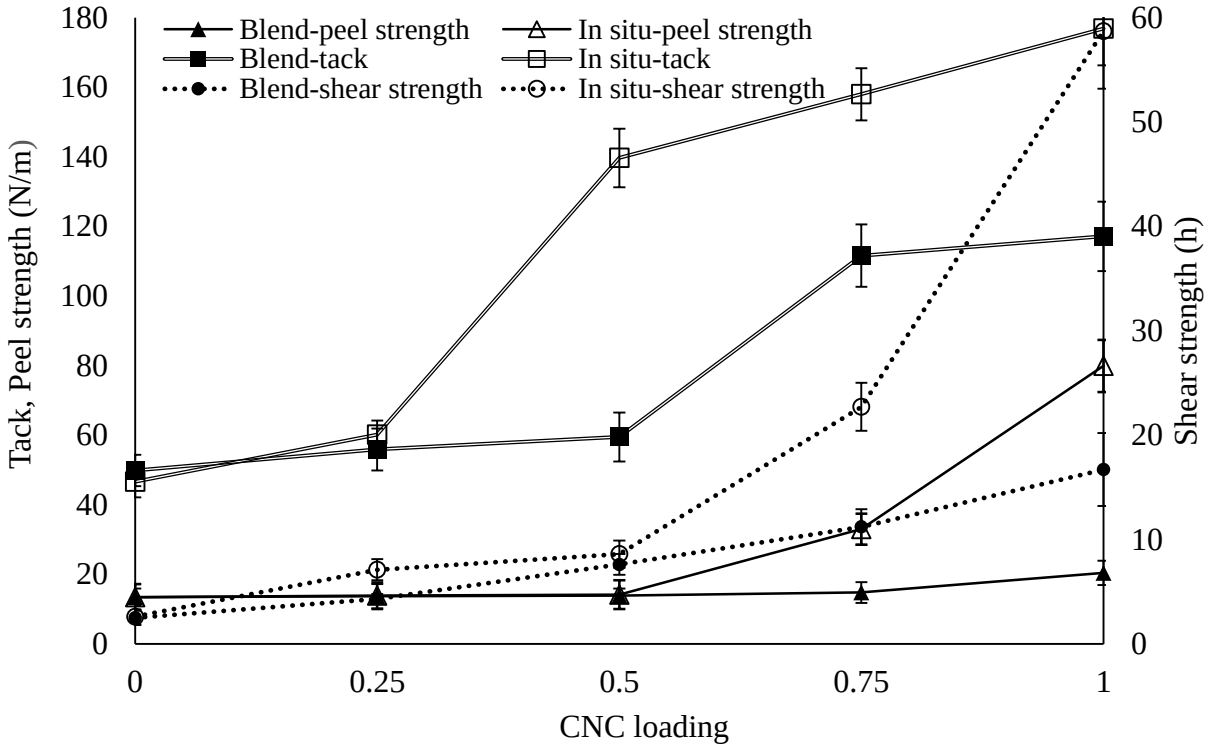

Figure 4.6 The effect of CNC loading in poly(BA/MMA) latexes on shear strength, tack, and peel strength. Closed symbols refer to samples from the blend technique while open symbols refer to samples produced using the in situ technique.

4.4 Conclusion

The mechanical performance of PSA films, specifically, shear strength, tack, and peel strength, was enhanced with increasing CNC loading either as a blended CNC/latex or as an *in situ* polymerized formulation. The increase in gel content along with CNC loading implied potential crosslinking activity of CNCs in the latex, which resulted in improved cohesive strength as reflected by an increased shear strength. Water contact angle results indicated that CNCs improved the surface interaction of PSA films with the stainless steel substrate and this resulted in increased tack and peel strength. The simultaneous increase in all three adhesive properties (as also confirmed by DMA results) for emulsion-based PSA films is an uncommon occurrence. This implies that beyond its safety and renewability, CNCs provide a solution to a well-known challenge in PSA production.

As noted above, the mechanical performance of PSA films prepared using a blending technique increased with CNC loading, but the PSA films resulting from the *in situ* technique showed significantly greater improvement, which we associate with the interaction of CNCs with the polymer matrix during the synthesis process for the *in situ* technique.

Acknowledgements: The authors gratefully acknowledge the financial support of CelluForce Inc., FPInnovations and the Natural Science and Engineering Research Council (NSERC) of Canada. We also acknowledge Michael Reid for providing the AFM image of CNC.

4.5 References

[1] Benedek I. Pressure-sensitive adhesives and applications. 2nd ed. New York: Marcel Dekker Inc; 2004.

[2] Jovanović R, Ouzineb K, McKenna TF, Dubé MA. Butyl acrylate/methyl methacrylate latexes: Adhesive properties. Macromol Symp 2004;206:43–56.

[3] Gower MD, Shanks RA. The effect of varied monomer composition on adhesive performance and peeling master curves for acrylic pressure-sensitive adhesives. J Appl Polym Sci 2004;93:2909–17.

[4] Satas D. Handbook of Pressure Sensitive Adhesive Technology. 2nd ed. New York: Van Nostrand Reinhold; 1989.

[5] Lovell, PA. ; El-Aasser MS. Emulsion Polymerization and Emulsion Polymers. New York: John Wiley & Sons, Chichester; 1997.

[6] Zosel A, Schuler B. The Influence of surfactants on the peel strength of water-based pressure sensitive adhesives. J Adhes 1999;70:179–95.

[7] Steward PA, Hearn J, Wilkinson MC. An overview of polymer latex film formation and properties. Adv Colloid Interface Sci 2000;86:195–267.

[8] Mallégol J, Gorce JP, Dupont O, Jeynes C, McDonald PJ, Keddie JL. Origins and effects of a surfactant excess near the surface of waterborne acrylic pressure-sensitive adhesives. Langmuir 2002;18:4478–87.

[9] Tobing SD, Klein A. Molecular parameters and their relation to the adhesive performance of acrylic pressure-sensitive adhesives. J Appl Polym Sci 2001;79:2230–2244.

[10] Tobing SD, Klein A. Molecular parameters and their relation to the adhesive performance of emulsion acrylic pressure-sensitive adhesives. II. Effect of crosslinking. J Appl Polym Sci 2001;79:2558–64.

[11] Fonseca GE, McKenna TFL, Dubé MA. Effect of bimodality on the adhesive properties of pressure sensitive adhesives: Role of bimodal particle size and molecular weight distributions. Ind

Eng Chem Res 2010;49:7303–12.

[12] Fonseca GE, McKenna TF, Dubé MA. Miniemulsion vs. conventional emulsion polymerization for pressure-sensitive adhesives production. Chem Eng Sci 2010;65:2797–810.

[13] Qie MA, Dubé L. Manipulation of chain transfer agent and cross-linker concentration to modify latex micro-structure for pressure-sensitive adhesives. Eur Polym J 2010.

[14] Qie L, Dubé MA. Manipulating latex polymer microstructure using chain transfer agent and cross-linker to modify psa performance and viscoelasticity. Macromol React Eng 2011;5:117–28.

[15] Marquis DM, Guillaume E and Chivas-Joly C. Properties of Nanofillers in Polymer. In: Cuppoletti J, editor. Nanocomposites Polym. with Anal. Methods, In Tech; 2011, p. 261–84.

[16] Wang T, Lei CH, Dalton AB, Creton C, Lin Y, Fernando KAS, et al. Waterborne, nanocomposite pressure-sensitive adhesives with high tack energy, optical transparency, and electrical conductivity. Adv Mater 2006;18:2730–4.

[17] Wang T, Colver PJ, Bon SAF, Keddie JL. Soft polymer and nano-clay supracolloidal particles in adhesives : synergistic effects on mechanical properties. Soft Matter 2009;5:3842–9.

[18] Kajtna J, Šebenik U. Microsphere pressure sensitive adhesives-acrylic polymer/montmorillonite clay nanocomposite materials. Int J Adhes Adhes 2009;29:543–50.

[19] Rana PK, Swain SK, Sahoo PK. Synthesis, characterization, and properties of intercalated poly(2-ethyl hexylacrylate)/silicate nanocomposites: XRD, TEM, IR, TGA, superabsorbency, pressure-sensitive adhesion, and biodegradation. J Appl Polym Sci 2004;93:1007–11.

[20] Patel S, Bandyopadhyay A, Ganguly A, Bhowmick AK. Synthesis and properties of nanocomposite adhesives. J Adhes Sci Technol 2006;20:371–85.

[21] Yamamoto Y, Fujii S, Shitajima K, Fujiwara K, Hikasa S, Nakamura Y. Soft polymer-silica nanocomposite particles as filler for pressure-sensitive adhesives. Polymer (Guildf) 2015;70:77–

87.

[22] Khalina M, Sanei M, Mobarakeh HS, Mahdavian AR. Preparation of acrylic/silica nanocomposites latexes with potential application in pressure sensitive adhesive. Int J Adhes Adhes 2015;58:21–7.

[23] Lee SW, Park JW, Park CH, Kwon YE, Kim HJ, Kim EA, et al. Optical properties and UV-curing behaviors of optically clear PSA-TiO 2 nano-composites. Int J Adhes Adhes 2013;44:200–8.

[24] Dufresne A. Preparation of cellulose nanocrystals. Nanocellulose From Nat. to High Perform.Tailord Mater., Betlin: GmbH, Walter de Gruyter; 2012:83–124.

[25] Habibi Y, Lucia LA, Rojas OJ. Cellulose nanocrystals: Chemistry, self-assembly, and applications. Chem Rev 2010.

[26] Moon RJ, Martini A, Nairn J, Simonsen J, Youngblood J. Cellulose nanomaterials review: structure, properties and nanocomposites. vol. 40. 2011.

[27] Bendahou A; Habibi Y; Kaddami H.; Dufresne A. A. Physico-chemical characterization of palm from phoenix dactylifera – l, preparation of cellulose whiskers and natural rubber–based nanocomposites. J Biobased Mater Bioenergy 2009;3:81–90.

[28] Bendahou, A.; Kaddami, H.; Dufresne A. A. Investigation on the effect of cellulosic nanoparticles' morphology on the properties of natural rubber based nanocomposites. Eur Polym J 2010;46:609–20.

[29] Grunert M, Winter WT. Nanocomposites of cellulose acetate butyrate reinforced with cellulose nanocrystals. J Polym Environ 2002;10:27–30.

[30] Kvien I, Tanem BS, Oksman K. Characterization of cellulose whiskers and their nanocomposites by atomic force and electron microscopy. Biomacromolecules 2005;6:3160–5.

[31] Petersson L, Oksman K. Biopolymer based nanocomposites: Comparing layered silicates and microcrystalline cellulose as nanoreinforcement. Compos Sci Technol 2006;66:2187–96.

[32] Cao X, Dong H, Li CM. New nanocomposite materials reinforced with cellulose nanocrystals in Waterborne Polyurethane. Biomacromolecules 2007;8:899–904.

[33] Li Y, Ren H, Ragauskas AJ. Rigid polyurethane foam reinforced with cellulose whiskers: Synthesis and characterization. Nano-Micro Lett 2010;2:89–94.

[34] Favier V, Canova G R, Cavaille JY, Chanzy H, Dufresne A, Gauthier C. Nanocomposite materials form latex and cellulose whiskers. Polym Adv Technol 1994;6:351–5.

[35] Helbert W, Cavaille JY, Dufresne A. Thermoplastic nanocomposites filled with straw cellulose whiskers . Part I : Processing and mechanical behavior. Polym Compos 1996;17:604–11.

[36] Hajji P, Cavaille JY, Favier V,. Gauthier C, Vigier G. Tensile behavior of nanocomposites from latex and cellulose whiskers. Polym Compos 1996;17:612–9.

[37] Ruiz MM, Cavaillé JY, Dufresne A, Gérard JF, Graillat C. Processing and characterization of new thermoset nanocomposites based on cellulose whiskers. Compos Interfaces 2000;7:117–31.

[38] Azizi Samir MAS, Alloin F, Dufresne A. Review of recent research into cellulosic whiskers, their properties and their application in nanocomposite field. Biomacromolecules 2005.

[39] Dufresne A. Processing of polymer nanocomposites reinforced with polysaccharide nanocrystals. Molecules 2010;15:4111–28.

[40] Roohani M, Habibi Y, Belgacem NM, Ebrahim G, Karimi AN, Dufresne A. Cellulose whiskers reinforced polyvinyl alcohol copolymers nanocomposites. Eur Polym J 2008;44:2489–98.

[41] Paralikar SA, Simonsen J, Lombardi J. Poly(vinyl alcohol)/cellulose nanocrystal barrier membranes. J Memb Sci 2008;320:248–58.

[42] Choi YJ, Simonsen J. Cellulose nanocrystal-filled carboxymethyl cellulose nanocomposites. J Nanosci Nanotechnol 2006;6:633–639.

[43] Dufresne A, Cavaille JY, Helbert W. Thermoplastic nanocomposites filled with wheat straw cellulose whisker. Part II: Effect of Processing and Modeling. Polym Compos 1997;18:198-210.

[44] Vatansever A, Dogan H, Inan T, Sezer S, Sirkecioglu A. Properties of na-montmorillonite and cellulose nanocrystal reinforced poly(butyl acrylate-co-methyl methacrylate) nanocomposites. Polym Eng Sci 2015;55:2922–8.

[45] Elmabrouk A Ben, Wim T, Dufresne A, Boufi S. Preparation of poly(styrene-co-hexylacrylate)/cellulose whiskers nanocomposites via miniemulsion polymerization. J Appl Polym Sci 2009. doi:10.1002/app.30886.

[46] Ben Mabrouk A, Kaddami H, Magnin A, Belgacem MN, Dufresne A, Boufi S. Preparation of nanocomposite dispersions based on cellulose whiskers and acrylic copolymer by miniemulsion polymerization: Effect of the silane content. Polym Eng Sci 2011;51:62–70.

[47] Kedzior SA, Marway HS, Cranston ED. Tailoring cellulose nanocrystal and surfactant behavior in miniemulsion polymerization. Macromolecules 2017;50:2645–55.

[48] Kajtna J, Šebenik U. Novel acrylic/nanocellulose microsphere with improved adhesive properties. Int J Adhes Adhes 2017;74:100–6.

[49] Dastjerdi Z, Cranston ED, Dubé MA. Synthesis of poly(n-butyl acrylate/methyl methacrylate)/CNC latex nanocomposites via in situ emulsion polymerization. Macromol. React. Eng. 20017. doi:10.1002/mren201700013.

[50] Reid MS, Villalobos M, Cranston ED. Cellulose nanocrystal interactions probed by thin film swelling to predict dispersibility. Nanoscale 2016;8:12247–57.

[51] Pressure Sensitive Tape Council. Test Methods for Pressure Sensitive Adhesive Tapes 2004,

Northbrook, Illinois.

[52] Kalashnikova I, Bizot H, Bertoncini P, Cathala B, Capron I. Cellulosic nanorods of various aspect ratios for oil in water pickering emulsions. Soft Matter 2013;9:952–9.

[53] Hu Z, Patten T, Pelton R, Cranston ED. Synergistic stabilization of emulsions and emulsion gels with water-soluble polymers and cellulose nanocrystals. ACS Sustain Chem Eng 2015;3:1023–31.

[54] Ghosh P, Dev D, Samanta AK. Graft copolymerization of acrylamide on cotton cellulose in a limited aqueous system following pretreatment technique. J Appl Polym Sci 1995.

[55] Misra BN, Mehta IK, Khetarpal RC. Grafting onto cellulose. VIII. Graft copolymerization of poly(ethylacrylate) onto cellulose by use of redox initiators. Comparison of initiator reactivities. J Polym Sci Polym Chem Ed 1984;22:2767–75.

[56] Zhou C, Wu Q, Yue Y, Zhang Q. Application of rod-shaped cellulose nanocrystals in polyacrylamide hydrogels. J Colloid Interface Sci 2011.

[57] Dahlquist CA. Pressure-Sensitive adhesives. In: Patrick R. L, editor. Treatise Adhes. Adhes., New York: Marcel Dekker Inc; 1969, p. 19–260.

[58] Jovanović R, Dubé MA. Emulsion-based pressure-sensitive adhesives: A Review. J Macromol Sci Part C Polym Rev 2004;44:1–51.

Chapter 5:

The Influence of CNC in the Presence of Microstructural Modifiers on the Mechanical Performance of PSAs

5.1 Introduction

Emulsion-based pressure sensitive adhesives (PSAs) have increased in popularity in the commercial PSA market due to strict regulations imposed on the use of volatile organic solvents [1]. However, emulsion-based PSAs do not exhibit the same properties as their solution-based counterparts. The mechanical performance of emulsion-based PSAs can be altered through the manipulation of reaction conditions such as monomer composition, seed properties, monomer and initiator feed rate, as well as initiator concentration [2-7]. The addition of microstructural modifiers such as crosslinkers and chain transfer agents to the reaction formulation can also be used to alter PSA performance [8, 9]. The use of nanoparticles in PSA production has been considered previously to modify adhesive performance [10-12]. Cellulose nanocrystals (CNCs) are renewable, nontoxic nano-reinforcement agents [13]. Although the inclusion of CNCs into a polymer matrix has been explored, there is limited information on the influence of CNCs on the mechanical performance of PSAs. Dastjerdi & Dubé reported the synthesis of CNC/poly(butyl acrylate/methyl methacryate) nanocomposites [14] and the impact of CNCs on PSA performance [15]. In the present study, the combined influence of microstructural modifiers and CNCs on the mechanical performance of PSAs was studied via seeded semi-batch emulsion polymerization of butyl acrylate/methyl methacrylate.

5.2 Experimental methods

5.2.1 Materials

n-Butyl acrylate (BA) and methyl methacrylate (MMA) monomers, sodium dodecyl sulfate (SDS) anionic surfactant, potassium persulfate (KPS) initiator, allyl methacrylate (AMA) crosslinking agent, 1-dodecanethiol (NDM) chain transfer agent, and hydroquinone (HQ) inhibitor

were all purchased from Sigma Aldrich. All the above chemicals were reagent grade and were used as received. Tetrahydrofuran (THF, HPLC grade) was obtained from EMD Chemicals. Poly (vinylidene fluoride) (PVDF) membrane filters with a pore size of 5.0 μm were purchased from EMD Millipore. Distilled deionized (DDI) water was used throughout all experiments. CNCs were obtained from CelluForce (Windsor, QC, Canada). Ashless Whatman filter paper (grade 542) was purchased from Fisher Scientific. Nitrogen gas was purchased from Linde Canada. Melinex$^{@}$ 453 polyethylene terephthalate (PET) films were obtained from Tekra.

5.2.2 Aqueous CNC dispersion preparation

A specified amount of spray dried CNC (1 wt.% based on total monomer weight) was dispersed into the required amount of DDI water and stirred with a magnetic stir bar for 4 h until it appeared to be well-dispersed according to visual inspection. Afterwards, the dispersion was sonicated using a Sonic Dismembrator Ultrasonic processor (500 W with 65% amplitude) for 15 min in an ice bath to avoid overheating. Finally, the CNC dispersion was filtered through ashless Whatman 542 filter paper by vacuum filtration.

5.2.3 Latex preparation

A seeded, semi-batch emulsion polymerization approach was employed to produce all latexes. The polymerization process included three stages: a batch stage to produce seed latex particles, a continuous feeding stage to grow the latex particles, and a cook stage to react any remaining monomer. A stable latex formulation reported previously for seeded semi-batch polymerization was used here [Chapter 4]. The BA/MMA weight ratio (90/10 w/w), and initiator amount were kept constant for all runs while the amounts of AMA and CTA were varied (0, 0.2, 0.4 phm) (Table 5.1). Final latex solids contents with 40 and 50 wt.% were synthesized for 1 wt.% CNC loading and 0 wt.% CNC loading, respectively.

All polymerization reactions were performed in a jacketed 1 L stainless steel LabMax™ (Mettler Toledo) reactor. The reactor was equipped with a nitrogen purge line, an anchor stirrer, a sampling line, a reflux condenser with a vent line, and two separate feed pumps. The reaction temperature (65 ^{o}C) and stirring speed (250 rpm) were controlled by iControl LabMax software during polymerization.

Table 5.1 *In situ* semi-batch polymerization formulation.

Component	**Latex seed (g)**	**Monomer emulsion feed (g)**	**Initiator feed (g)**	**Total (g)**	**Total (phm)***
n-Butyl acrylate (BA)	19.8	178.2	-	**198**	**90**
Methyl methacrylate (MMA)	2.2	19.8	-	**22**	**10**
Allyl methacrylate (AMA)	-	0, 0.44, 0.88	-	**-**	**0,0.2,0.4**
1-dodecanethiol (NDM)	-	0, 0.44, 0.88	-	**-**	**0,0.2,0.4**
Potassium persulfate (KPS)	0.06	-	0.54	**0.6**	**0.27**
Sodium dodecyl sulfate (SDS)	0.36, 0.7	2.6	-	**2.96, 3.3**	**1.35,1.5**
Cellulose nanocrystals (CNCs)	0,2.2	-	-	**0, 2.2**	**0, 1**
Distilled de-ionized (DDI) water	40,95[a]/ 0,165[b]/3[c]	68	54	**220, 330**	**100,150**

[a]Water used for SDS solution in seed production stage
[b]Water used for aqueous CNC dispersion
[c]Water used for initiator solution in seed production stage
*phm= parts per hundred parts monomer

To begin, a SDS solution and aqueous CNC dispersion were charged to the reactor at room temperature (Latex seed, Table 5.1). The stirring speed was set to 250 rpm and maintained throughout the run. The reactor was then purged with nitrogen and the reactor temperature increased to 60^{o}C (within 30 min). Next, the monomer mixture and initiator solution were charged

to the reactor (Latex seed, Table 5.1). The temperature was then increased to 65 ^{o}C within 5 min, and the seed stage was continued for 30 min. After completion of the seed stage, the monomer emulsion feed and initiator feed (Table 5.1) were charged separately to the reactor using two feed pumps at constant rates and feeding times of 3.5 and 4 h, respectively. At the completion of the feed stage, the polymerization was allowed to proceed for an additional 60 min to increase the monomer conversion (cooking stage). Additional runs containing a crosslinker and chain transfer agent without CNC were also prepared for comparative purposes.

5.2.4 PSA Film Characterization

8 g of each *in situ* latex was cast onto a 50 µm Melinex$^{@}$ sheet with a #30 Meyer rod. The cast films were dried at a controlled temperature (23 ± 1 ^{o}C) and relative humidity (50% ± 5) for 24 h prior to testing. The PSA film thickness was 36 ± 2 µm.

Loop tack, 180^{o} peel strength and shear strength were measured at 23 ± 1^{o}C and relative humidity of 50% ± 5 according to the Pressure Sensitive Tape Council standards PSTC-6, PSTC-1 and PSTC-7, respectively [51]. A Universal Instron tester was used to measure the loop tack and peel strength of the PSA films, and home-built shear tester was used to measure the shear strength of the PSA films. The average of five measurements with (±SD) was used in the analysis of adhesive performance.

A 1″ × 6″ strip was cut from the PSA film and formed into a loop with the adhesive side facing out-ward. Approximately 1″ at both ends of the strip was masked with tape and inserted into the upper grip of the Instron tester. The instrument moved the upper grip downward at a speed of 1 mm/s until an area of 1 inch^{2} came into contact with the stainless steel substrate mounted into the lower grip. Next, the tester moved the upper grip upward at the same speed while recording

the force needed to de-bond the loop from the substrate. The maximum force per meter necessary to remove the adhesive was reported as loop tack in N/m.

A 1″ × 5″ strip of the PSA film was used to measure peel strength. The strip was laminated onto a stainless steel substrate with the help of a 2040 g roll coater. The roll coater was passed through the film front-to-back twice (i.e., along the length of the film). The substrate and the strip were immediately inserted into the grips and the upper grip was set to move upward at a speed of 1 mm/s. The average force (N) per m required to peel the strip from the substrate was recorded and reported as peel strength at a peel angle of 180^{o}.

A 1" x 5" strip of the PSA film was laminated onto a stainless steel substrate with a contact area of 1/2" x 1/2" and then placed in the shear tester using a C-clamp. A 500 g weight was suspended at the end of the strip. The time needed for the PSA film to fall off the testing panel was recorded automatically as the shear strength using Labview™ software.

Samples of 0.05 g of dry polymer were sealed in PVDF membranes and immersed in 20 mL of THF. The samples in their pouches were left to swell under gentle shaking for 24 h at room temperature. The sample pouches were then dried in a fume hood until a constant weight was reached. The gel content was calculated as the ratio between the mass of dried sample after removing the soluble components and the mass of the initial polymer.

5.3 Results and Discussion

Several latexes containing a crosslinker (allyl methacrylate, AMA) and/or CTA (n-dodecyl mercaptan, NDM), with or without CNCs were synthesized to study their influence along with that of the CNCs on PSA performance. As expected, the addition of crosslinking agent decreased the peel strength and tack while improving the shear strength significantly (B, C in Figure 5.1; Table

5.2). The addition of the CNC to the latex containing the crosslinker (B1) had no considerable impact on peel strength and tack (Figure 5.1) but significantly enhanced the shear strength (Table 5.2). In comparison, the addition of CNC without crosslinker (A1), resulted in a substantial increase in all three adhesive measurements (peel strength, tack and shear strength). Comparing A1 to B1 reveals that the presence of crosslinker either alone or in the presence of CNC results in little to no improvement in peel strength and tack although shear strength does increase greatly. It is possible that the crosslinker reacted with the CNC and prevented the CNC from interacting favourably with the polymer. Latex B1 also showed a very high viscosity compared to the other reactions, which supports this idea.

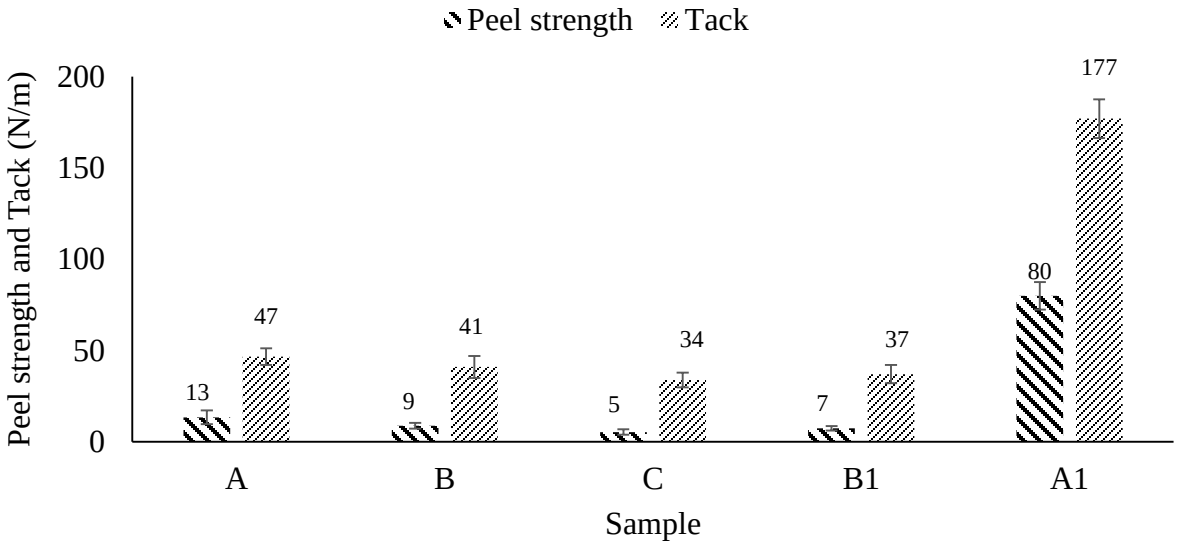

Figure 5.1 The effect of crosslinker loading with or without CNC on peel strength and tack.

Table 5.2 The effect of crosslinker loading with or without CNC on shear strength and gel content.

Sample	Crosslinker (phm)	CNC (phm)	Shear strength (h)	Gel content (%)
A	0	0	2.6	33
B	0.2	0	4	84
C	0.4	0	8	95
A1	0	1	58.7	62
B1	0.2	1	240	97

As shown in Figure 5.2, the inclusion of CTA in the polymerization formulation considerably increased both peel strength and tack, while greatly decreasing the shear strength (see samples D, E, D1 and E1 in Figure 5.2 and Table 5.3). Cohesive failure, indicated by a residue left on the substrate after the test is completed, was observed in the peel strength and tack results for samples D and E; this is an indicator of poor cohesive strength and is reflected in the low shear strength values. The addition of CNC had a slight negative effect on the peel strength, a stronger negative effect on tack (D1 and E1 in Figure 5.2) and a strong positive effect on shear strength (Table 5.2).

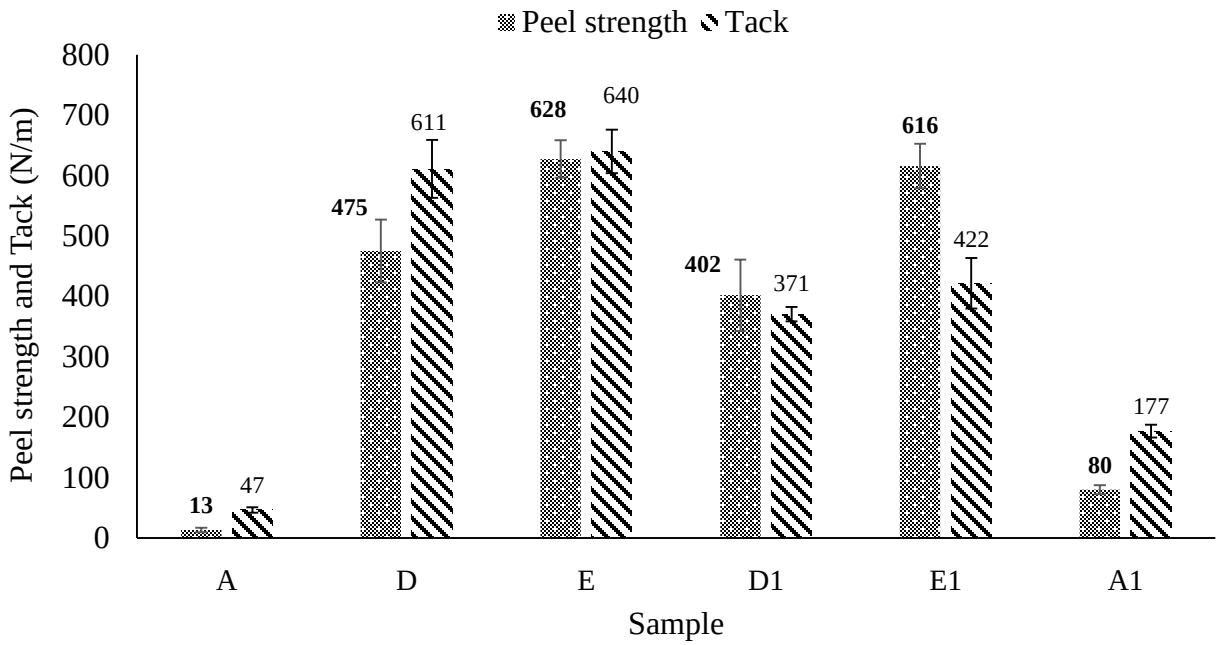

Figure 5.2 The effect of CTA loading with or without CNC on the peel strength and tack.

Table 5.3 The effect of CTA loading with or without CNC on shear strength and gel content.

Sample	CTA (phm)	CNC (phm)	Shear strength (s)	Gel content (%)
A	0	0	2.6 (h)	33
D	0.2	0	26	10
E	0.4	0	8	8
A1	0	1	58.7 (h)	62
D1	0.2	1	157	11
E1	0.4	1	33	8

Formulations with both CTA and crosslinker, with and without CNC were synthesized. Results using CNC alone (A1) were comparable, if not better than runs with CTA and crosslinker (F and F1) in Figure 5.3 and Table 5.4. Thus, the use of CNCs *alone* would be recommended rather than using the more hazardous CTA and crosslinker.

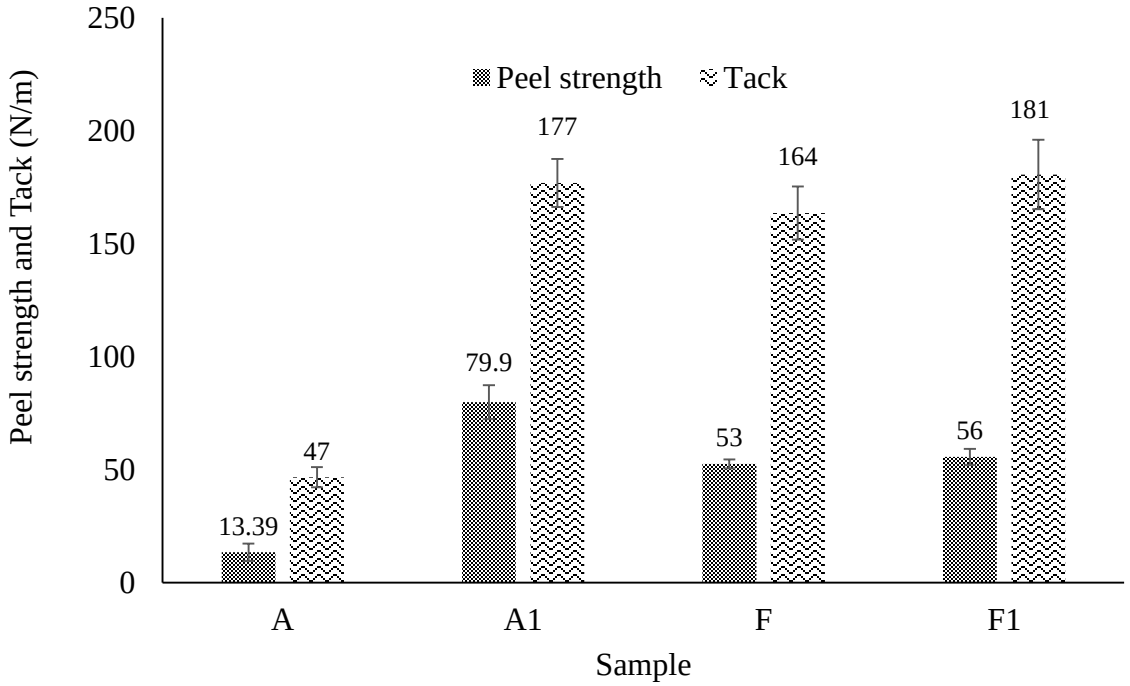

Figure 5.3 The effect of CNC on peel strength and tack for base latex and base latex containing crosslinker & CTA.

Table 5.4 The effect of CNC on shear strength and gel content.

Sample	Crosslinker (phm)	CTA (phm)	CNC (phm)	Shear strength (h)	Gel content (%)
A	0	0	0	2.6	33
A1	0	0	1	58.7	62
F	0.2	0.2	0	3.1	70
F1	0.2	0.2	1	16	91

5.4 Conclusion

The addition of CNC to latex containing modifiers such as crosslinker or CTA improved shear strength in all cases. However, improvements to tack and peel strength were non-significant in direct contrast to their effect when crosslinker and CTA were not used. In some cases, at the

very least, the increases to shear strength did not come at the expense of tack or peel strength. Further exploration of the effect of CNC when the formulation results in low tack and peel strength is warranted. In any case, it can be concluded that CNC is ideally suited for use to improve shear strength in a nontoxic manner.

5.5 References

[1] Lovell, PA., El-Aasser MS. Emulsion Polymerization and Emulsion Polymers. New York: John Wiley & Sons, Chichester; 1997.

[2] Jovanović R, Ouzineb K, McKenna TF, Dubé MA. Butyl acrylate/methyl methacrylate latexes: Adhesive properties. Macromol Symp 2004;206:43–56.

[3] Gower MD, Shanks RA. The effect of varied monomer composition on adhesive performance and peeling master curves for acrylic pressure-sensitive adhesives. J Appl Polym Sci 2004;93:2909–17.

[4] Tobing SD, Klein A. Molecular parameters and their relation to the adhesive performance of acrylic pressure-sensitive adhesives. J Appl Polym Sci 2001;79:2230–2244.

[5] Tobing SD, Klein A. Molecular parameters and their relation to the adhesive performance of emulsion acrylic pressure-sensitive adhesives. II. Effect of crosslinking. J Appl Polym Sci 2001;79:2558–64.

[6] Fonseca GE, McKenna TFL, Dubé MA. Effect of bimodality on the adhesive properties of pressure sensitive adhesives: Role of bimodal particle size and molecular weight distributions. Ind Eng Chem Res 2010;49:7303–12.

[7] Fonseca GE, McKenna TF, Dubé MA. Miniemulsion vs. conventional emulsion polymerization for pressure-sensitive adhesives production. Chem Eng Sci 2010;65:2797–810.

[8] Qie MA, Dubé L. Manipulation of chain transfer agent and cross-linker concentration to modify latex micro-structure for pressure-sensitive adhesives. Eur Polym J 2010.

[9] Qie L, Dubé MA. Manipulating latex polymer microstructure using chain transfer agent and cross-linker to modify psa performance and viscoelasticity. Macromol React Eng 2011;5:117–28.

[10] Wang T, Lei CH, Dalton AB, Creton C, Lin Y, Fernando KAS. Waterborne, nanocomposite pressure-sensitive adhesives with high tack energy, optical transparency, and electrical conductivity. Adv Mater 2006;18:2730–4.

[11] Wang T, Colver PJ, Bon SAF, Keddie JL. Soft polymer and nano-clay supracolloidal particles in adhesives : synergistic effects on mechanical properties. Soft Matter 2009;5:3842–9.

[12] Kajtna J, Šebenik U. Microsphere pressure sensitive adhesives-acrylic polymer/montmorillonite clay nanocomposite materials. Int J Adhes Adhes 2009;29:543–50.

[13] Dufresne A. Preparation of cellulose nanocrystals. Nanocellulose From Nat. to High Perform.Tailord Mater., Betlin: GmbH, Walter de Gruyter; 2012:83–124.

[14] Dastjerdi Z, Cranston ED, Dubé MA. Synthesis of poly(n-butyl acrylate/methyl methacrylate)/CNC latex nanocomposites via in situ emulsion polymerization. Macromol. React. Eng. 20017. doi:10.1002/mren201700013.

[15] Dastjerdi Z, Cranston ED, Dubé MA. Pressure sensitive adhesive property modification using cellulose nanocrystals. Int J Adhes Adhes. 20017 (under review).

Chapter 6:

General Discussion

General Discussion, Conclusion and Recommendations

In recent decades, due to environmental concerns, policy makers have imposed strict regulations on the use of volatile organic compounds (VOCs) [1]. As a result, the commercial pressure sensitive adhesive (PSA) market has shifted towards the production of emulsion-based PSAs as opposed to solution-based PSAs. Despite being produced via a clearly more sustainable process, emulsion-based PSAs tend to exhibit inferior adhesive performance compared to their solution-based counterparts [2]. The adhesive performance of PSA films is commonly evaluated by shear strength, tack, and peel strength. Depending on their final application, the PSA films may require a balanced combination of these three properties. An important challenge is that, in most cases, the modification of one of these properties, often results in a deterioration of another. For example, attempts to increase an emulsion-based PSA film's shear strength often results in a decrease in its peel strength and tack. Efforts to overcome this issue were discussed in Chapter 3 [3–7]. One such effort involves the use of crosslinking and/or chain transfer agents (CTAs). In this thesis, we have presented the use of a cellulose nanocrystal (CNC) nanofiller to achieve PSA property modification.

The application of nanofillers in PSAs has been considered by many researchers to improve the mechanical performance of PSAs [8–12]. Nanofillers are effective modifiers for polymeric materials due to their extremely high surface to volume ratio. They significantly improve polymer properties such as thermal, optical, barrier, and mechanical properties even at very low concentrations (<5 wt.%) [13]. CNCs have been widely investigated in recent years due to their unique properties such as high elastic modulus, high aspect ratio, abundance of surface hydroxyl groups, renewability, and nontoxicity [14]. As there is limited information on the subject, this

thesis explores the synthesis of CNC/latex nanocomposites via *in situ* emulsion polymerization as well as the influence of CNCs on adhesive performance.

An important first step and major challenge in this work was to achieve stable latex polymerization formulations. As a result of extensive effort, the buffer was eliminated from the formulation, the potassium persulfate (KPS) initiator concentration was lowered from 0.38 phm to 0.1 phm, and the SDS concentration relative to the CNC concentration and latex solids content was modified. All of these modifications served to achieve a stable latex formulation (Table 6.1). Additionally, the aqueous CNC dispersion was charged to the reactor by feed pump in 30 min during the initial heating and mixing period in the batch polymerization. Subsequent characterization of the CNC/latex nanocomposites revealed that the CNC content had no considerable effect on monomer conversion, polymer particle size, and glass transition temperature (T_g) while significant increases in storage and loss modulus, gel content (Table 6.2), and latex viscosity (Figure 6.1) with increasing CNC loading were observed. These results were attributed to the crosslinking ability of CNCs through their surface hydroxyl groups and their intermolecular interactions between CNCs via their hydroxyl groups (particularly at the highest CNC loadings (2 phm)), and their high specific surface area.

Table 6.1 *In situ* batch emulsion polymerization formulation.

Component	**Amount**	
	(g)	(phm)*
Butyl acrylate (BA)	135	90
Methyl methacrylate (MMA)	15	10
Sodium dodecyl sulfate (SDS)	3	2
Potassium persulfate (KPS)	0.15	0.1
Cellulose nanocrystals (CNC)	0-3	0-2
Deionized distilled water (DDI H_2O)	300	200

*phm = parts per hundred parts monomer

Table 6.2 Gel content of poly(BA/MMA) latexes with different CNC loadings.

CNC loading (phm)	Gel content (wt.%)
0	28±1.9
0.5	53±2.3
1	62±1.7
2	69±2.5

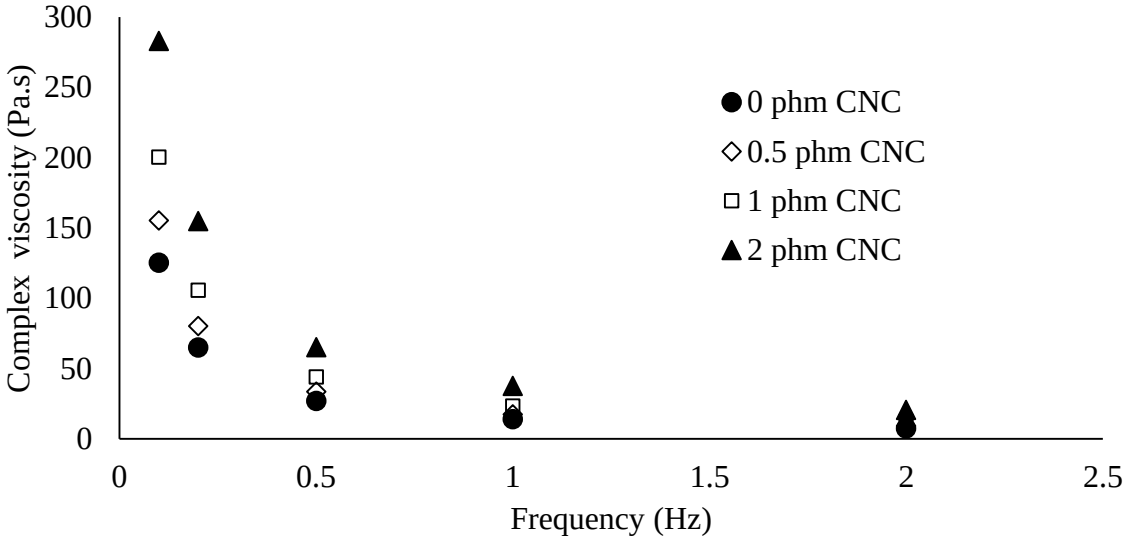

Figure 6.1 Complex viscosity vs. frequency of the dried nanocomposite films for different CNC loadings.

After overcoming the stability challenges, establishing a stable polymerization formulation, and achieving desirable impacts of CNC loading on the latex properties, CNC/PSA

nanocomposites were synthesized through a seeded semi-batch polymerization, a more industrially relevant synthetic method. The process formulation is shown in Table 6.3.

Table 6.3 *In situ* semi-batch emulsion polymerization formulation.

Component	**Latex seed (g)**	**Monomer emulsion feed (g)**	**Initiator feed (g)**	**Total (g)**	**Total (phm)***
n-Butyl acrylate (BA)	19.8	178.2	-	**198**	**90**
Methyl methacrylate (MMA)	2.2	19.8	-	**22**	**10**
Potassium persulfate (KPS)	0.06	-	0.54	**0.6**	**0.27**
Sodium dodecyl sulfate (SDS)	0.36-0.7	2.6	-	**2.96 - 3.3**	**1.35-1.5**
Cellulose nanocrystals (CNCs)	0-2.2	-	-	**0, 0.55 1.1, 1.65, 2.2**	**0, 0.25, 0.5, 0.75, 1**
Distilled de-ionized (DDI) water	40-95[a]/ 0-165[b]/3[c]	68	54	**220-330**	**100-150**

[a]Water used for SDS solution in seed production stage
[b]Water used for aqueous CNC dispersion
[c]Water used for initiator solution in seed production stage

Shear strength, tack, and peel strength were simultaneously improved with increasing CNC content in the nanocomposites (Figure 6.2). The improvements in shear strength were attributed to the crosslinking activity of the CNC with the latex polymer which was confirmed by an increasing gel content. Increases to both tack and peel strength with increasing CNC loading were associated with improved interfacial properties of the CNC/PSA films with the stainless steel substrate via the CNC surface hydroxyl group.

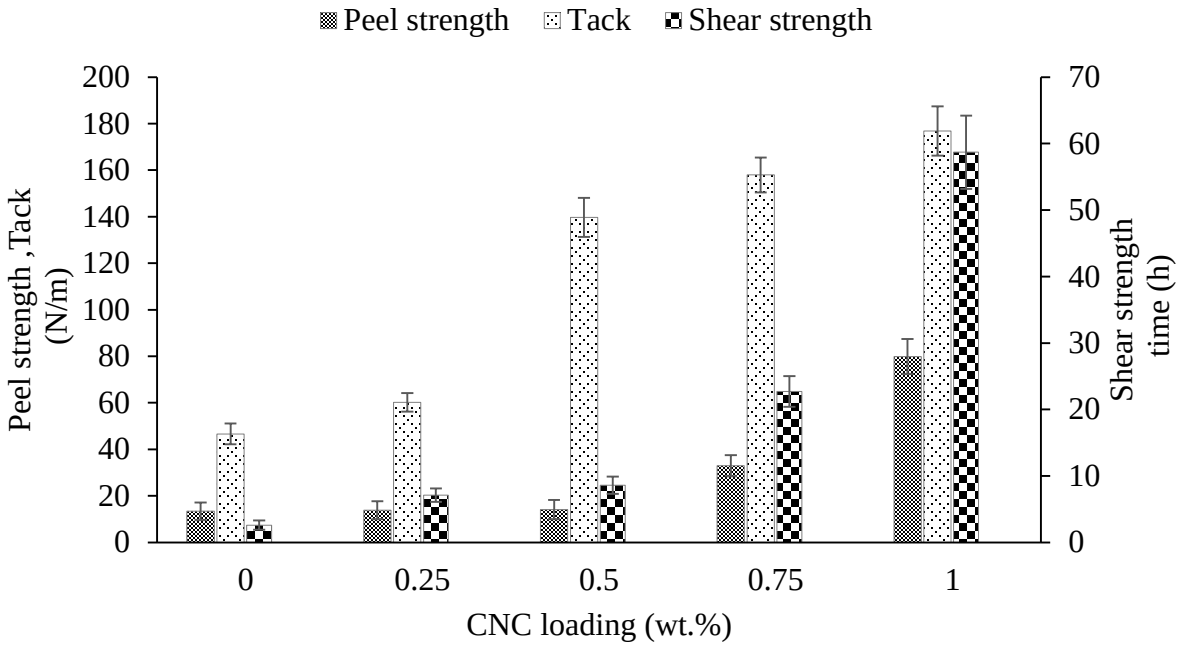

Figure 6.2 The effect of CNC loading on shear strength, tack, and peel strength.

Inclusion of CNCs in the latex using a blending technique also enhanced PSA performance (Figure 6.3). However, the CNC/PSA films synthesized using the *in situ* technique exhibited a significantly better adhesive performance (Figure 6.3). It is likely that the longer contact time (5 h) at an elevated temperature (65 ^{o}C) provided better interaction between the CNC and the latex compared to the blending technique (room temperature for 30 min). Furthermore, aqueous CNC dispersions have a tendency to agglomerate during film formation if they are not well dispersed and anchored to the polymer matrix [15]. Given that a possible graft reaction through the CNC occurred during *in situ* polymerization, this may have facilitated the anchoring of the CNC to the polymer.

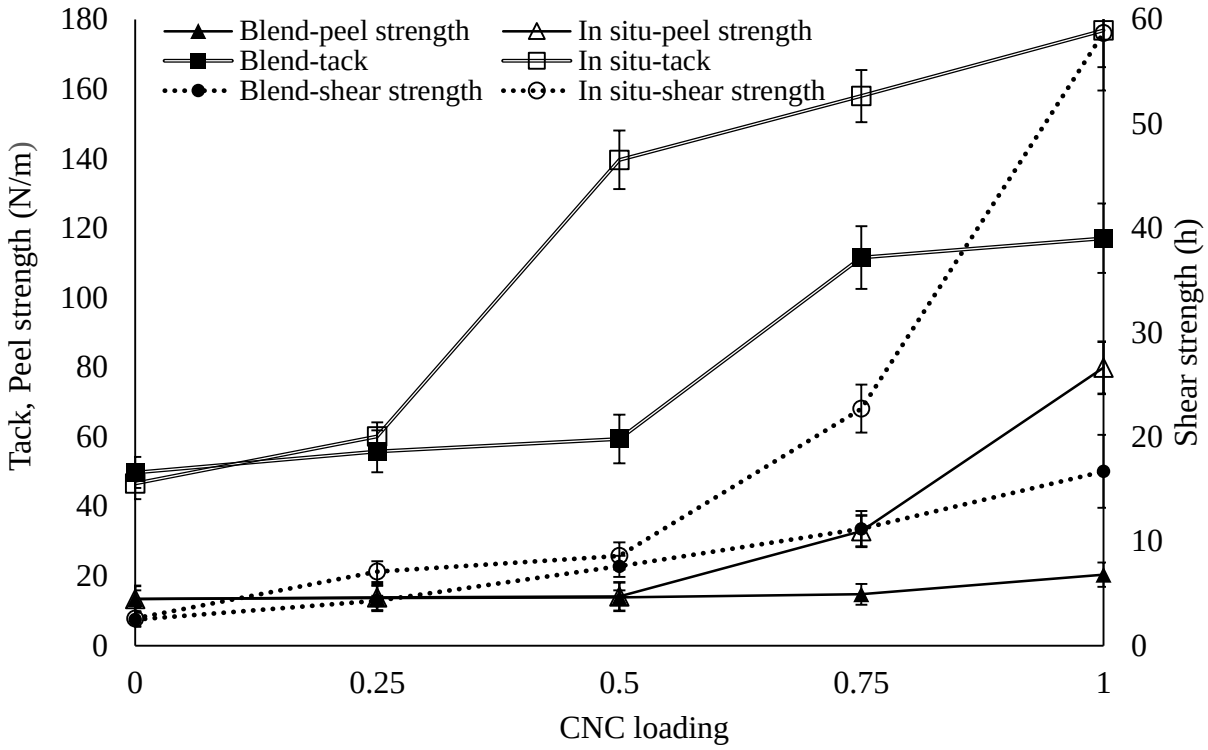

Figure 6.3 The effect of CNC loading on peel strength and tack. Closed symbols refer to samples from the blend technique while open symbols refer to samples from the in situ technique.

In the final part of our study, several latexes containing a crosslinker (allyl methacrylate, AMA) and/or CTA (n-dodecyl mercaptan, NDM), with or without CNCs were also prepared to study their influence along with that of the CNCs on PSA performance (Table 6.4).

Table 6.4 The mechanical performance of PSAs containing modifiers with or without CNC.

Sample	CTA (phm)	Crosslinker (phm)	CNC (phm)	Shear strength (s or h)	Tack (N/m)	Peel strength (N/m)
A	0	0	0	2.6 (h)	13	47
B	0.2	0.2	0	3.1 (h)	53	164
C	0	0	1	58.7 (h)	80	177
D	0.2	0	0	26 (s)	475	611
E	0.2	0	1	157 (s)	402	371
F	0	0.2	0	4 (h)	9	41
G	0	0.2	1	240 (h)	7	37
H	0.2	0.2	1	16 (h)	56	181

As expected, the addition of CTA greatly increased peel strength and tack while decreasing the shear strength from hours to seconds (Table 6.4 A & D). Conversely, the addition of a crosslinking agent decreased the peel strength and tack while improving the shear strength (Table 6.4 A & F). The addition of CNCs to latex formulations containing both crosslinker and CTA improved the shear strength but did not have a positive influence on peel strength and tack (Table 6.4 E & G). Further study of the influence of CNC on PSA performance in the presence of CTA and crosslinker alone or in tandem is clearly required.

6.1 Conclusion

Poly(n-butyl acrylate-co-methyl methacrylate)/CNC latexes were successfully synthesized via *in situ* emulsion polymerization after several attempts to modify a standard emulsion polymerization formulation to overcome latex stability issues. The CNC/latexes showed increasing storage modulus, gel content, and viscosity with increasing CNC loading. These observations were attributed to the crosslinking ability of CNC through its surface hydroxyl groups and its high specific surface area. Following the promising influence of CNC loading on CNC/latex

properties, a series of PSA/CNC nanocomposite films were prepared to investigate the effect of CNC loading on adhesive properties. Surprisingly, all three adhesive properties including peel strength, tack, and shear strength were significantly improved with increased CNC loading. It appeared that CNC improved the hydrophilicity of the nanocomposite films and consequently improved their surface interaction with stainless steel, which resulted in improved peel strength and tack. In addition, the crosslinking activity of CNC through its surface hydroxyl groups led to the enhancement of shear strength. The addition of CNC to latex containing modifiers such as crosslinker or CTA did not have the same influence on the adhesive properties. It can be concluded that the CNC alone can serve as an appropriate, nontoxic property modifier in PSA production as a part of a more sustainable product development.

6.2 Recommendations

This work offers a novel and promising approach of adding CNC to poly(n-butyl acrylate-co-methyl methacrylate) latex using emulsion polymerization. Considering the desirable impact of CNC on adhesive properties, the following recommendations are proposed to broaden the application of CNCs in latexes.

The synthesis of stable CNC/latex was the main challenge in this study as the negatively charged CNC surfaces destabilized the negatively charged growing polymer particles, the use of a cationic initiator (i.e., 2,2'-Azobis (2-methyl-propionamidine dihydrochloride)) along with a cationic surfactant (i.e., hexadecyl trimethyl ammonium bromide, CTAB) is recommended to produce a positively charged polymer particle surface to overcome the destabilizing issue. In addition, the surfactants play an important role in PSA adhesive properties. Therefore, it is

recommended to investigate the use of a cationic surfactant and/or a cationically-modified CNC on latex stability and eventually, on adhesive properties.

The use of polymeric surfactants such as macrosurfactants and polymerizable surfactants with CNC/latex nanocomposites should be studied. Macrosurfactants (e.g., PBA-b-PAA) consist of hydrophobic-hydrophilic block copolymers with a tunable hydrophilicity of one or both blocks. They usually show pH- or temperature-dependent micellization and surface activity. Since the CNCs are hydrophilic, macrosurfactants might stabilize the colloidal latex through their tunable hydrophilicity. Polymerizable surfactants (e.g., dodecyl allyl sulfosuccinate) usually bear functional groups which can be chemically incorporated into polymer molecules. Therefore, they become immobilized and cannot diffuse toward the latex film surface and as a result, will not produce the same negative effects on PSA adhesive properties as encountered with surfactants such as SDS. Aside from their positive influence on PSA properties, polymerizable surfactants may also interact with CNCs.

An image of CNC/latex would provide helpful information about the incorporation of CNCs into the polymer matrix. Transmission electron microscopy (TEM) is usually used for the visual analysis of nanocomposite latexes. As a small amount of CNC was used in the polymerization (i.e., 1 phm) and further dilution was required for sample preparation, we were unable to locate CNCs in our polymer matrix. Therefore, it is recommended to synthesize CNC/latexes with higher CNC loading (>2 phm) and very low solids content (<30%) in order to verify the location of the CNCs in the polymer matrix. However, the changes in reaction conditions may also affect CNC location. In addition, the use of a larger proportion of a monomer with a higher polymer T_g (e.g., MMA) in the reaction formulation is recommended to facilitate the

imaging process as BA yielded very soft polymer particles that lost their shape and "melted" during the course of TEM analysis.

According to the shear strength results, it was found that the improvement in shear strength of PSA nanocomposite films resulted from the crosslinking activity of the CNCs. Hence, the addition of ceric ammonium nitrate initiator, at the seed stage, may provide a means to encourage CNC grafting reactions and perhaps alter its hydrophobicity to encourage better incorporation into the polymer particles.

Another property of interest to commercial latex manufacturers is the shelf life of the material. The effect of CNC on latex shelf life should be investigated.

Because of the functionality of the CNC surfaces, modification of the CNCs can be undertaken. In this case, a broad range of modified CNCs can be used to examine their effect on latex stability, CNC loading, CNC polymer interaction and ultimately, CNC/latex nanocomposite end-use properties.

6.3 References

[1] Lovell, P. A. ; El-Aasser MS. Emulsion Polymerization and Emulsion Polymers. New York: John Wiley & Sons, Chichester; 1997.

[2] Zosel A. Shear strength of pressure sensitive adhesives and its correlation to mechanical properties. J Adhes 1994;44:1–16.

[3] Jovanović R, Ouzineb K, McKenna TF, Dubé MA. Butyl acrylate/methyl methacrylate latexes: Adhesive properties. Macromol Symp 2004;206:43–56.

[4] Fonseca GE, McKenna TFL, Dubé MA. Effect of bimodality on the adhesive properties of pressure sensitive adhesives: Role of bimodal particle size and molecular weight distributions. Ind Eng Chem Res 2010;49:7303–12.

[5] Fonseca GE, McKenna TF, Dubé MA. Miniemulsion vs. conventional emulsion polymerization for pressure-sensitive adhesives production. Chem Eng Sci 2010;65:2797–810.

[6] Qie MA, Dubé L. Manipulation of chain transfer agent and cross-linker concentration to modify latex micro-structure for pressure-sensitive adhesives. Eur Polym J 2010.

[7] Qie L, Dubé MA. Influence of polymer microstructure on the performance of post-treated latex-based pressure sensitive adhesives. J Appl Polym Sci 2012;124:349–64.

[8] Wang T, Lei CH, Dalton AB, Creton C, Lin Y, Fernando KAS, et al. Waterborne, nanocomposite pressure-sensitive adhesives with high tack energy, optical transparency, and electrical conductivity. Adv Mater 2006;18:2730–4.

[9] Wang T, Colver PJ, Bon SAF, Keddie JL. Soft polymer and nano-clay supracolloidal particles in adhesives : synergistic effects on mechanical properties. Soft Matter 2009;5:3842–9.

[10] Lee SW, Park JW, Park CH, Kwon YE, Kim HJ, Kim EA, et al. Optical properties and UV-curing behaviors of optically clear PSA-TiO 2 nano-composites. Int J Adhes Adhes 2013;44:200–8.

[11] Li HAO, Yang Y, Yu Y. Acrylic emulsion pressure-sensitive adhesives (PSAS) reinforced with layered silicate. J Adhes Sci Technol 2004;18:1759–70.

[12] Khalina M, Sanei M, Mobarakeh HS, Mahdavian AR. Preparation of acrylic/silica nanocomposites latexes with potential application in pressure sensitive adhesive. Int J Adhes Adhes 2015;58:21–7.

[13] Hanemann T, Szabó DV. Polymer-nanoparticle composites: From synthesis to modern

applications. vol. 3. 2010.

[14] Moon RJ, Martini A, Nairn J, Simonsen J, Youngblood J. Cellulose nanomaterials review: structure, properties and nanocomposites. Chem Soc Rev Chem Soc Rev 2011;40:3941–94.

[15] Ben Mabrouk A, Kaddami H, Magnin A, Belgacem MN, Dufresne A, Boufi S. Preparation of nanocomposite dispersions based on cellulose whiskers and acrylic copolymer by miniemulsion polymerization: Effect of the silane content. Polym Eng Sci 2011;51:62–70.

Appendix A

Table A.1 Starved seeded semi-batch emulsion polymerization with 47 wt.% solids content.

Component	Initial charge (g)	Monomer emulsion stock solution (g)	Initiator solution (g)	Total (g)	Total (phm)*
Butyl acrylate (BA)	10.8	304.6	-	315.4	90
Methyl methacrylate (MMA)	1.2	33.8	-	35	10
Potassium persulfate (KPS)	0.45	-	0.9	1.35	0.38
Sodium bicarbonate	0.05	-	-	0.05	0.01
Sodium dodecyl sulphate (SDS)	0.45	6.7	-	7.15	2
Deionized distilled water (DDI water)	202[a]/15 [b]	89	90	396	113

[a]water used for buffer and surfactant solution
[b]water used for initiator solution in seed stage
*phm= parts per hundred parts monomer

The 2 phm CNC loading was considered as the starting CNC loading for *in situ* emulsion polymerization but it was gradually decreased to lower amounts in each polymerizations due to coagulation results (Table A.2).

Table A.2 *In situ* starved seeded semi-batch emulsion polymerization with 47 wt.% solids content resulted in coagulation.

Component	Initial charge (g)	Monomer emulsion stock solution (g)	Initiator solution (g)	Total (g)	(phm)*
Butyl acrylate (BA)	10.8	304.6	-	315.4	90
Methyl methacrylate (MMA)	1.2	33.8	-	35	10
Potassium persulfate (KPS)	0.45	-	0.9	1.35	0.38
Sodium bicarbonate	0.05	-	-	0.05	0.01
Sodium dodecyl sulphate (SDS)	0.45	6.7	-	7.15	2
Cellulose nanocrystals (CNC)	0.35,0.7 1.75,3.5,7	-	-	0.35,0.7 1.75,3.5, 7	0.1,0.2 0.5,1,2
Deionized distilled water (DDI water)	170[a]/32[b]/15[c]	89	90	396	113

[a]water used for CNC dispersion
[b]water used for buffer and surfactant solution
[c]water used for initiator solution in seed stage
*phm= parts per hundred parts monomer

According to the coagulation results from the above polymerization formulations, the lowest CNC loading and lower solids content (42% and 37%) were selected for the following polymerization formulations.

Table A.3 *In situ* starved seeded semi-batch emulsion polymerization with 42 wt.% solids content and 0.1 phm CNC resulted in coagulation.

Component	Initial charge (g)	Monomer emulsion stock solution (g)	Initiator solution (g)	Total (g)	(phm)*
Butyl acrylate (BA)	10.8	304.6	-	315.4	90
Methyl methacrylate (MMA)	1.2	33.8	-	35	10
Potassium persulfate (KPS)	0.45	-	0.67	1.35	0.38
Sodium bicarbonate	0.05	-	-	0.05	0.01
Sodium dodecyl sulphate (SDS)	0.45	6.7	-	7.15	2
Cellulose nanocrystals (CNC)	0.35	-	-	0.35	0.1
Deionized distilled water (DDI water)	258[a]/32[b]/15[c]	89	90	484	113

[a]water used for CNC dispersion
[b]water used for buffer and surfactant solution
[c]water used for initiator solution in seed stage
*phm= parts per hundred parts monomer

Table A.4 *In situ* starved seeded semi-batch emulsion polymerization with 37 wt.% solids content and 0.1 phm CNC loading resulted in coagulation.

Component	Initial charge (g)	Monomer emulsion stock solution (g)	Initiator solution (g)	Total (g)	(phm)*
Butyl acrylate (BA)	8.1	228.45	-	236.55	90
Methyl methacrylate (MMA)	0.9	25.35	-	26.25	10
Potassium persulfate (KPS)	0.34	-	0.67	1.01	0.38
Sodium bicarbonate	0.05	-	-	0.05	0.01
Sodium dodecyl sulphate (SDS)	0.34	5.02	-	5.36	2
Cellulose nanocrystals (CNC)	0.262	-	-	0.262	0.1
Deionized distilled water (DDI water)	66[a]/236.5[b]/11.3[c]	66.7	67.5	448	113

[a]water used for CNC dispersion
[b]water used for buffer and surfactant solution
[c]water used for initiator solution in seed stage
*phm= parts per hundred parts monomer

In order to set up a stable polymerization formulation, the polymerization reaction procedure was simplified from semi-batch to batch procedure at lower solids content (33.3%) for the rest of polymerizations.

Table A.5 *In situ* emulsion batch polymerization with 33 wt.% solids content resulted in coagulation.

Component	Amount	
	(g)	(phm)
Butyl acrylate (BA)	135	90
Methyl methacrylate (MMA)	15	10
Potassium persulfate (KPS)	0.57	0.38
Sodium bicarbonate	0.57	0.38
Sodium dodecyl sulfate (SDS)	3	2
Cellulose nanocrystals (CNC)	0.15	0.1
Deionized distilled water (DDI)	300	200

Table A.6 *In situ* emulsion batch polymerization with 33 wt.% solids content resulted in coagulation.

Component	Amount	
	(g)	(phm)
Butyl acrylate (BA)	135	90
Methyl methacrylate (MMA)	15	10
Potassium persulfate (KPS)	0.57	0.38
Sodium bicarbonate	0.28	0.19
Sodium dodecyl sulfate (SDS)	3	2
Cellulose nanocrystals (CNC)	0.15	0.1
Deionized distilled water (DDI)	300	200

According to the interaction study was reported in chapter3 (page 71) and coagulation resulted from above mentioned formulations (Table A.2-A.6), the buffer was removed from emulsion polymerization and initiator concentration was reduced to 0.1 phm for the following reported emulsion polymerization formulations. The CNC dispersion was also charged to the reactor through pump in 30 min during the course of heating procedure.

The stable CNC/latex was successfully synthesized through the polymerization formulation (Table A.7) along with the new CNC feed protocol.

Table A.7 Stable i*n situ* emulsion batch polymerization with 33 wt.% solids content.

Component	Amount	
	(g)	(phm)
Butyl acrylate (BA)	135	90
Methyl methacrylate (MMA)	15	10
Potassium persulfate (KPS)	0.15	0.1
Sodium dodecyl sulfate (SDS)	3	2
Cellulose nanocrystals (CNC)	1.5	1
Deionized distilled water (DDI)	300	200

In order to test whether the new CNC feed protocol contributed in successful run or not, another polymerization with standard batch emulsion procedure was performed and resulted in coagulation (Table A.8).

Table A.8 Stable i*n situ* emulsion batch polymerization with 33wt,% solids content resulted in coagulation as polymerization was conducted in a standard procedure.

Component	Amount	
	(g)	(phm)
Butyl acrylate (BA)	135	90
Methyl methacrylate (MMA)	15	10
Potassium persulfate (KPS)	0.15	0.1
Sodium dodecyl sulfate (SDS)	3	2
Cellulose nanocrystals (CNC)	1.5	1
Deionized distilled water (DDI)	300	200

The common emulsifiers such as EF-800, CTAB, and their combination with Disponil at different concentrations (1, 1.5, 2 phm) were used in the following polymerization formulations. Although the new CNC feed protocol was employed, all polymerizations were ended up to coagulations.

Table A.9 *In situ* emulsion batch polymerization with 33 wt.% solids content resulted in coagulation.

Component	Amount	
	(g)	(phm)
Butyl acrylate (BA)	135	90
Methyl methacrylate (MMA)	15	10
Potassium persulfate (KPS)	0.15	0.1
EF-800	1.5,2.25,3	1,1.5,2
Cellulose nanocrystals (CNC)	1.5	1
Deionized distilled water (DDI)	300	200

Table A.10 *In situ* emulsion batch polymerization with 33wt.% solids content resulted in coagulation.

Component	Amount	
	(g)	(phm)
Butyl acrylate (BA)	135	90
Methyl methacrylate (MMA)	15	10
Potassium persulfate (KPS)	0.15	0.1
CTAB	1.5,2.25,3	1,1.5,2
Cellulose nanocrystals (CNC)	1.5	1
Deionized distilled water (DDI)	300	200

Table A.11 *In situ* emulsion batch polymerization with 33% solids content resulted in coagulations.

Component	Amount	
	(g)	(phm)
Butyl acrylate (BA)	135	90
Methyl methacrylate (MMA)	15	10
Potassium persulfate (KPS)	0.15	0.1
EF-800/Disponil*	1.5,2.25,3	1,1.5,2
Cellulose nanocrystals (CNC)	1.5	1
Deionized distilled water (DDI)	300	200

*Different combinations of EF-800/Disponil (1:1, 1:2 wt.%) were considered for each emulsifier concentration (phm).

Table A.12 *In situ* emulsion batch polymerization with 33% solids content resulted in coagulations.

Component	Amount	
	(g)	(phm)
Butyl acrylate (BA)	135	90
Methyl methacrylate (MMA)	15	10
Potassium persulfate (KPS)	0.15	0.1
CTAB/Disponil*	1.5,2.25,3	1,1.5,2
Cellulose nanocrystals (CNC)	1.5	1
Deionized distilled water (DDI)	300	200

* Different combinations of CTAB-800/Disponil (1:1, 1:2 wt.%) were considered for each emulsifier concentration (phm).

Table A.13 *In situ* emulsion batch polymerization with 40% solids content resulted in coagulations.

Component	Amount	
	(g)	(phm)
Butyl acrylate (BA)	135	90
Methyl methacrylate (MMA)	15	10
Potassium persulfate (KPS)	0.15	0.1
Sodium dodecyl sulfate (SDS)	3	2
Cellulose nanocrystals (CNC)	1.5,2.25,3	1,1.5,2
Deionized distilled water (DDI)	225	200

Table A.14 Stable *In situ* emulsion batch polymerization with 40% solids content.

Component	Amount	
	(g)	(phm)
Butyl acrylate (BA)	135	90
Methyl methacrylate (MMA)	15	10
Potassium persulfate (KPS)	0.15	0.1
Sodium dodecyl sulfate (SDS)	2.25	1.5
Cellulose nanocrystals (CNC)	1.5	1
Deionized distilled water (DDI)	225	200

Table A.15 Stable in situ emulsion batch polymerization with 33.3 wt.% solids content and higher KPS concentrations.

Component	Amount	
	(g)	(phm)
Butyl acrylate (BA)	135	90
Methyl methacrylate (MMA)	15	10
Potassium persulfate (KPS)	0.22,0.3,0.41	0.15,0.2,0.27
Sodium dodecyl sulfate (SDS)	3	2
Cellulose nanocrystals (CNC)	1.5	1
Deionized distilled water (DDI)	300	200

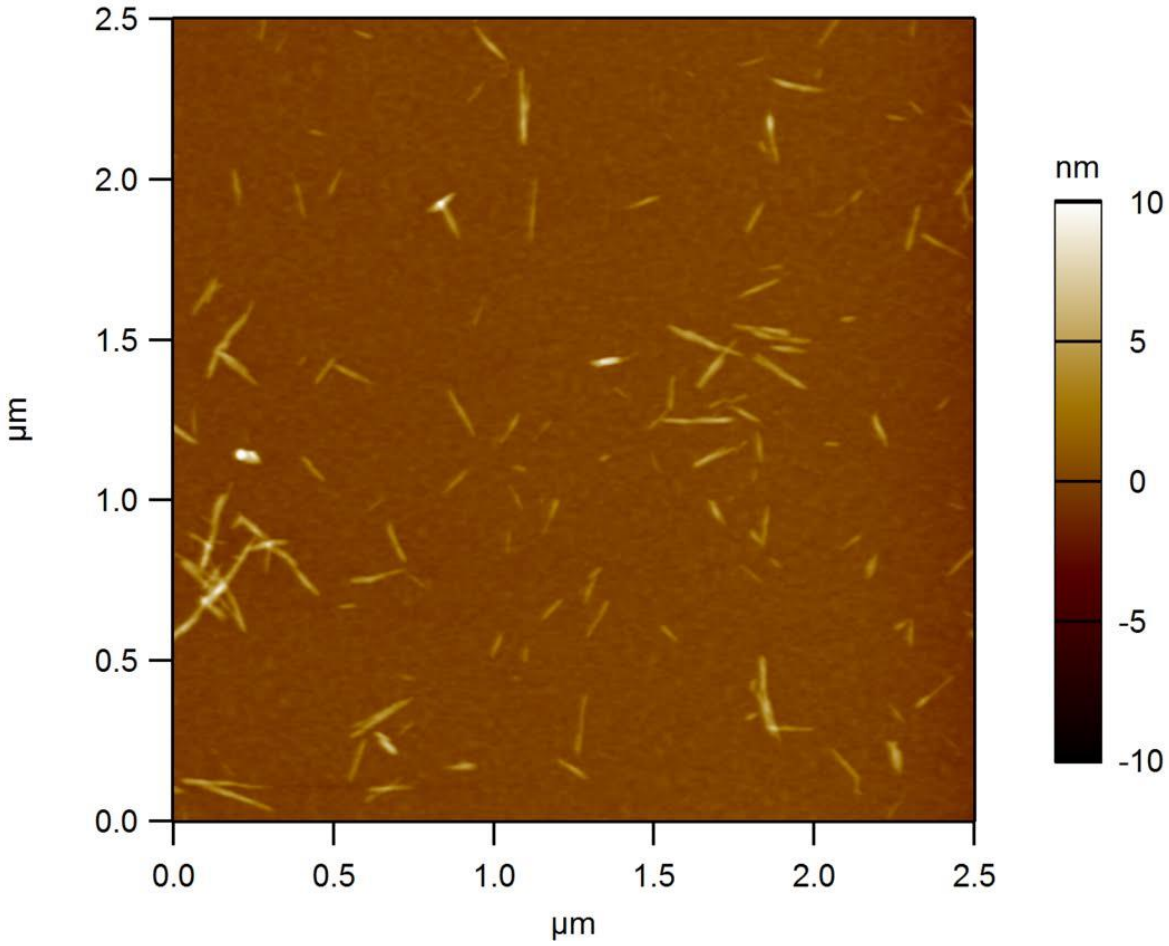

Figure A.1 AFM image of aqueous CNC dispersion (0.001wt.%).

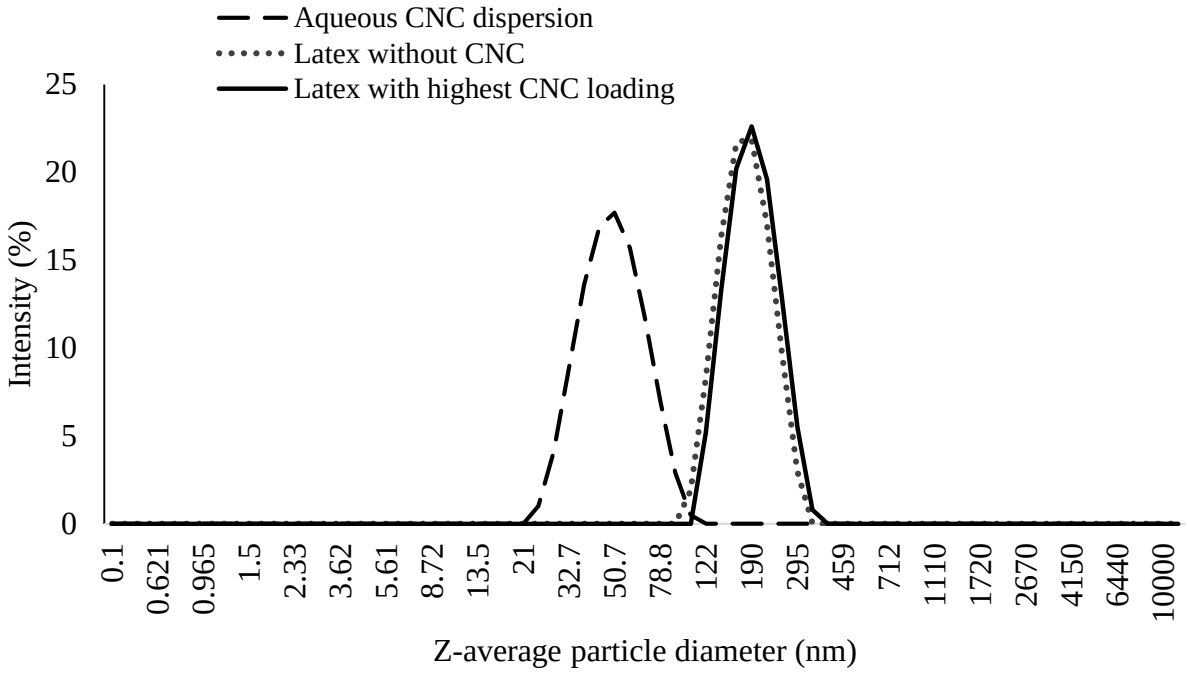

Figure A.2 Particle size of CNC/latex dispersion.

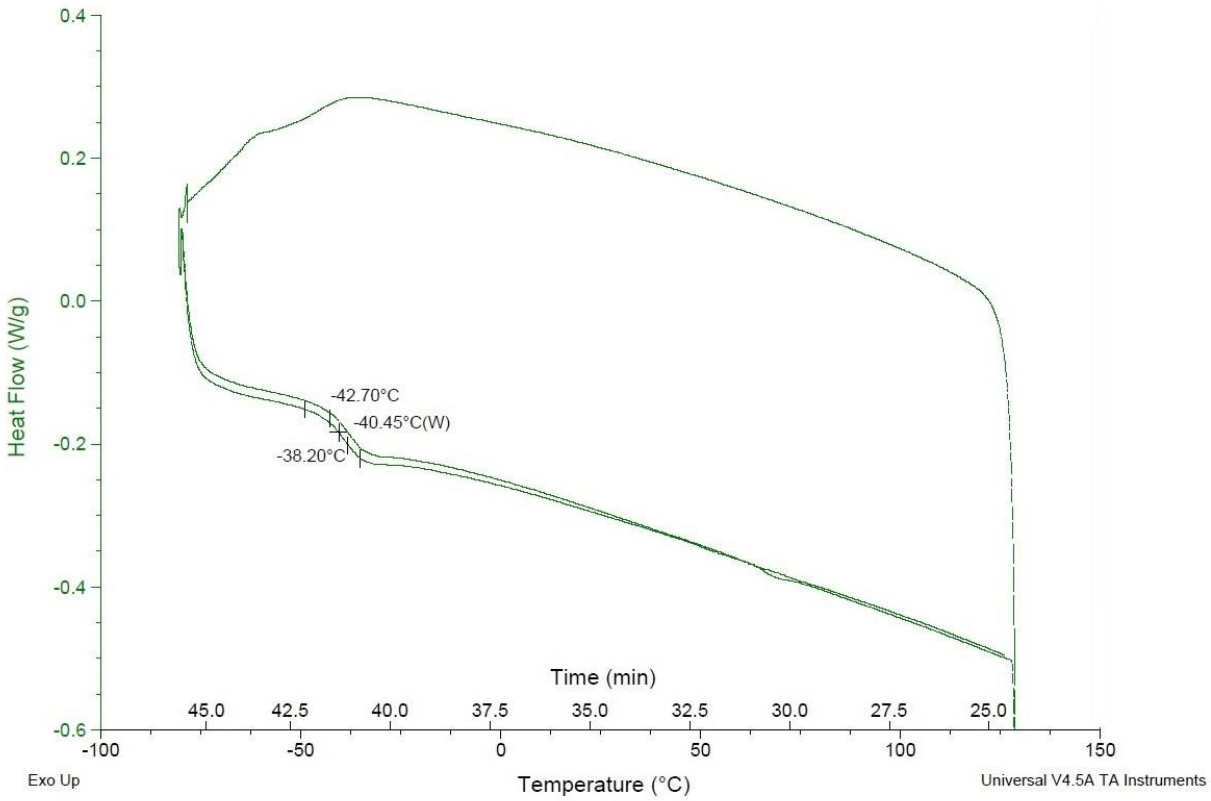

Figure A.3 DSC thermograph of poly(BA/MMA, 90:10).

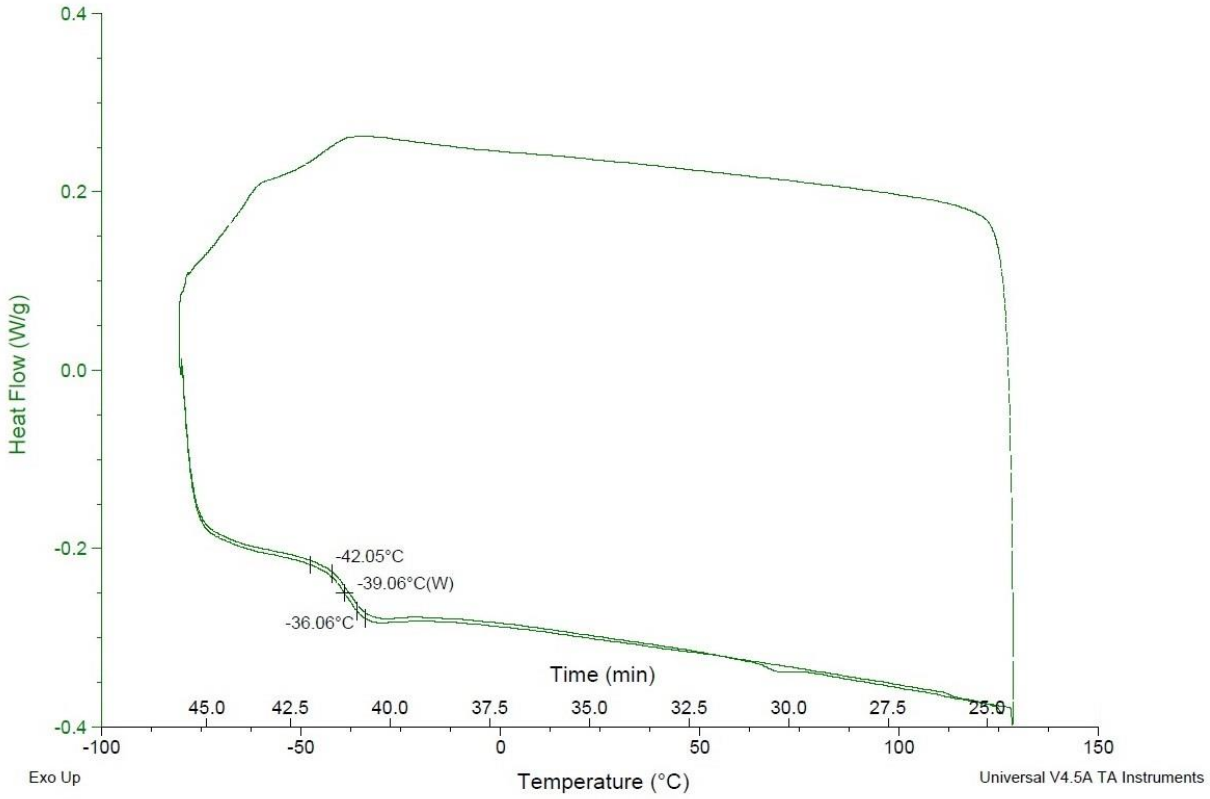

Figure 4 DSC thermograph of CNC/poly(BA/MMA, 90:10) at 0.5 wt.% CNC loading.

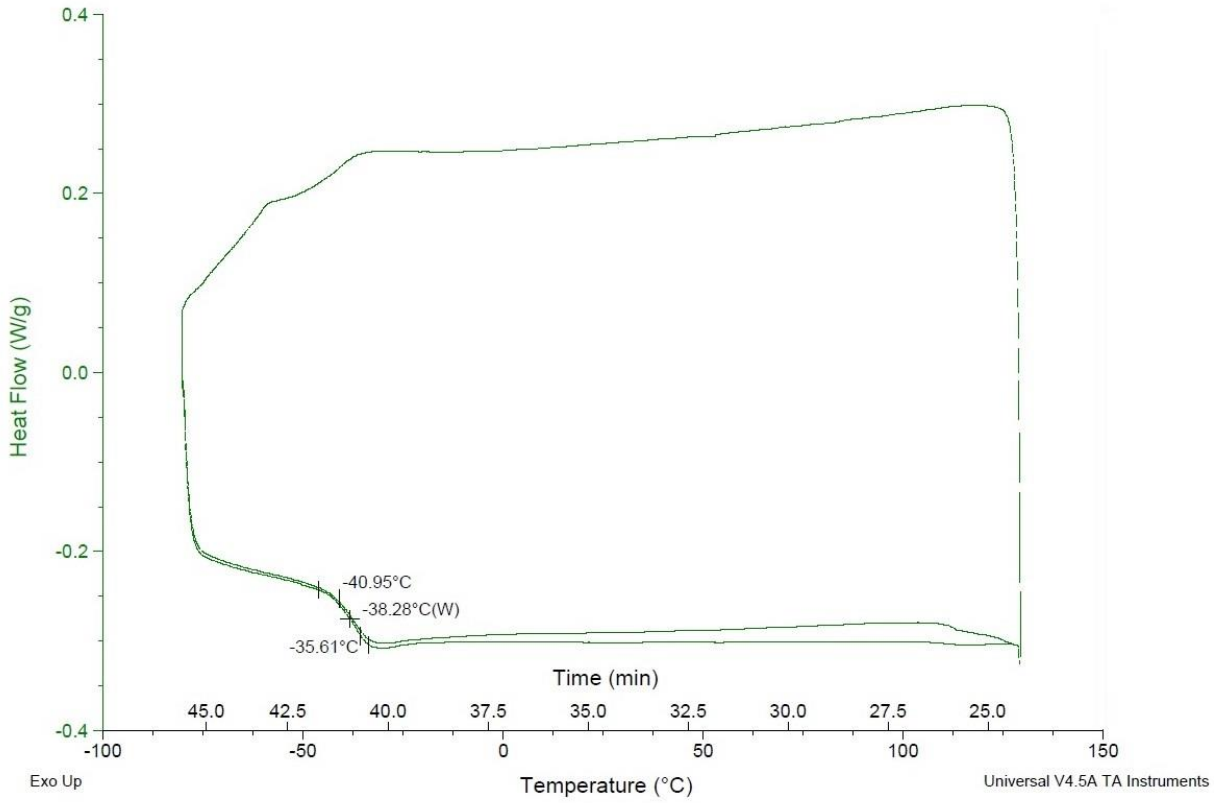

Figure A.5 DSC thermograph of CNC/poly(BA/MMA, 90:10) at 1 wt.% CNC loading.